

STEREOCHEMICAL AND CALORIMETRIC STUDIES

OF

SOME OCTAHEDRAL GROUP IVB COMPLEXES

by

H. EDWIN BLAYDEN

A THESIS SUBMITTED TO

THE UNIVERSITY OF SOUTHAMPTON

FOR

THE DEGREE OF

MASTER OF PHILOSOPHY

SOUTHAMPTON

MAY 1971

ACKNOWLEDGEMENTS

I wish to express my deep gratitude to my supervisors, Professor I. R. Beattie and Dr. M. Webster, for providing me with the opportunity to present this thesis and for their continued help and encouragement. I also wish to thank Dr. G. A. Ozin for a gift of $\text{SiCl}_4 \cdot 2\text{PMe}_3$ crystals; Dr. J. S. Wood and my colleagues for many helpful discussions; the computer staff of the National Centre for Computation, Imperial College, and the Atlas Computing Laboratory where the X-ray 63 System was used. Special thanks are due to Mrs. A. Jones who typed the thesis.

I am particularly indebted to Pamela without whose enduring patience, help and encouragement this thesis would never have been written.

H. Edwin Tslayden.

Dedicated with love and gratitude

to Pamela and to my parents

ABSTRACT

FACULTY OF SCIENCE

CHEMISTRY

Master of Philosophy

STEREOCHEMICAL AND CALORIMETRIC STUDIES OF SOME OCTAHEDRAL
GROUP IVB COMPLEXES

By H. Edwin Blayden

The factors which influence the preferred stereochemistries of octahedral Group IV complexes are briefly discussed and methods of investigating CIS-TRANS isomerism are surveyed.

Results published during the period (1968-1970) relating to simple five and six co-ordinate complexes of silicon IV, germanium IV and tin IV are critically reviewed. The tabulation is thought to be comprehensive for firm stereochemical and calorimetric evidence concerning six co-ordinate species, and for stereochemical evidence concerning five co-ordinate species.

The crystal structure of tetrachlorotin IV-bis-acetonitrile ($\text{SnCl}_4 \cdot 2\text{MeCN}$) has been determined from photographically collected, three dimensional X-ray diffraction data. The complex crystallizes in the space group $P2_1/c$ with $z = 4$ in a unit cell of dimensions $a = 6.12$; $b = 13.72$; $c = 13.38 \text{ \AA}$ and $\beta = 100.4^\circ$. The molecules of $\text{SnCl}_4 \cdot 2\text{MeCN}$ are CIS octahedral. Sn-Cl distances are comparable with those obtained in previous work on SnCl_4 adducts. Sn-N distances (2.33 , 2.34 \AA) are comparable with the value found in the analogous glutaronitrile complex (2.29 \AA) (130).

The crystal structure of bis(trimethylphosphine)tetrachloro-silicon IV ($\text{SiCl}_4 \cdot 2\text{PMe}_3$) has been determined from counter collected, three dimensional X-ray diffraction data. The data is of modest quality due to a poor crystal of plate like habit and the Pyrex capillary enclosure ($R = 0.142$). The complex crystallizes in the space group $\text{P2}_1/\text{c}$ with $a = 6.65$; $b = 8.26$; $c = 13.10 \text{ \AA}$; $\beta = 101.8^\circ$ and $z = 2$. The structure consists of discrete centrosymmetric TRANS $\text{SiCl}_4 \cdot 2\text{PMe}_3$ molecules. Angles around the central silicon atom are approximately 90° and the pertinent bond lengths (STD. DEV in parenthesis) are $\text{Si-Cl}(1) = 2.30(1)$; $\text{Si-Cl}(2) = 2.20(1)$; $\text{Si-P} = 2.26(1)$; $\text{P-C} = 1.83(4), 1.89(4) \text{ \AA}$.

The design and testing of a microcalorimeter (effective volume 30 cc) is described suitable for measuring the formation enthalpies of oxygen and moisture sensitive complexes. The heats of formation of crystalline $\text{MX}_4 \cdot 2\text{py}$ ($M = \text{Si, Ge, Sn}$; $X = \text{Cl, Br}$) adducts have been measured from the pure constituents (in excess pyridine). Apart from the (suspect) value for $\text{SnCl}_4 \cdot 2\text{py}$ differences between members of the series vary neither greatly nor in a systematic manner.

CONTENTS

	Page
Chapter 1. Introduction and Chemical Background	1
Chapter 2. Recent work on five and six-co-ordinate complexes of Silicon IV, Germanium IV and Tin IV	7
Chapter 3. The application of spectroscopic techniques (and dipole moment measurements) to problems of CIS-TRANS isomerism in Group IVB	24
Chapter 4. Background to X-ray crystallographic work	45
Chapter 5. The crystal structure of tetrachlorotin IV-bis-acetonitrile	58
Chapter 6. The crystal structure of bis(trimethylphosphine)tetrachlorosilicon IV	73
Chapter 7. Calorimetric studies of some $\text{MX}_4 \cdot 2\text{py}$ complexes	84
Appendix A Experimental (X-ray section)	111
B Observed and calculated structure factors	112
C References	117
Plate 1 - The Calorimeter	

PART 1

CHAPTER 1

INTRODUCTION AND CHEMICAL BACKGROUND

CHAPTER 1

INTRODUCTION AND CHEMICAL BACKGROUND

(1:1) INTRODUCTION

During the last decade the spectroscopic techniques used to study the 's' and 'p block' elements have been developed to a very high degree of sophistication. This has led to a renewed interest in a field of chemistry which for some time has been neglected in favour of the more spectroscopically accessible transition elements. In contrast to the transition elements, whose properties are largely influenced by the presence of partially filled 'd shells', interest in these groups lies, generally speaking, in the very fact that their 'd shells' are either empty or filled. In Group IVB the outermost electron shell is four short of the next inert gas configuration. The gain or loss of four electrons to give ionic species is unlikely on a charge-radius basis. Thus compounds such as Al_4C_3 are best regarded as covalent. Similarly, four covalent bonds are formed in the hydrides and tetrachlorides where the central atom is tetrahedral and may be regarded as sp^3 hybridized.

A complete range of the simple tetrahalides has been prepared with the exception of the tetrabromide and tetraiodide of lead, the non-existence of these being attributed to the strongly oxidizing properties of Pb IV, which presumably converts the heavy halide ion to free halogen. The tetrafluorides of carbon, silicon and germanium, are gaseous at room temperature; SnF_4 and PbF_4 which are fluorine bridged polymers in the solid state are involatile. The other tetrahalides are generally volatile liquids or easily melted solids. A number of mixed halides are known, e.g. SiF_3I , SiCl_2Br_2 , although as far as the author is aware the ultimate mixed species MFClBrI which would be a racemic mixture, has

never been prepared.

The majority of the complexes of silicon, germanium, tin, and the Group IV A element titanium, can be regarded as arising from the Lewis acid behaviour of the tetrahalides towards halide ions and donor ligands (Lewis bases) containing nitrogen, oxygen, phosphorus, or sulphur as electron donors. The hexafluoro complex $[\text{SiF}_6]^{2-}$ formed when SiF_4 is hydrolyzed is well known. A range of similar hexafluoro species are known for the other elements. With monodentate ligands the most commonly occurring stoichiometries (Acceptor:Donor) are 1:1 and 1:2, although ratios greater than these, (1:3 and 1:4) are by no means unknown. When complexation takes place, the central metal atom increases its co-ordination number from four, usually to become either five or six co-ordinate. Five-co-ordinate species may be considered to be sp^3d hybridized in valence bond language, with trigonal bipyramidal shapes. Six-co-ordinate species are usually approximately octahedral (sp^3d^2) conformations, and with monodentate ligands both CIS and TRANS isomers are possible. Bidentate donors generally give 1:1 six-co-ordinate octahedral complexes. Higher co-ordination numbers are occasionally found for tin, e.g. TROP_3SnCl (1) where the central atom is seven co-ordinate, and $\text{Sn}(\text{TROP})_4$ (2) where the central atom is eight co-ordinate. (TROP = TROPOLONATO).

(1:2) FACTORS DETERMINING THE PREFERENTIAL FORMATION OF CIS AND TRANS ISOMERS.

Beattie (3), and more recently Dyer and Ragsdale (4), have discussed the factors which might be expected to influence the stereochemistry of octahedral $\text{MX}_4\cdot 2\text{L}$ complexes. Arguments are based principally on the effects of steric repulsion, symmetry, and $\text{p}\pi - \text{d}\pi$ bonding. It is likely that these factors are interrelated to some extent, but for present purposes they are considered individually.

From a consideration of idealized CIS and TRANS isomers (Fig.1), in which all bond angles were 90° , and the ligands were represented by single atoms, it has been pointed out (3,4) that on the basis of X-X repulsions alone a TRANS isomer is preferred if the donor atom is small relative to the halogen, since five X-X interactions are expected for the CIS conformation, compared to only four for the TRANS. On the other hand, Beattie (3) has reasoned that if the geometry of the MX_4 moiety approximates to the original tetrahedral symmetry of the halide, then a CIS configuration is stereochemically feasible. This is particularly likely if the ligand is shaped in such a way as to allow it to 'penetrate' the tetrahedron. The 'pointed' acetonitrile ligand has been pictured behaving in just this manner (3) to produce a conformation which is effectively CIS. In a situation in which the donor atom or ligand is no longer small in comparison to the halide, the L-X repulsions become significant and the TRANS isomer may be favoured.

The TRANS isomer has a higher symmetry (D_{4h}) than that of the CIS isomer (C_{2v}) so that in the absence of steric effects the change in entropy ΔS for the equilibrium $TRANS \rightleftharpoons CIS$ (Fig.1) should be positive. Consequently, with increasing temperature the equilibrium will be displaced to the right, since $\Delta G (= \Delta H - T\Delta S)$ would become increasingly negative (4). Several such temperature dependent equilibria have been observed for the β diketonate complexes (see Chapter 2).

The ability to form M-X π bonds apparently favours the formation of the CIS isomer (4). If appropriate vacant metal d-orbitals are available the halogens are thought to arrange themselves so as to achieve the greatest stability through p π - d π bonding (3,4). ^{19}F N.M.R. spectra of $MF_4 \cdot 2L$ complexes ($M = Ti, Sn$) (4,5) have been examined in some detail, and it has been shown that the effectiveness of the fluorine atoms and ligands in bonding via the available d π - orbitals is reflected

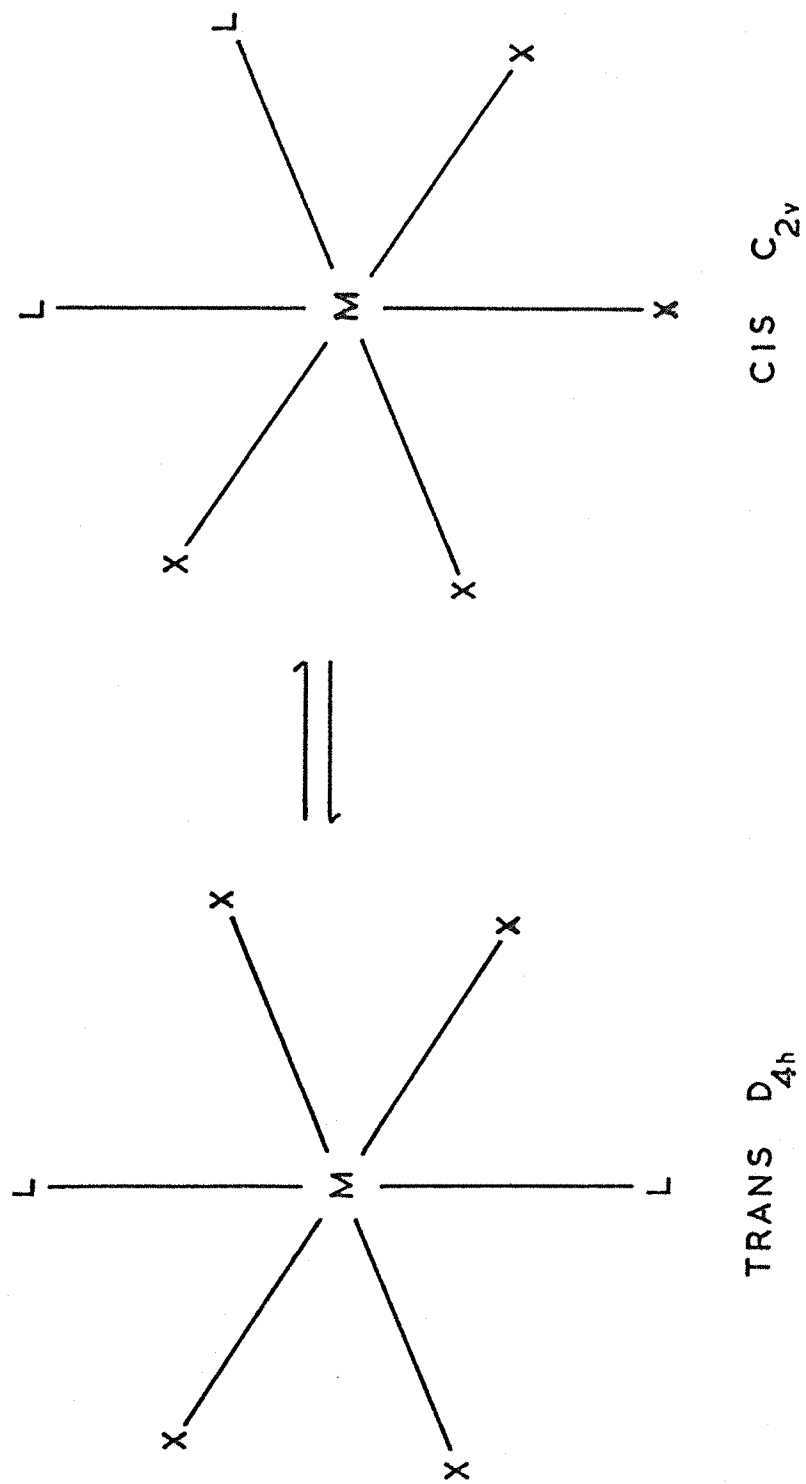


FIGURE.I. CIS AND TRANS $\text{MX}_4\cdot 2\text{L}$

in the chemical shifts of the equivalent fluorine pairs. For $\text{TiF}_4 \cdot 2\text{L}$ complexes, F-M π bonding is important and explains the stability of the CIS isomer. Earlier work (4), however, has suggested that p π - d π bonding decreases in importance for M-O bond formation as the metal d-orbitals become more diffuse with increasing atomic number. Both CIS and TRANS $\text{SnF}_4 \cdot 2\text{EtOH}$ (7) are known in ethanol solution, whereas only the CIS form has been detected for $\text{TiF}_4 \cdot 2\text{EtOH}$ (8). Dyer and Ragsdale (4) have argued that the large differences observed in the ^{19}F chemical shift data for the tin and titanium complexes (1 p.p.m. and 60 p.p.m. respectively) are also indicative of decreased π bonding in tin complexes, in which the 3d level is filled. If this is true steric effects and the magnitude of X-X repulsions would seem to be decisive in determining the stereochemistry of octahedral tin complexes, particularly those involving small halogen atoms.

(1:3) STABILITY AND DONOR-ACCEPTOR STRENGTH

The 'stability' sequence for a series of related adducts is sometimes obvious. For example, although the stability of $\text{SiCl}_4 \cdot 2\text{py}$ is little effected by the substitution of one or more of its chlorines by other electronegative groups, the inclusion of only a single alkyl or aryl group may grossly alter the acceptor properties of the central atom. $\text{SiCl}_4 \cdot 2\text{py}$ is stable under anhydrous conditions at room temperature, while only a very unstable complex is formed under the same conditions with methyl trichlorosilane. When further alkyl groups are introduced no reaction takes place at all (9). The range of $\text{MX}_4 \cdot 2\text{py}$ complexes (M = Si, Ge, Sn, X = F, Cl, Br) are all stable and very insoluble at normal temperatures so that the exact stability sequence is by no means so obvious.

Calorimetry offers one of the most suitable methods of studying stability trends in solution. Complexes formed by the Group III halides have been extensively studied in this way (10,11). In cases where an insoluble complex is precipitated, the situation is complicated by the fact that the lattice energy is unknown. Nevertheless, for a closely related series of adducts, all of which are very insoluble, it is reasonable to assume that the 'heat of reaction' is at least an approximate measure of the donor-acceptor bond strength providing the lattice energies are of similar magnitudes. This is particularly likely for the $\text{MX}_4 \cdot 2\text{py}$ ($\text{M} = \text{Si}, \text{Ge}, \text{Sn}$) complexes, since all these are now thought to be (TRANS) isostructural^{*}. (See Chapter 2). Available thermochemical data for the formation of the $\text{MX}_4 \cdot 2\text{py}$ complexes is remarkably discordant with respect both to the magnitude of the reaction enthalpies and the exact sequence of donor-acceptor strengths within the series. Enthalpy changes for the $\text{MX}_4 \cdot 2\text{py}$ systems are particularly sensitive to hydrolysis, and it seems probable that at least some of these results are in error.

^{*} Though not necessarily isomorphous.

(1:4) PURPOSE OF THE PRESENT STUDY

There has been a serious shortage of X-ray diffraction work to act as a firm foundation for the interpretation of spectroscopic data. The complexes $\text{SnCl}_4 \cdot \text{MeCN}$ (12-22) and $\text{SiCl}_4 \cdot 2\text{PMe}_3$ (23,24) have been characterised by infra-red and Raman studies, which have indicated CIS and TRANS molecular structures respectively. It is important that the structures of several typical examples of CIS and TRANS isomers should be confirmed by single crystal X-ray analysis.

Part I of the present work has therefore as its objective the determination of refined crystal and molecular structures for

- a) TETRACHLOROTIN IV BIS-ACETONITRILE ($\text{SnCl}_4 \cdot 2\text{MeCN}$) and
- b) BIS(TRIMETHYL PHOSPHINE)TETRACHLOROSILICON IV ($\text{SiCl}_4 \cdot 2\text{PMe}_3$).

Part II will be concerned with the design and testing of a microcalorimeter suitable for the measurement of the reaction enthalpies of moisture and (in some cases) oxygen sensitive $\text{MX}_4 \cdot 2\text{L}$ complexes. An attempt will be made to interpret the data for $\text{MX}_4 \cdot 2\text{py}$ ($\text{M} = \text{Si}, \text{Ge}, \text{Sn}$ and $\text{X} = \text{Cl}, \text{Br}$) adducts in terms of their relative stabilities.

CHAPTER 2

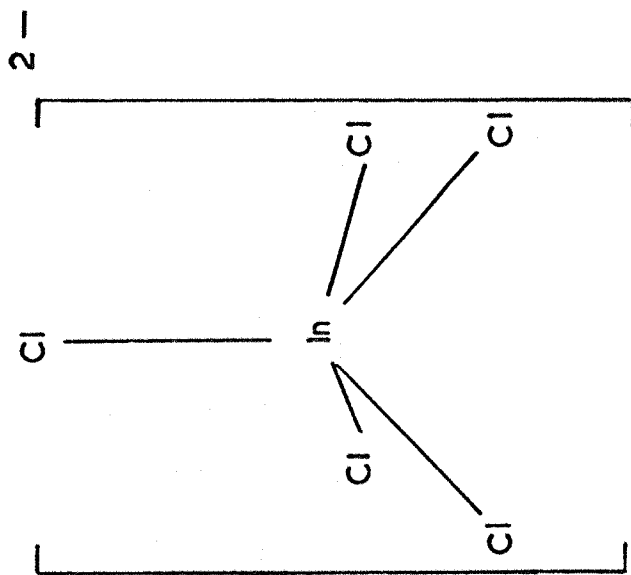
RECENT WORK ON FIVE AND SIX-CO-ORDINATE COMPLEXES

OF SILICON IV GERMANIUM IV AND TIN IV

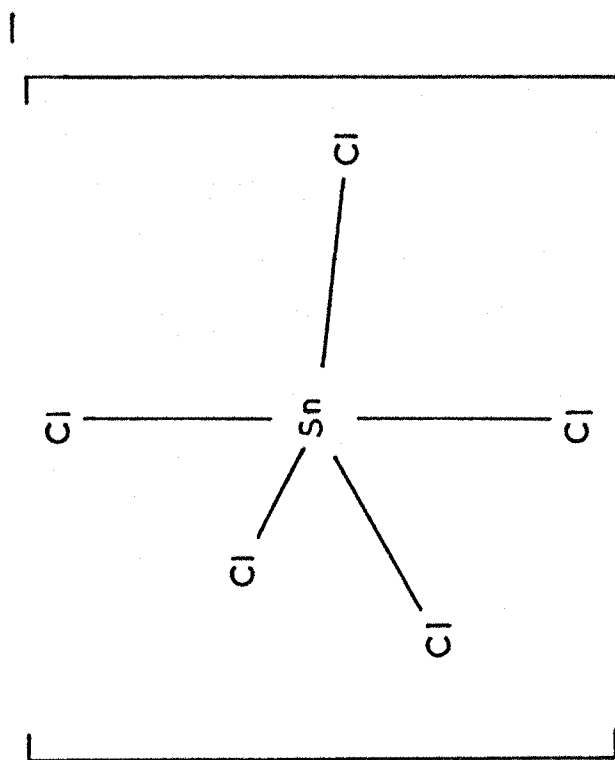
RECENT WORK ON FIVE AND SIX-CO-ORDINATE COMPLEXES OF
SILICON IV, GERMANIUM IV AND TIN IV

(2:1) Co-ordination compounds of the quadri-positive Group IV B elements (Si, Ge, Sn, Pb) have been reviewed by Beattie (3) 1963, Gielen and Sprecher (25) 1966, and more recently by Aylett (26) 1968. Germanium complexes have been discussed in detail by Lavigne and Tancrede (27) 1962, and by Webster (28) 1962 (tetrahalides only). A very large number of tin tetrahalide complexes have been detailed by Rule (29) 1964. Aylett's article is comprehensive, (1968) especially with regard to stereochemical studies. The present chapter attempts to bring together the more important results published during the period 1968-1970 for five and six co-ordinate silicon, germanium and tin addition compounds. The tabulation is thought to be comprehensive for firm evidence concerning the stereochemistries and stabilities of simple six-co-ordinate complexes, and for the stereochemistries of simple five-co-ordinate species. A large number of tin complexes have been reported and these are simply listed with a minimum of detail. For the sake of continuity a number of earlier references are included, all of which are cited in Ref.26.

Stereochemical interest in six-co-ordinate species naturally centres around the question of CIS-TRANS isomerism. Examples of five-co-ordination in the solid state are comparatively rare outside the transition metal series. Considerable interest surrounds the stereochemical configurations adopted by such species. The anion InCl_5^{2-} is unusual in that it displays a square-pyramidal (C_{4v}) geometry in its tetraethyl ammonium salt (30,31). Apart from the analogous TlCl_5^{2-} salt (32) this geometry is unknown for other simple non transition metal complexes. Five-co-ordinate species so far reported for Group IV B, e.g. SnCl_5^- , (33,34) and $\text{Me}_2\text{SnCl}_3^-$, (35) appear to have trigonal-bipyramidal shapes. (See Fig.2)



SQUARE PYRAMIDAL InCl_5^{2-} C_{4v}



TRIGONAL BIPYRAMIDAL SnCl_5^- D_{3h}

(2:2) FIVE CO-ORDINATE SILICON

This is the least studied aspect of silicon chemistry, and until relatively recently (1965) there remained real doubts as to its occurrence. By 1968, however, Aylett (26) was able to cite studies relating to molecular (e.g. $\text{SiCl}_4 \cdot \text{NMe}_3$ (36), $\text{CHF}_2\text{CF}_2\text{SiH}_3 \cdot \text{NMe}_3$ (37)), anionic, e.g. $[\text{PtCl}(\text{CO})(\text{PET}_3)_2]^\text{+} \text{SiF}_5^-$, $\text{Ph}_4\text{As}^\text{+} \text{SiF}_5^-$ (38,39), cationic e.g. $[\text{Ph}_3\text{Si}(\text{bipy})]^\text{+} \text{I}^-$ (40), $[\text{SiH}_3\text{ZL}]^\text{+} \text{M}(\text{CO})_n^-$ (41) and polymeric species e.g. $(\text{Me}_2\text{NSiH}_3)_5^\text{+}$ (42). The reaction of the weaker bases with some halogen or pseudohalogen substituted silanes has been shown to result in cationic four-co-ordinate species such as $[\text{SiH}_3 \cdot \text{NMe}_3]^\text{+} \text{I}^-$, $[\text{Me}_3\text{SiNMe}_3]^\text{+} \text{ClO}_4^-$ (43,44).

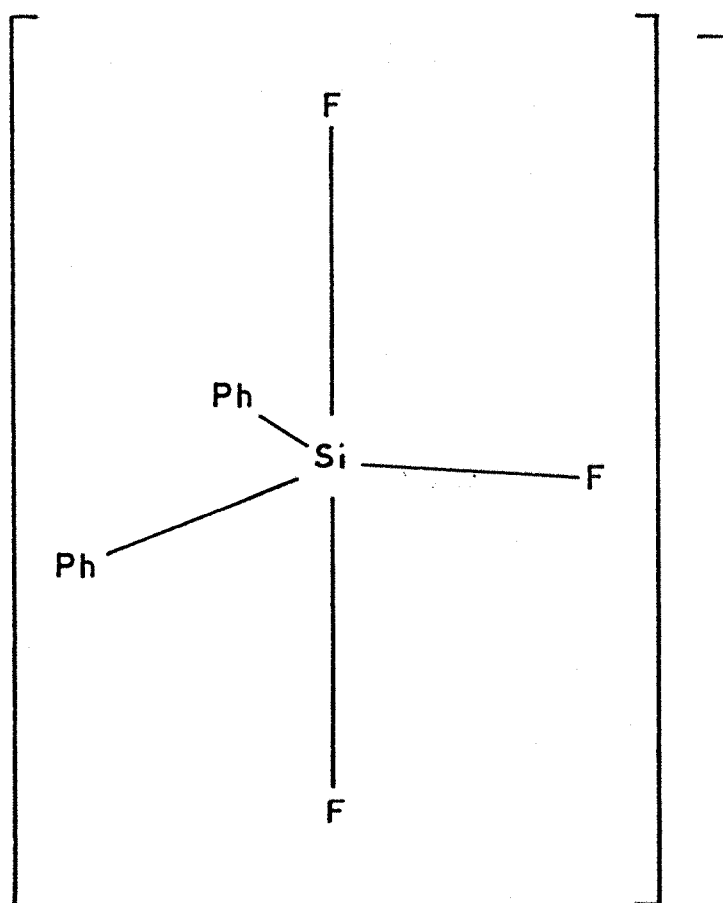
Klanberg and Muetterties (45) have now demonstrated the existence of the anions SiF_5^- , RSiF_4^- , (R = alkyl, aryl) and $(\text{Ph})_2\text{SiF}_3^-$, in solvents of low polarity using ^{19}F N.M.R. and P.M.R. spectra. Low temperature spectra of SiF_5^- and RSiF_4^- showed spectroscopic equivalence of all the fluorine atoms suggesting a rapid intramolecular rearrangement. For $(\text{Ph})_2\text{SiF}_3^-$ they were able to establish two types of fluorine atom environment, and assigned a trigonal-bipyramidal (C_{2v}) configuration for the anion (see Fig.3). Above -40°C the two fluorine environments were averaged out to a single resonance.

Beattie and Ozin (23) have reported detailed vibrational studies which suggest that $\text{SiCl}_4 \cdot \text{NMe}_3$ is probably monomeric and five co-ordinate with C_{3v} symmetry. For the 1:1 adducts of silicon tetrafluoride with trimethylamine and trimethylphosphine a C_{3v} model was found to be acceptable but not proved.

Attempts to prepare $[\text{SiCl}_3 \cdot 2\text{NMe}_3]^\text{+}$ by reacting SiCl_3I with trimethylamine have proved unsuccessful (46). However, in the presence

* Five co-ordinate molecular pentamer with symmetrical Si-N-Si bridges.

FIGURE 3 .



TRIGONAL BIPYRAMIDAL $\text{Ph}_2\text{SiF}_3^-$ C_{2v}

of one equivalent of silver perchlorate, similar experiments led to the species $[\text{SiCl}_3 \cdot 2\text{NMe}_3]^+ \text{ClO}_4^-$ (46), and spectral data were found to be 'not inconsistent' with that expected of a monomeric cation of D_{3h} symmetry. The analogous germanium complex was similarly prepared, but in the case of the tin compound a more complex reaction occurred (46). $[\text{SiCl}_3 \cdot 2\text{PMe}_3]^+ \text{ClO}_4^-$ was prepared (47) by reacting trimethylphosphine with $[\text{SiCl}_3 \cdot 2\text{NMe}_3]^+ \text{ClO}_4^-$, (in MeCN) demonstrating the stability sequence $\text{Me}_3\text{P} > \text{Me}_3\text{N}$ towards SiCl_3^+ . (See Table 14).

(2:3) SIX CO-ORDINATE SILICON

Although six-co-ordinate silicon has been known for a considerable time in SiO_2 (rutile form) and in the anion SiF_6^{2-} , it is only relatively recently that evidence for other six co-ordinate species has accumulated. In general these have been formulated as either molecular octahedral, (AL_2 or AL) or alternatively, as cationic species. e.g. $[\text{Si}(\text{trop})_3]^+$ (49), $[\text{SiI}_2(\text{py})_4]^{2+} 2\text{I}^-$ (50,51). The majority of investigations have employed vibrational spectroscopy. In 1968 (26) there was an almost complete absence of X-ray diffraction data to act as a basis for the interpretation of such spectroscopic studies, and a significant proportion of stereochemical work prior to this is suspect.

The $\text{MX}_4 \cdot 2\text{py}$ series, and the silicon complexes in particular, have attracted a good deal of attention. Campbell-Fergusson and Ebsworth (43) were first to question the earlier CIS (50) assignment for $\text{SiCl}_4 \cdot 2\text{py}$. Single crystal X-ray studies have now shown that $\text{SiF}_4 \cdot 2\text{py}$ (52), and $\text{SiCl}_4 \cdot 2\text{PMe}_3$ (53)[‡] are all TRANS octahedral structures. Beattie et al (51) have demonstrated through more detailed vibrational studies that it is not possible to decide between CIS and TRANS $\text{SiCl}_4 \cdot 2\text{py}$ from vibrational

[‡] Reported in this thesis.

data alone. Guertin and Onyszchuk (54) reached similar conclusions regarding the 1:2 complexes formed by SiF_4 with pyrrolidine and ~~pyridine~~^{PIPERIDINE}. ^{19}F N.M.R. results (54) have confirmed the CIS chelate structure for $\text{SiF}_4 \cdot \alpha\alpha'$ -dipyridyl.

For the compounds $\text{SiCl}_3^+ \cdot 3\text{py}$ and $\text{SiCl}_2^{2+} \cdot 4\text{py}$, thought to contain cationic silicon halide species, C_{2v} and D_{4h} symmetries respectively have been suggested from vibrational data (51). The compound $\text{SiCl}_3\text{I} \cdot 3\text{py}$ appears to be the first well characterized 1:3 adduct of a tetrahalogen silicon IV species (51).

The ability of 2,2'-bipyridyl to complex with the methyl substituted chlorosilanes has proved controversial. Tanaka et al (55) interpreted conductometric and spectroscopic measurements to indicate univalent electrolytes for Me_3SiCl and $\text{Me}_2\text{SiCl}_2/\text{bipy}$ systems in acetonitrile. ($[\text{Me}_3\text{Si}(\text{bipy})]^+ \text{Cl}^-$ in 1:1 mole ratios donor:acceptor). However, Beattie, Jones and Webster (56) doubt that a complex is formed between Me_2SiCl_2 and bipyridyl. They obtained a near non electrolyte when rigorously purified acetonitrile was used. In the light of this result, the observations of Tanaka et al (57) that $(\text{Me})_3\text{SiCl}$, $(\text{Me})_2\text{SiCl}_2$ and SiCl_4 form 1:1, 1:2 and 1:3 complexes respectively with bipyridyl, to give siliconium cations in solution, seem very surprising. Complex formation seems to be less inhibited when the number of substituent methyl groups is reduced to one. For example, Kummer et al (58) have reported the formation of a comparable 1:1 complex between the disilane $(\text{Cl}_2\text{CH}_2\text{Si} \cdot \text{SiCH}_2\text{Cl}_2)$ and bipyridyl under non polar conditions. The 1:1 composition is confirmed by P.M.R. spectra and analysis, and the results are in accordance with a structure in which the donor is bound to only one silicon of a molecular adduct, the two $\text{Si}-\text{Me}_3$ groups being non equivalent in the N.M.R. sense. No prediction is forwarded for the stereochemistry of the ligand with respect to the silicon. The authors mention,

however, that a single crystal X-ray structural analysis is in progress (1969).

Beattie and Ozin (59) predicted that the five-coordinate ion $[\text{SiCl}_3 \cdot 2\text{PMe}_3]^+$ (isoelectronic with $\text{AlCl}_3 \cdot 2\text{PMe}_3$) would be stable. This led them to examine the reactions of the tetrahalides with trimethylphosphine. In contrast to the behaviour of SiX_4 with trimethylamine, they obtained the adducts $\text{SiCl}_4 \cdot 2\text{PMe}_3$ and $\text{SiBr}_4 \cdot 2\text{PMe}_3$ and found them to have vapour pressures < 2 m.m.Hg at 25°C (47,23). They further noted the non existence of $\text{SiF}_4 \cdot 2\text{PMe}_3$ under similar conditions, and pointed out that this is an almost exact reversal of the stability sequence with trimethylamine. Trimethylamine forms 1:1 and 1:2 adducts with SiF_4 ; 1:1 with SiCl_4 ; and no adduct with SiBr_4 (at -78°C) (47). The vibrational spectra of the 1:2 adducts strongly suggested a TRANS octahedral shape (23)[‡].

The dichlorobis(acetylacetonato) complexes of germanium and tin have attracted attention from several quarters. In general they appear to be chelated molecular monomers having predominantly CIS structures. Thompson (60) has reported the first silicon complex of this type, $\text{Si}(\text{acac})_2\text{Cl}_2$. Infra-red data indicate that the complex is a chelated enolate. Unfortunately solubility problems precluded molecular weight and conductivity measurements, which might have helped to establish the polymerization and any saltlike character of the complex. Uncertainties arising from the P.M.R. spectra made it difficult to assign the stereochemical configuration with any certainty. Comparisons with other complexes suggested that $\text{Si}(\text{acac})_2\text{Cl}_2$ may be ionic or unsymmetrical. Related work on $\text{M}(\text{acac})_2\text{X}_2$ complexes (where $\text{M} = \text{Ge}, \text{Sn}$) strongly support molecular structures in solution (61,62,63).

Very recently, Dean and Evans (64) reported a ^{19}F N.M.R. study of anions of the general type $\text{MF}_{6-2x} \text{L}_x^{2-}$ ($\text{M} = \text{Si}, \text{Ge}, \text{Ti}$; L = bidentate ligand)

[‡] This work suggested the present X-Ray analysis of $\text{SiCl}_4 \cdot 2\text{PMe}_3$

TABLE 1

RECENT STUDIES IN FIVE AND SIX CO-ORDINATE SILICON

Compound	Prob. Structure/Comment	Evidence	Ref.
SiF_5^- , RSiF_5^- , PhSiF_5^- $(\text{Ph})_2\text{SiF}_3^-$ (Soln) (Cation R_4N)	[5] Anionic	^{19}F 'H N.M.R.	45
$\text{SiCl}_4 \cdot \text{NMe}_3$ (S & Soln)	[5] Monomeric Molecular (C_{3v})	IR. R.	23
$\text{SiF}_4 \cdot \text{NMe}_3$	[5] Monomeric Molecular (C_{3v})		
$\text{SiF}_4 \cdot \text{PMe}_3$	[5] Monomeric Molecular (C_{3v})		
$[\text{SiCl}_3 \cdot 2\text{NMe}_3]^+ \text{ClO}_4^-$ (S & Soln)	[5] Monomeric Cation (D_{3h}) ?	IR. R.	46
$[\text{SiCl}_3 \cdot 2\text{PMe}_3]^+ \text{ClO}_4^-$ (S)	$\text{PMe}_3 > \text{NMe}_3 / \text{SiCl}_3^+$		47
$(\text{Ph})_2\text{RSi}(\text{acac})$	Open Cation Enol Struc.	N.M.R.	48
$(\text{Ph})_2\text{MeSi}(\text{acac})$ (Soln)	[5]		
$[\text{Si}(\text{TROP})_3]^+$ (Soln)	[6] Cation	U.V. circular dichroism	49
$\text{SiCl}_3^+ 3\text{py}$	Probably (C_{2v}) [6]	IR. R. Solid & Soln	51
$\text{SiCl}_2^{2+} 4\text{py}$	Probably (D_{4h}) [6]		
$\text{SiH}_2\text{I}_2 4\text{py}$	[6]		
$\text{SiI}_2^{2+} 4\text{py}$	[6]		
$\text{SiF}_4 \cdot 2\text{py}$ (S)	Molecular Trans [6]	X-Ray	52
$\text{SiCl}_4 \cdot 2\text{py}$	Molecular Trans [6]		52
$\text{SiCl}_4 \cdot 2\text{PMe}_3^+$ (S)	Molecular Trans [6]	X-Ray	53
$\text{SiCl}_4 \cdot 2\text{PMe}_3$, $\text{SiBr}_4 \cdot 2\text{PMe}_3$	Molecular Trans Octahedral [6]	IR. R.	47/23
$\text{SiCl}_4 \cdot 2\text{py}$ (S)	[6] Molecular	IR. R.	51
$\text{SiF}_4 \cdot 2$ Pyrrolidine	[6] Molecular	IR. R.	54
$\text{SiF}_4 \cdot 2$ Piperidine			
$\text{SiF}_4 \cdot 2\text{py}$ (S)			
$\text{SiF}_4 \cdot \text{en}$			

Table 1 (Continued)

Compound	Prob. Structure/Comment	Evidence	Ref
$\text{SiF}_4 \cdot \text{dipyridyl}$	CIS chelate	^{19}F NMR	66
$\text{Me}_3\text{SiCl}/\text{bipy}$	$[\text{Me}_3\text{Si bipy}]^+\text{Cl}^-$	UV/Cond	49
$\text{Me}_2\text{SiCl}_2/\text{bipy}$	$[\text{Me}_2\text{Si 2bipy}]^{2-} 2\text{Cl}^-$		55
Soln. MeCN			57
$\text{Me}_2\text{SiCl}_2/\text{bipy}$	No complex/near non electrolyte	Cond.	56
Soln. MeCN			
$\text{Cl}_2\text{CH}_3\text{Si} - \text{SiCH}_3\text{Cl}_2$ -bipy (S)	1:1 complex molecular $[\text{6}]$ bipy co-ordinated to only one Si	NMR	58
$\text{Si}(\text{acac})_2\text{Cl}_2$ (S)	Chelated enolate. Structure uncertain.	IR/NMR	60
$\text{SiF}_6^{2-} \cdot 2\text{L}$ M = Si, Ge, Ti L = bidentate	Redistribution studies with MF_6^{2-} (Soln.)	^{19}F NMR	64
$\text{SiCl}_4 \cdot \text{SiBr}_4$	Acceptor prop. toward Me_3 and PMe_3	V.P. measurements	47 24
$\text{SiCl}_4 \cdot \text{SiBr}_4$	Acceptor properties towards py	calorimetry	67
SiCl_4 SiBr_4 SiF_4 and Ge.Sn	Acceptor properties py/isoquinoline	Calorimetry	68,69
$\text{SiF}_4 \cdot \text{benzidine}$	$[\text{6}]$ Molecular	IR/	70
$\text{SiF}_4 \cdot \text{C}_{12}\text{H}_{12}\text{N}_2$ (S)		P. X-Ray	

The work is complementary to their earlier study of the analogous tin fluoro complexes (65). Quantitative studies of the redistribution reaction between $M(\text{oxalate})_3^{2-}$ and MF_6^{2-} are reported ($M = \text{Si, Ge, Sn, Ti}$).

(2:4) FIVE CO-ORDINATE GERMANIUM

The stereochemistries five co-ordinate silicon and germanium are generally very similar. Only a very small number of five co-ordinate germanium IV complexes are known with any degree of certainty, but these include examples of neutral, cationic and anionic species. Bleidelis et al (71) have reported an X-ray study of 1-ethylgermatrane $\text{C}_8\text{GeH}_{17}\text{NO}_3$ (Fig.4). This appears to be the first such examination of a five co-ordinate germanium compound. The molecule is trigonal bipyramidal with nitrogen and carbon atoms at the apices. Vibrational spectra of $\text{GeCl}_4 \cdot \text{NMe}_3$ including both solution and orientated single crystal Raman measurements support a C_{3v} model (36,23).

Prior to 1968 the only reasonably well established five co-ordinate cation was $[\text{Ph}_3\text{Gebipy}]^+$ (72). Now the anion $[\text{GeCl}_3 \cdot 2\text{NMe}_3]^+$ (46) is known; analogous to the silicon complex mentioned earlier (46). The most likely symmetry is D_{3h} (46). Beattie et al (34) have observed that the addition of chloride ions to a solution of germanium tetrachloride in nitromethane results in the formation of the previously unknown anion GeCl_5^- . The infra-red and Raman spectra are tentatively assigned to a trigonal bipyramidal species. It is, of course, possible to obtain GeCl_5^- ions in the gas phase by bombarding the tetrahalide with low energy electrons in a mass spectrometer. Cradock et al (73) have observed GeCl_5^- together with several other anionic species, both monomeric and associated.

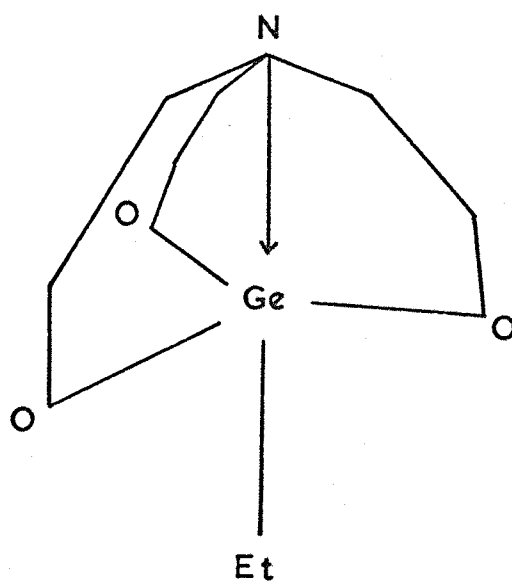


FIGURE 4 1 ETHYL GERMATRANE $C_8GeH_{17}NO_3$

(2:5) SIX-CO-ORDINATE GERMANIUM

Here again neutral, cationic and anionic species are all well known, though in much smaller numbers than for six-co-ordinate silicon. The neutral adduct $\text{GeCl}_4 \cdot 2\text{py}$ was the first of the series to be unambiguously assigned the TRANS octahedral configuration (74). Neutral CIS chelate species are also well established, e.g. $\text{GeX}_4 \cdot \text{bipy}$ (20,72) both in the solid state and in solution. Tanaka et al (55) have observed the quadripositive cation $[\text{Ge}(\text{bipy})_3]^{4+}$ in acetonitrile solution. Some control over the degree of ionization appears to be possible by using a solvent of the appropriate dielectric constant; thus conductivity measurements have indicated $[\text{GeI}_2(\text{bipy})_2]^{2+}$ and $[\text{GeI}_3(\text{terpy})]^{+}$ in nitrobenzene (72). Nazarenco et al (75) have more recently reported the cation $[\text{Ge}(\text{D.N.P.})_3]^{4+}$ (D.N.P. = dinitroprocatechol).

The anionic species GeF_6^{2-} (76) and GeCl_6^{2-} (77) as their rubidium and caesium salts were studied by X-Ray methods as early as 1940. Very recently Dean and Evans (64) have characterized anions of the types $\text{GeF}_{6-2x}\text{L}_x^{2-}$, $\text{GeF}_5\text{OR}^{2-}$, and $\text{GeF}_5\text{O}_2\text{CR}^{2-}$ in solution using ^{19}F N.M.R. spectroscopy. Beattie et al (34) have reported complete vibrational data for GeCl_6^{2-} as the caesium and tetrabutyl ammonium salts.

The vibrational spectrum of the neutral adduct $\text{GeCl}_4 \cdot 2\text{PMe}_3$ strongly suggests a TRANS octahedral structure (23). Onyszchuk et al (66) have recorded the ^{19}F N.M.R. spectra of a number of $\text{GeF}_4 \cdot 2\text{L}$ and $\text{GeF}_4 \cdot \text{L}'$ complexes (L = 6 aminohexanoic acid lactam, δ -valerolactam, 2,6 dimethyl- γ -pyrone, tetramethylurea. L' = tetramethylenediamine, $\alpha\alpha'$ -bipyridyl). The spectra of the $\text{GeF}_4 \cdot 2\text{L}$ species showed broad resonances at room temperature. On cooling, two triplets of an AX_2X_2 spectrum appeared, indicating that exchange was occurring at room temperature, and that the CIS isomer was present at lower temperatures. A single line, also present in $\text{MX}_4 \cdot 2\text{L}$ spectra, was tentatively assigned to the TRANS isomer. Spectra of $\text{MX}_4 \cdot \text{L}'$

complexes are typical of chelated CIS species at room temperature.

Both infra-red (78) and dipole moment (79) measurements have suggested CIS structures for complexes of the type $M(\text{acac})_2\text{Cl}_2$. ($M = \text{Ge}, \text{Sn}$). An early N.M.R. study of $\text{Ge}(\text{acac})_2\text{Cl}_2$ in deuteriochloroform solution gave apparently clear evidence for the CIS conformation (80). However, recent studies of the similar complexes $\text{Ge}(\text{D.P.M.})_2\text{Cl}_2$ and $\text{Ge}(\text{P.V.A.C.})_2\text{Cl}_2$ (where $\text{D.P.M.} = (\text{t-C}_4\text{H}_9)\text{COCHCO}(\text{t-C}_4\text{H}_9)^-$ and $\text{P.V.A.C.} = (\text{t-C}_4\text{H}_9)\text{COCHCOCH}_3^-$) have established the existence of both CIS and TRANS isomers (81). The spectra in benzene solution at 17°C were in close accordance with that expected of a TRANS structure. After a period of 2-5 hours at 37°C additional lines were observed, and the spectrum was attributed to an equilibrium mixture containing both the CIS (C_2) and the TRANS (D_{2h}) isomers. A reinvestigation of the N.M.R. spectrum of $\text{Ge}(\text{acac})_2\text{Cl}_2$ (81) showed the dominance of the CIS isomer, but here again additional lines were observed indicating the presence of an appreciable quantity of the TRANS molecule. Evidence is accumulating which suggests that perhaps the majority of complexes of this type exist in both isomeric forms in solution.

FIVE CO-ORDINATE TIN (See Table 3)

SIX CO-ORDINATE TIN (See Table 3)

TABLE 2

RECENT STUDIES IN FIVE AND SIX CO-ORDINATE GERMANIUM

Compounds	Structure/Comment	Evidence	Ref.
$\text{C}_8\text{GeH}_{17}\text{NO}_3$	[5] Ge. Trigonal Bipyramidal Ge — N = 2.25 Å, N-Ge-C = 176°	X-ray	71
$\text{GeCl}_4 \cdot \text{NMe}_3$ S + Soln. + Cryst.	[5] C_{3v} Neutral	IR/R	36,23
$[\text{GeCl}_3 \cdot 2\text{NMe}_3]^+$ S + Soln. ClO_4^-	D_{3h} ? [5] Cationic	IR/R	46
NR_4GeCl_5 Soln. in nitro- methane	[5] Anion GeCl_5^-	IR/R	34
GeCl_5^- (gas)	also Ge_2F_4^- and Ge_2F_8^- [5]	Mass Spec.	73
Ge.3DNP	DNP = 3,5,dinitropyrocatechol [6] Ge^{4+} Cation	Potentiometric Spectro Photo- metric	75
$\text{GeF}_{6-2x}\text{L}_x^{2-}$	CIS:TRANS Ratios [6] anions. Redistribution reaction. $\text{M}(\text{OX})_3^{2-}$ and MF_6^{2-} studied quantitatively.	^{19}F N.M.R.	64
$(\text{NR}_4)_2\text{GeCl}_6$ Cs_2GeCl_6	GeCl_6^{2-} [6] Anion O_h GeCl_6^{2-} [6] Anion O_h	IR/R	34
$\text{GeCl}_4 \cdot 2\text{PMe}_3$	[6] Neutral TRANS octahedral D_{4h}	IR/R	23
$\text{GeF}_4 2\text{L}$ (I) $\text{GeF}_4 \text{L}'$ (II)	L = Monodentate, L' = Bidentate (see text) I CIS/TRANS. II CIS	^{19}F N.M.R.	66
$\text{Ge}(\text{DPM})_2\text{Cl}_2$ $\text{Ge}(\text{PVAC})_2\text{Cl}_2$ $\text{Ge}(\text{acac})_2\text{Cl}_2$	CIS/TRANS Equilibrium Temperature Dependent	N.M.R.	81
$\text{GeX}_4 \cdot 2\text{py}$ X = F, Cl, Br	Donor Acceptor Properties	Calorimetry	68,69
$\text{GeCl}_4/\text{bipy}$	1:3 Adduct		
$(\text{CH}_3)_2\text{GeCl}_2/\text{bipy}$	1:2 Adduct Cationic (?)	U.V. Cond.	57
$(\text{CH}_3)_3\text{GeCl}/\text{bipy}$ in acetonitrile	1:1 Adduct (See also Ref. 56)		

Table 3

RECENT STUDIES IN FIVE AND SIX CO-ORDINATE TIN IV

Compound/System	Structure/Comment	Evidence	Ref.
$\text{Me}_2\text{SnCl}(\text{S}_2\text{CNMe}_2)$ (dmdtc) (S)	Distorted trig.bipyramidal. Two Me Groups in Equatorial Position [5]	X-Ray	82
$\text{MeSnCl}(\text{S}_2\text{CNMe}_2)$		N.M.R.	83
$\text{Me}_2\text{SnCl}(\text{S}.\text{SeCNMe}_2)$ S and Soln.	Trig. Bipyramidal [5]	IR	84
$\text{R}_4\text{N}^+\text{SnCl}_5^-$ $\text{R}_4\text{N}^+\text{SnBr}_5^-$ (S) Methylene chloride soln.	R_4M = Tri-p-tolyl R_4N = Di-p-tolylphenyl Monomeric Trig.Bipyramidal [5]	X-Ray IR Mössbauer	85
$\text{Bu}_4\text{N}^+\text{SnCl}_5^-$ (Soln) MeNO_2	Partial Data. Tentative Assignment [5]	IR	34
$\text{R}^1.\text{Ph}.\text{R}.\text{SnClDMSO}$	1:1 [5]	N.M.R.	86
Me_2SnXL X = Cl, Br, I. L = Tropolone	Trigonal Bipyramidal [5] Two methyl groups probably equatorial	IR N.M.R.	87
SnX_4 FAN SnX_4 DMAF	DMAF = N,N,dimethylaminomethyl -ferrocene FAN = Ferroceneacetonitrile M-X, M-N stretching vibration assigned [5]	IR	88
$\text{SnCl}_4.\text{P}(\text{Ph})_3$	[5] Molecular monomer	IR	89
$\text{SnCl}_4.2\text{MeCN}$	Molecular CIS Octahedral [6]	X-Ray ^I IR/R	90
$\text{SnX}_4.2\text{L}$	X = Cl, Br, I. L = MeCN, PhCN, DMF, 2,2dipyridyl - Earlier assignments reversed for Sn-Cl Sn-N	IR	21
$\text{SnCl}_4.2\text{MeCN}$ ($\text{SnCl}_4.3\text{MeCN}$)	Several other adducts / MeCN co-ord. via N	IR/R X-Ray (P)	91
$\text{SnCl}_4.2\text{L}$	10 complexes. L = alkyl/aryl- phosphine. Molecular TRANS	IR/R Mössbauer	92

Table 3 (Continued)

Compound/System	Structure/Comment	Evidence	Ref.
$\text{SnCl}_4 \cdot 2\text{Me}_2\text{SeO}$	Prob. CIS Molecular. Co-ord. via oxygen. Co-ordination power comparable to Me_2SO	IR	93
$\text{SnX}_4 \cdot 2\text{L}$ $(\text{Bu}_3\text{P})\text{SnCl}_4$	L = variety ligands. O,N,S,P Donor atoms. 25 complexes. Q.S. Q.S. 1mm/sec. Prob. Trans	Mössbauer	94
$\text{SnCl}_4 \cdot 2\text{PMe}_3$	Molecular TRANS	IR/R	23
$\text{SnX}_4 \cdot 2\text{L}$	L = $\text{P}(\text{Ph})_3$, $\text{As}(\text{Ph})_3$ Tentative Assign. Sn-P	IR	89
$\text{SnX}_4 \cdot 2\text{L}$	X = F, Cl, Br, I. L = PMe_3O , NMe_3O . NMe_3O better donor than both PMe_3O and Py N oxide	IR	95
$\text{SnCl}_4 \cdot 2\text{py}$ $\text{SnBr}_4 \cdot 2\text{py}$	Molecular TRANS Octahedral	X-Ray	96
$\text{SnF}_4 \cdot 2\text{L}$	L = 4 substituted pyridine 1-6oxides and 4 substituted quinoline 1 - 6oxides	IR	97
$\text{SnCl}_4 \cdot 2\text{L}$	L = py and isoquinoline. Donor Acceptor strengths relative to $\text{MX}_4 \cdot 2\text{L}$ (M = Si, Ge)	Cal.	68 69
$\text{SnCl}_4 \cdot 2\text{py}$	CIS Molecular ?	IR	98
$\text{SnI}_4 \cdot 2\text{L}$ $\text{SnI}_4 \cdot \text{L}'$	L = NMe_3 , py, Ph_3PO L' = TMEN, bipy, 1,10, Phen	IR Mössbauer	99
$\text{SnCl}_4 \cdot 2\text{POCl}_3$ $\text{SnCl}_4 \cdot \text{PSCl}_3$ $\text{SnCl}_4 \cdot 2\text{EtOH}$ $\text{SnCl}_4 \cdot 2\text{EtO}$ $\text{SnCl}_4 \cdot (\text{CH}_2\text{OMe})_2$ $\text{SnCl}_4 \cdot (\text{CH}_2\text{CH}_2\text{OMe})_2$	CIS No Complex CIS TRANS TRANS TRANS	N.Q.R.	100
$\text{SnCl}_4 \cdot 2\text{POCl}_3$	Assignment M-Cl vibrations via known crystal structure.	N.Q.R.	101

Table 3 (Continued)

Compound/System	Structure/Comment	Evidence	Ref
$\text{SnCl}_4 \cdot 2\text{L}$	Molecular $\left[6\right]$. L = Aliphatic Alcos. and Esters	Mössbauer	102
$\text{SnCl}_4 \cdot 2\text{L}$	Molecular $\left[6\right]$. L = Several Aromatics	Mössbauer	103
$\text{SnCl}_4 \cdot 2\text{L}$	L = Oxygen donors	Mössbauer	104
$\text{SnCl}_4 \cdot 2\text{COCl}_2$ (liq)	COCl_2 very weak base	IR	105
$\text{SnX}_4 \cdot 2\text{L}$	X = Cl, Br. L = Aromatic Aldehyde	Cond. DM	106
		IR Cal.	107
$\text{Me}_2\text{SnCl}_2(\text{py-N-oxide})$ S	Mössbauer spectra in powerful magnetic field. Quadrupole interaction negative.	Mössbauer	108
$\text{R}_2\text{SnX}_2\text{L}_2$	R = Ph. X = Cl, Br, I. L = py, $\frac{1}{2}\text{bipy}$, $\frac{1}{2}\text{dipyam}$, $\frac{1}{2}\text{tripyam}$. R = Et, X = Cl, Br. L = $\frac{1}{2}\text{dipyam}$, $\frac{1}{2}\text{tripyam}$ TRANS Organo groups	Mössbauer	109
$\text{Ph}_2\text{SnX}_2\text{py}_2$	CIS Halogeno by Mössbauer		110
Alkyl and Aryl-Tin IV complexes (Large number)	Q.S. and nature of Sn ligand bond. Q.S. data for large number of trig.bipyramidal, Cis and Trans octahedral complexes of known structure.	Mössbauer	111
$(\text{Et}_4\text{N}^+)_2\text{SnX}_6^{2-}$ $(\text{Et}_4\text{N}^+)_2\text{SnX}_4\text{Y}_2^{2-}$	Linear relationship between isomer shift and the sum of the (Mullikan) Electronegativities.	Mössbauer	112
Me_2SnCl_2 Me_2SnF_2	Associated/near octahedral $\left[6\right]$ Associated/octahedral $\left[6\right]$	X-Ray Mössbauer	113
$\text{Me}_2\text{SnCl}_2 \cdot 2\text{DMSO}$	CIS-dichloro-Cis-Bis(dimethylsulph oxide)TRANS-dimethyl tin IV	X-Ray	114
$(\text{Me})_2(\text{C}_5\text{H}_5\text{NO})_2\text{SnCl}_2$	Dichlorodimethylbis(pyridine-n-oxide)tin IV. Symmetrical	X-Ray	115
$\text{Me}_2\text{SnX}_2 \cdot 2\text{py}$ $\text{Et}_2\text{SnCl}_2 \cdot 2\text{py}$	X = Cl, Br, I. Octahedral TRANS alkyl, CIS halogen	IR	98
$\text{Et}_n\text{SnCl}_{4-n}/\text{py}$	$\left[6\right]$	PMR IR/R	116 132

Table 3 (Continued)

Compound/System	Structure/Comment	Evidence	Ref.
$R_2SnCl_2 \cdot 2L$	L = dimethylselenoxide		
$Me_2SnBr_2 \cdot 2L$	Me_2SeO Co-ord. via. Oxygen TRANS Alkyl. CIS Halogen	IR	93
$Ph_3SnCl_3 \cdot 2L$	L = Variety N (amine) donors some species probably ionic	Cond. IR	117
$Ph_3SnCl \cdot L$	L = Variety oxygen donors I.S. and Q.S. data	M	118
$Me_3SnCl \cdot L$	L = Variety donors incl. py [5] I.S. and Q.S. data		136
$(CH_3)_2Sn(DMDTC)_2$	DMDTC = dimethyldithiocarbamate Distorted TRANS octahedral	IR N.M.R.	83
$Ph_2Sn \left[\begin{array}{c} \diagup S_2CNR_2 \diagdown \\ \diagdown S_2CNR_2 \diagup \end{array} \right]_2$	CIS Octahedral	*	
$R_2'Sn \left[\begin{array}{c} \diagup S_2CNR''_2 \diagdown \\ \diagdown S_2CNR''_2 \diagup \end{array} \right]_2$	TRANS Octahedral	Mössbauer	119
$R_2Sn \cdot 2L$	CIS Octahedral	*	
$R_2SnX_2 \cdot L$	TRANS Octahedral L = bidentate - oxin, acac bipy, phen	Mössbauer	120
$R_2Sn(D.M.DS.C)$	D.M.DS.C. = dimethyldiseleno- carbamate (R = Me, Et) chelated co-ordinating power Se \approx S	IR PMR	121
$Sn(acac)_2Cl_2$ $Sn(oxim)_2Cl_2$ $Sn(oxim)_2(Cl_3CCO_2)_2$	Identical Mössbauer Spectra	Mössbauer	122
$Ph_2Sn(acac)_2$ (Soln)			
$XX'Sn(acac)_2$ (Soln. CCl_3)			
$SnX_2(2-SpyO)_2$	X = F, Cl, Br, I. Prob. CIS X	Mössbauer	
$R_2Sn(2-SpyO)_2$	R = Ph, Bu. Prob. TRANS R (2-SpyO) = 2-pyridinethiol-1-oxide	IR DM	125
$R_2Sn(salem)$	salem. quadridentate schiff base NN'-ethylenebis(salicylalimine) R Groups CIS by N.M.R.	IR NMR Mass.Spec. Cond	126

* See Chapter 3.

Table 3 (Continued)

Compound/System	Structure/Comment	Evidence	Ref.
$\text{Me}_2\text{Sn L}_2^*$	L = tropolone	IR	
$\text{R}_2\text{SnX L}_2$	R = alkyl phenyl. X = Cl, Br, I	NMR	87
SnX_2L_2	*Highly distorted octahedral		
$\text{R}_n\text{SnX}_{4-n}\cdot\text{L}$	L = 2,2,bipy, 1-10 phen. R = Me, Et, Bu, X = Cl, Br, I Several M-L fundamentals assigned	IR	127
$\text{R}_2\text{SnX}_3\text{L}$ (a)	R = Ph, Bu, X = Cl, NCS	Mössbauer	
$\text{R}_2\text{SnXL}'_2$ (b)	L = $\alpha\alpha'$ -dipyridyl, o-phen, 8-aminoquinoline, L' = oxinate, (2-SpyO) a) Two X groups TRANS b) R and X are CIS	IR DM	128
a) $\text{SnY}_2(\text{OXH})_2$ b) $\text{SnY}_2\text{SALH}_2$ c) $\text{SnCl}_{4-n}\text{OX}_n$ d) $\text{SnX}_4\cdot 2\text{OXH}$ e) $\text{SnX}_4\cdot 2\text{SALH}$	OXH = 8-hydroxyquinoline SALH = salicylaldehyde Y = halogen, alkyl, aryl. a) Carbons Prob. CIS d) Oxygens Prob. CIS e) Prob. TRANS	Mössbauer	129
$\text{SnCl}_4\text{NC}(\text{CH}_2)_3\text{CN}$	Tin IV chloride glutaronitrile one-dimensional polymer with glut. acting as a bridging ligand between SnCl_4 units. Octahedral with nitrogen atom CIS.	X-Ray	130
$\text{SnCl}_4\cdot\text{L}$ S and Soln	L = 1,2,ethylene bis diphenyl phosphine, and 1,4,butylenebisdiphenylphosphine and arsine analogues. 1:1 molecular octahedral.	Cond IR	131
$\text{SnF}_{6-n}\text{X}_n^{2-}$ Soln.	Approx. 100 anions. X = wide range unidentate or half bidentate ligand. (See Chapter 3)	N.M.R.	65
$(\text{Et}_4\text{N})_2\text{SnCl}_6$ Soln. MeNO_2	SnCl_6^{2-}	IR	34
$(\text{CH}_3)_2\text{SnX}_4^{2-}$	$\text{X}^- = \text{F}^-, \text{Cl}^-, \text{Br}^-, \text{NCS}^-$ NCS co-ord. via N TRANS octahedral	IR, R (PMR)	133

TABLE 3 (Continued)

Compound/System	Structure/Comment	Evidence	Ref.
$[(\text{Et})_4\text{N}]_2\text{SnX}_4\text{Y}_2$ (S)	SnX_4Y_2^- X = Cl, Br, I. Y = F, Cl, Br, I. Shifts related to Mulliken Electronegativities	Mössbauer	134
$((\text{Me})_4\text{N})_2\text{SnX}_4\text{Y}_2$	SnCl_6^{2-} , SnBr_6^{2-} , SnI_6^{2-} , $\text{SnCl}_4\text{Br}_2^{2-}$, $\text{SnCl}_2\text{Br}_4^{2-}$, $\text{SnCl}_2\text{I}_4^{2-}$, $\text{SnBr}_2\text{I}_4^{2-}$ Shifts related to Pauling Electronegativities. $\text{SnBr}_4\text{I}_2^-$ and $\text{SnCl}_4\text{I}_2^-$ Iodines may be CIS.	IR Mössbauer	135 112

CHAPTER 3

THE APPLICATION OF SPECTROSCOPIC TECHNIQUES TO PROBLEMS

OF CIS-TRANS ISOMERISM IN GROUP IV B

THE APPLICATION OF SPECTROSCOPIC TECHNIQUES TO PROBLEMS
OF CIS-TRANS ISOMERISM IN GROUP IV B

(3:1) The most powerful methods available for determining the molecular structures of Group IV B co-ordination compounds in the solid state are those of X-ray diffraction, vibrational spectroscopy and Mössbauer spectroscopy. Nuclear magnetic resonance spectroscopy (N.M.R.), nuclear quadrupole resonance spectroscopy (N.Q.R.) and vibrational spectroscopy are particularly rewarding when applied to the liquid and solution states. In the vapour phase, electron diffraction and vibrational spectroscopy are the most useful. X-ray diffraction techniques are definitive. Their use, however, is usually confined to crystalline solids. Since a large part of this thesis is concerned with the use of X-ray diffraction methods to differentiate between the CIS and TRANS isomers of octahedral molecules, it is appropriate to discuss briefly the ways in which spectroscopic methods may be used to approach the same problem. This is demonstrated with reference to a few selected examples.

(3:2) VIBRATIONAL SPECTROSCOPY

The terms 'slow' and 'fast' are often used to describe the time scales of the various spectroscopic methods. Such descriptions cannot be applied in the same sense to diffraction techniques because of the time averaging which is involved. X-ray data may be used to define the mean position of the atoms in a molecule; directly they yield little information about the atomic vibrations. Vibrational spectroscopy is considered to be an extremely 'fast' technique in that few kinetic processes normally occurring in molecules are too fast for it to follow. The time scale involved is in the order of 10^{-13} secs. Compared to this even the N.M.R. experiment is 'slow', (10^{-1} - 10^{-9} secs).

Infra-red and Raman techniques yield complementary information about molecules. Until only a few years ago, however, Raman spectroscopy had only very limited applications, particularly for solids, mainly because of the extreme feebleness of the effect. With the advent of lasers as sources of exciting energy the situation completely changed, and Raman spectra, even of coloured compounds, may now be obtained so conveniently that the technique is used in a routine fashion for identification and diagnostic purposes.

In the sodium chloride region infra-red spectroscopy has been applied most fruitfully to the fields of organic and organometallic chemistry, usually to obtain information about the number and type of functional groups present. However, most metal-ligand vibrations of interest to the structural inorganic chemist lie at very much lower frequencies, and this has led to the development of highly sophisticated instrumentation capable of high resolution in the $30\text{--}400\text{ cm}^{-1}$ range. The introduction of instruments such as the Beckman I.R.11 infra-red spectrometer, the Cary 81 and Spex Raman spectrometers has given access to virtually the complete vibrational spectrum of many molecules.

In favourable cases in which the molecular vibrations are relatively 'pure', a detailed study of the infra-red and Raman fundamental modes, their coincidences, and in the solution state of their depolarization ratios, may enable the stereochemistries of quite complex molecules to be decided. The techniques have been used extensively, with varying degrees of success, to differentiate between the CIS and TRANS isomers of many octahedral complexes. The following examples will show how such problems have been approached with respect to Group IV B.

Beattie et al (20) have shown that instead of referring to the entire spectrum, the symmetry of an octahedral molecule may be studied from the point of view of the radically altered acceptor skeleton. If

discrete octahedral species are assumed, it is then required to differentiate between the two MX_4 configurations shown in Fig.5. Of the numerous tetrahalide complexes studied using this approach, those formed with pyridine and with trimethylamine have been extensively examined, and are used here as examples.

Assuming that the M-L force constant is small, it is feasible to regard the TRANS complex simply as a perturbed square planar unit, and the CIS complex as the distorted tetrahedral entity shown in Fig.5. Reference to the character tables allows us to predict the number and activities of the fundamental vibrational modes expected for the MX_4 unit in these configurations.

TETRAHEDRAL MX_4

The MX_4 molecule of symmetry (T_d) has $3n - 6 = 9$ normal vibrational modes, four of which are observed as separate frequencies (f_2 symmetry vibrations are triply degenerate).

$$a_1(\nu_1) + e(\nu_2) + 2f_2(\nu_3 \text{ and } \nu_4)$$

All are Raman active but only ν_3 and ν_4 are infra-red active. For the Group IV tetrahalides (except, of course, for polymeric species) these frequencies have been comprehensively reported (137).

SQUARE PLANAR MX_4 'TRANS'

The square planar model of symmetry (D_{4h}) has nine normal modes. These can be divided into the following symmetry classes, the e_u modes being doubly degenerate:

$$a_{1g}(\nu_1) + a_{2u}(\nu_2) + b_{1g}(\nu_3) + b_{1u}(\nu_4) + b_{2g}(\nu_5) + 2e_u(\nu_6 \text{ and } \nu_7)$$

The molecule is centrosymmetric so that the exclusion rule is operative; no Raman active vibration is therefore also infra-red active, and no infra-red active mode is also Raman active. Thus ν_2 , ν_6 , ν_7 are infra-red active, ν_1 , ν_4 and ν_5 are Raman active. ν_3 is inactive.

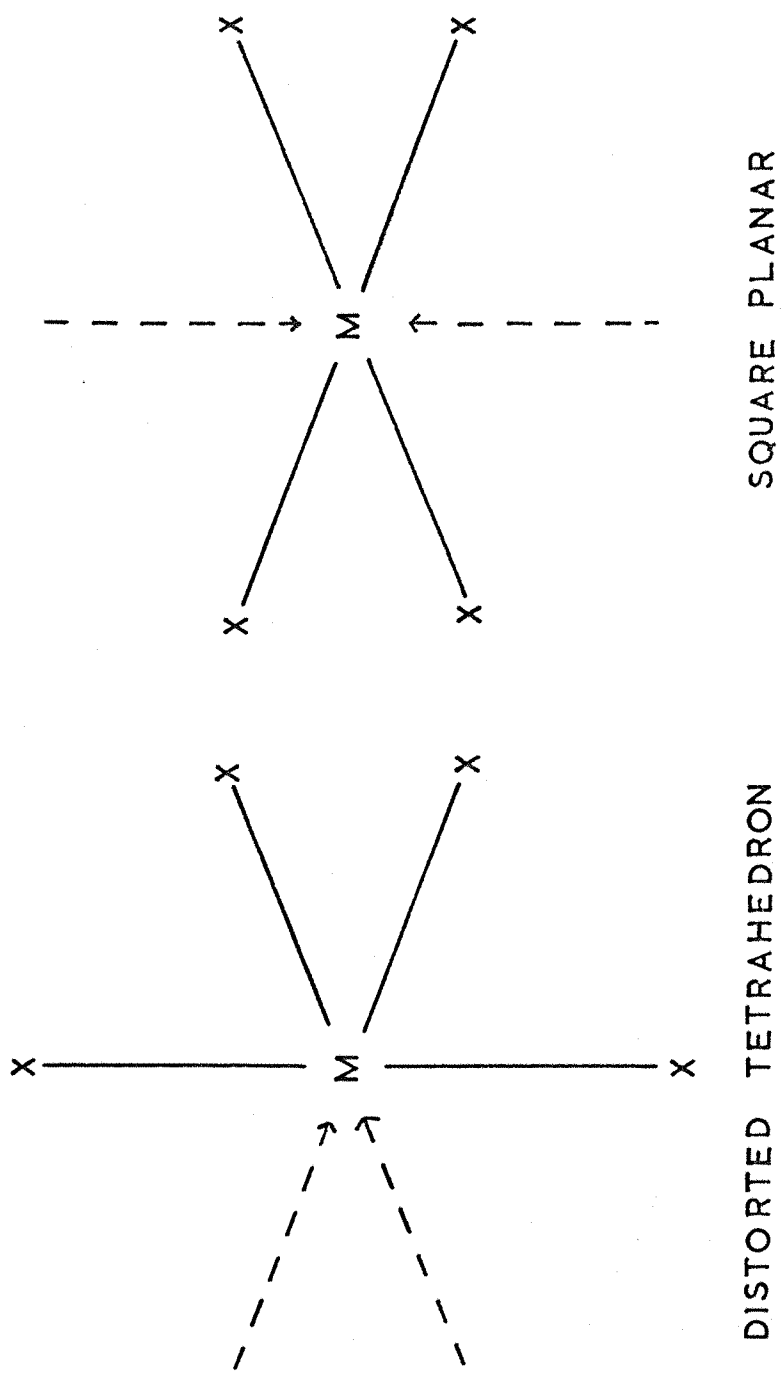


FIGURE 5 CONFIGURATION OF MX_4 RESIDUES FOR CIS & TRANS ISOMERS

MX₄ - 'CIS'

The 'distorted tetrahedral' CIS MX₄ residue has C_{2v} symmetry and has nine fundamental vibrational modes, none of which are degenerate:

$$4a_1 + a_2 + 2b_1 + 2b_2$$

These are all Raman active and all but the a₂ species are infra-red active. Another way of arriving at the same result is to consider the effect of decreasing the symmetry of the tetrahedral MX₄ acceptor from T_d → C_{2v} (138,50). When this happens as a result of co-ordination the doubly degenerate e_u, and triply degenerate f₂ vibrations are resolved as follows:

<u>SYMMETRY T_d</u>		<u>SYMMETRY C_{2v}</u>
a ₁ (R)		a ₁ (IR) (R)
e (R)	→	a ₁ (IR) (R) + a ₂ (R)
f ₂ (IR) (R)		a ₁ + b ₁ + b ₂ (IR) (R)

OCTAHEDRAL MX₆²⁻

The octahedral MX₆²⁻ ion has (O_h) symmetry. Of the fifteen normal modes six are individual frequencies, since e_g is doubly degenerate, and each of the f type vibrations is triply degenerate. They belong to the following species:

$$a_{1g}(\nu_1) + e_g(\nu_2) + 2f_{1u}(\nu_3, \nu_4) + f_{2g}(\nu_5) + f_{2u}(\nu_6)$$

ν₃ and ν₄ are infra-red active; ν₁, ν₂ and ν₅ are Raman active and ν₆ is inactive.

For the CIS and TRANS conformations we have to decide which are metal-halogen stretching vibrations, where they are likely to occur, and how many there will be for each species. Two vibrations in the tetrahedral molecule may be considered to be essentially stretching modes (ν₁, ν₃). The octahedral MX₆²⁻ ion also has two metal-halogen stretching vibrations (ν₁ and ν₃). Experimentally it is found that in both the above species,

and in $\text{MX}_4 \cdot 2\text{L}$ complexes, these stretching frequencies occur in approximately the same region. Now, as shown above, the a_1 and f type stretching modes of the tetrahedral MX_4 model, when resolved, give four frequencies, all of which are both infra-red and Raman active. Strictly speaking this is true only for small distortions of tetrahedral symmetry, whereas in practice the distortion ($T_d \longrightarrow C_{2v}$) is considerable. Observations of other molecules (139,28) have shown that only three well defined high frequency stretching vibrations are found experimentally. By taking into account the weakening of the metal-halogen bond on co-ordination, Beattie et al (50) predicted that one of the expected four vibrations should occur at a markedly lower frequency. They also pointed out that this fourth vibration should be relatively weak in the infra-red. Thus three infra-red and Raman active high frequency modes are expected for, for example, CIS $\text{MX}_4 \cdot 2\text{L}$. For $\text{SiCl}_4 \cdot 2\text{py}$ (50) these are expected to occur around 500 cm^{-1} . The single low intensity vibration is expected around 320 cm^{-1} .

Calculations (50,140) have shown that of the nine normal modes of the TRANS MX_4 entity, only the e_u and a_{2u} types (both infra-red active) are likely to appear in the same region as the set of three absorptions mentioned for the CIS adduct. If, however, the metal-ligand force constant is small compared to the metal-halogen value then the a_{2u} vibration will occur at a significantly lower frequency. Thus in the metal-halogen stretching region, and in the absence of complicating effects, the infra-red spectrum of the two isomers should be very different, (TRANS 2 bands, CIS 3 bands) and in principal it is possible to distinguish between them.

Unfortunately, there are in practice numerous pitfalls associated with this simple approach, the effect and importance of which have recently been underlined (51). Perhaps the most frequently encountered in the solid state are crystal field effects, which may resolve degenerate vibrations.

Thus in a crystalline $\text{MX}_4 \cdot 2\text{L}$ TRANS complex, crystal field resolution of the doubly degenerate e_u mode would result in the appearance of two bands. The simultaneous appearance of such an effect, together with a relatively high frequency a_{2u} vibration, could give a spectrum similar to that expected for a CIS adduct. A good example of crystal field splitting is provided by symmetrical SiF_6^{2-} , where the triply degenerate f_{1u} fundamental is resolved into two separate bands in the crystalline compound BaSiF_6 (20). In the regular octahedron found in the potassium and ammonium salts this splitting is not observed (20). Fermi resonance (141) may make a combination band sufficiently intense to be mistaken as a fundamental. Furthermore, an extremely weak fundamental might escape detection. If such a band had been predicted from group theoretical considerations, it is not difficult to imagine a situation in which the spectra could be misinterpreted. The possibility of accidental degeneracies should not be ruled out, nor should the possibility that bands lying close to one another might remain unresolved.

With the advent of modern computing techniques (142,143) vibrational analyses of fairly complicated molecules are now possible. As a rule, force constants are transferred from simple related molecules of high symmetry whose structure and vibrational parameters are firmly established. Although a highly suspect procedure on theoretical grounds, and necessitating the (arbitrary) assumption that many of the interaction terms are zero, useful results are obtained which give a semi-quantitative picture as to the nature of the normal modes. The normal co-ordinate analysis carried out by Beattie, Webster and Chantry (140) on CIS and TRANS $\text{MX}_4 \cdot 2\text{L}$ is an obvious example. By making reasonable assumptions about the magnitude of force constants, and by comparing observed and calculated spectra, Beattie and Rule were able to unambiguously assign the TRANS structure to complexes of the type $\text{MCl}_4 \cdot 2\text{NMe}_3$ ($\text{M} = \text{Si, Ge, Ti, Sn}$) (144).

The difficulties involved in interpreting vibrational spectra in the presence of interfering effects are clearly demonstrated by the work of Beattie, Gilson and Ozin (51) on the virtually insoluble complex $\text{SiCl}_4 \cdot 2\text{py}$ and species related to it. Their initial work (144) indicated a CIS stereochemistry for $\text{SiCl}_4 \cdot 2\text{py}$; an incorrect assignment being made on the grounds of inadequate data. X-ray analysis (52) subsequently showed the structure to be TRANS. In the light of this result a more rigorous spectroscopic study was carried out (51). The first problem which had to be overcome in this work was to unambiguously assign a metal-nitrogen stretching vibration in order to obtain a reasonable force constant. This they were able to do from detailed vibrational analyses of $\text{SnCl}_4 \cdot 2\text{NMe}_3$ and $\text{SnCl}_4 \cdot 2\text{N}(\text{CD}_3)_3$. By applying the force constant obtained for the tin-nitrogen bond to $\text{SiCl}_4 \cdot 2\text{py}$ they found it possible to make meaningful comparisons between the observed and calculated ($\text{SiCl}_4 \cdot 2\text{py}$) spectra. An inspection of the silicon-chlorine stretching region ($\approx 500 \text{ cm}^{-1}$) showed that the calculated infra-red spectrum contained bands due to splitting of the e_u vibration, a mixed mode due to a combination of Si-N and Si-Cl frequencies, and a ligand mode. The other bands correspond to the ones they had previously allocated to the silicon-chlorine stretching vibrations of a CIS adduct (50). The single intense Raman band at 324 cm^{-1} provided little help in resolving this ambiguity, since a similar band, thought to be an ~~axial~~ ^{LINEAR} SiCl_2 symmetric stretching mode, is present in the spectrum of CIS $\text{SiCl}_4 \cdot \text{bipy}$. The authors point out that even though they were able to obtain excellent experimental and computed data for $\text{SiCl}_4 \cdot 2\text{py}$, they found it impossible to decide on a CIS or TRANS structure on the basis of vibrational data alone. The absence of solution data obviously made the problem a particularly difficult one. However, even when such data are available a complete and unambiguous assignment is by no means certain, as is demonstrated by the amount of discordant work on $\text{SnCl}_4 \cdot 2\text{MeCN}$. (See Ref. 90 and references therein).

(3:3) NUCLEAR MAGNETIC RESONANCE SPECTROSCOPY

The circulating charges associated with atomic nuclei having inherent spin give rise to magnetic moments. Whenever a molecule contains magnetic nuclei, for example ^1H , ^{19}F , ^{31}P , ^{11}B , etc. the nuclear magnetic resonance spectrum may give valuable information about its structure. Compared to vibrational spectroscopy the N.M.R. experiment is rather slow (10^{-1} - 10^{-9} secs) and it is important to interpret data with reference to the appropriate time scale, since the rate of exchange in many molecules is of the same order.

Three distinct parameters may contribute directly towards the solution of a structural problem; the position of the resonances (the chemical shifts), their intensities, and the fine structure due to 'spin-spin splitting'. The latter effect can result from both like and unlike nuclei provided only that both species possess a magnetic moment.

The non-magnetic nature of ^{12}C and ^{16}O results in the simplification of the spectra of organic molecules, so that full use may be made of the intense N.M.R. signal produced by the hydrogen nuclei. Furthermore, organic compounds are frequently liquids or solids easily soluble in non-polar solvents and are thus a particularly rewarding field of study. On the other hand, inorganic compounds are often solids of low solubility, and those containing nuclei which have a nuclear spin $I = \frac{1}{2}$ with a zero quadrupole moment are in the minority. Those nuclei with spin $(I) \gg 1$ possessing quadrupole moments produce spectra having characteristically large line widths. Organometallics offer, in general, an ideal group of compounds for study by N.M.R., since if not liquids they are frequently soluble in organic solvents. An additional advantage is that if the metal nucleus has a magnetic moment, spin-spin coupling to nuclei in attached groups may be observed. The majority of stereochemical studies of inorganic compounds involving high resolution N.M.R. measurements have

been made either in the vapour, liquid or solution states, with ^1H and ^{19}F the most frequently studied nuclei. A substantial quantity of inorganic N.M.R. work has now been published, and its application to inorganic stereochemistry in general has been reviewed by White (145). Many authors have discussed in detail the analysis of N.M.R. spectra and much of this work has been summarized by Emsley et al (146) (1965).

The technique has proved particularly useful in establishing the structures of the hydrides (where X-ray diffraction methods are strictly limited) since the situation in which an H is bonded directly to a metal is characterized by particularly large chemical shifts ($\delta \approx 30$). The chelated complex $\text{RuHCl}[\text{Et}_2\text{P}(\text{Cl})_2\text{CH}_2\text{PEt}_2]_2$ is a good example (147) ($\delta = 31.8$). The same complex (147) offers a classical example of the way in which N.M.R. spectroscopy may be used to distinguish between CIS and TRANS isomers (Fig.6). In general, nuclei of spin $I = \frac{1}{2}$ show spin-spin splitting with (n) neighbouring nuclei (of identical coupling constant J) to produce a resonance split into $n + 1$ peaks with intensities following binomial coefficients. Similar effects result from interaction with nuclei having spin I greater than $\frac{1}{2}$. For a nucleus of spin $I = 1$ there are three equally probable orientations for the precessing nucleus and interaction with a second nucleus will show a signal having three lines of equal intensity. The magnitude of the coupling constant J depends on the proximity of the interacting nuclei and the nature of the bonds connecting them. Thus interaction with chemically identical, but magnetically non-equivalent species, results in different splitting patterns and coupling constants. The relevance of magnetic non equivalence to high resolution N.M.R. has been discussed by Van Gorkam and Hall (148). Two otherwise identical atoms are chemically non equivalent if they are unrelated by a molecular symmetry axis. Nuclei which produce identical chemical shifts must experience equal magnetic environments and are termed isochronous (148,149,150). Chemically equivalent nuclei are isochronous, but the

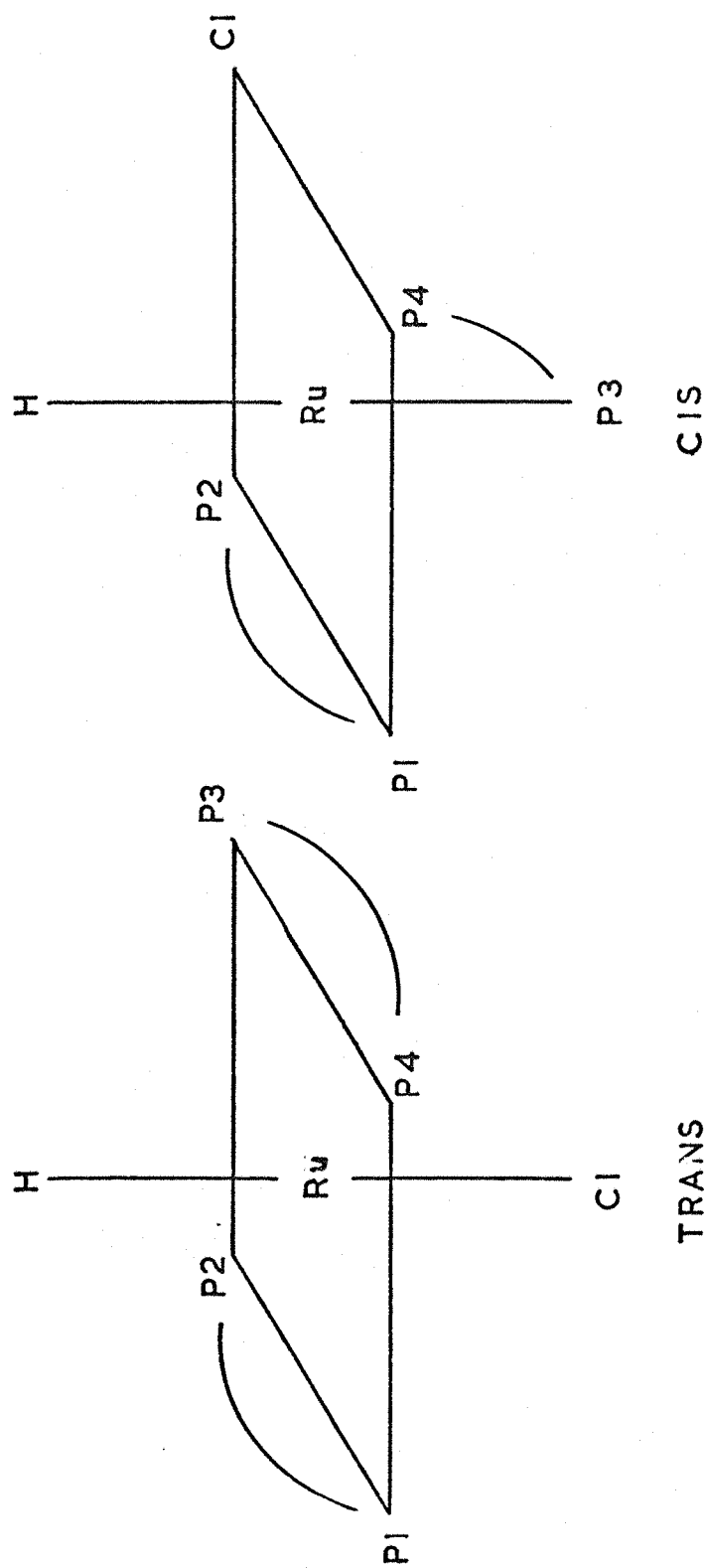


FIGURE 6 CIS AND TRANS $\text{RuHCl}[\text{Et}_2\text{P}(\text{CH}_2\text{CH}_2\text{PEt}_2)_2]_2$

reverse is not always true. For nuclei to be magnetically equivalent with respect to the N.M.R. experiment they must be both isochronous and display identical coupling constants to any other magnetically active nucleus.

Consider the ruthenium complex mentioned above. Both CIS and TRANS conformations are possible and in each case a very different spectrum is expected (147). The two forms are distinguishable since in the TRANS model all four ^{31}P nuclei are magnetically equivalent. This is not true of the CIS complex. In the TRANS isomer the hydrido nucleus shows spin-spin coupling to all four magnetically equivalent ^{31}P nuclei, ($I = \frac{1}{2}$) giving rise to a symmetrical quintet set of signals of predictable relative intensity. In the case of the CIS form however, coupling occurs between three distinct groups of ^{31}P nuclei, one containing P_2 and P_4 , the others P_1 and P_3 . The first pair will produce a triplet, while coupling with the other two will each give rise to doublets. The resulting triplet spectrum, exhibiting a more complex spin-spin splitting pattern, is therefore very different from that of the TRANS model. Experimentally, Chatt and Hayter (147) observed only the simple (quintet) spectrum showing that $\text{RuHCl}[\text{Et}_2\text{PCH}_2\text{CH}_2\text{PEt}_2]_2$ is in fact TRANS.

N.M.R. studies of many Group IV B complexes are restricted by their marginally favourable nuclear properties, suitable isotopes being low in natural abundance and sensitivity. The majority of stereochemical information has therefore been obtained almost exclusively from ^1H and ^{19}F spectra. Of particular relevance to the type of complex described in this thesis is the work of Muettert et al. (151) and of Ragsdale and Stewart (7) on the stereochemistry of complexes based on the metal tetrafluorides ($\text{M} = \text{Si}, \text{Ge}, \text{Sn}, \text{Ti}$). The work of Dean and Evans (65) on the ^{19}F N.M.R. of anions of the general type $\text{SnF}_{6-n}\text{L}_n^{2-}$ is also particularly noteworthy.

The earlier of these studies (151) gave fairly conclusive

evidence for octahedral symmetry in complexes of the type $\text{MF}_4 \cdot 2\text{L}$ and $\text{MF}_4\text{L}'$. ($\text{M} = \text{Sn}, \text{Ti}$, $\text{L} = \text{monodentate}$, $\text{L}' = \text{bidentate}$). At temperatures within a range $+15^\circ\text{C}$ to the freezing point of the solvent, the spectra consisted of two resonances of equal intensity, each of which was split into triplets. This is consistent with two types of fluorine environment having equivalent populations, and was therefore interpreted as resulting entirely from the CIS complex. The spectra were found to be temperature dependent; the fine structure being lost on warming the solution. This was interpreted as being due to an exchange process (order of magnitude 10^{-3} sec at $0 \pm 30^\circ\text{C}$) involving the base molecules. The ^{19}F spectra of SiF_4 and GeF_4 complexes (151) consisted of only a single resonance, superficially indicating a TRANS structure. However, such a spectrum would also result from fast ligand exchange, and the authors were therefore unable to make an unambiguous assignment. In contrast to this work, however, Ragsdale and Stewart (7) found unambiguous evidence for a CIS-TRANS equilibrium in the system $\text{SnF}_4 \cdot 2\text{EtOH}/\text{EtOH}$. A complex multiplet containing six lines they assigned to the CIS complex since the observed intensities agreed well with that predicted for an A_2B_2 spectrum. A separate single resonance they assigned to the TRANS complex. At -50°C the concentrations of the CIS and TRANS forms were found to be the same. The concentration of the TRANS isomer was found to decrease continuously on warming until at room temperature the CIS isomer predominated.

In their elegant ^{19}F N.M.R. study Dean and Evans (65) examined approximately one hundred anions of the general type $\text{SnF}_{6-n}\text{X}_n^{2-}$, where X represents a wide range of unidentate or half a bidentate ligand. For many of these species CIS/TRANS ratios are reported. Most extensively reported are ions of the type $\text{SnF}_4\text{X}_2^{2-}$. In general such systems are particularly amenable to study by ^{19}F N.M.R. spectroscopy, since fluorine exchange is normally slow on the N.M.R. time scale, and the complexes may

be studied in labile equilibrium. In addition, tin has two relatively abundant isotopes with spin $I = \frac{1}{2}$. (^{117}Sn 7.61% and ^{119}Sn 8.58%). The spin-spin splitting due to interaction between these nuclei and ^{19}F acted as a useful interpretative aid. Species present in solution were identified by the order of the appearance of the resonance lines as ionic concentrations were varied, and by the fine structure observed on the lines. The equilibrium constants for CIS and TRANS redistributions involving ligands such as NCO , Cl , Br , I , CF_3COO , MeCOO and $\text{Me}_3\text{C.COO}$, are particularly interesting. The equilibrium constant is a measure of the ease of replacing a fluorine in $\text{SnF}_5\text{X}^{2-}$ by X , compared to a similar replacement in SnF_6^{2-} . The results show that for the halogenofluoro stannates, it is easier to replace a fluorine in a CIS position with increasing atomic number, and less easy to replace a fluorine in a TRANS position. However, the authors draw attention to the fact that K is less than the statistically predicted value for $\text{X} = \text{Cl}$, suggesting that the ease of replacing the second halogen depends on more than one factor. $[\text{SnI}_2\text{F}_4]^{2-}$ is exclusively CIS. Very recently the same authors (64) have reported a complementary study of anions of the same general form, but with $\text{M} = \text{Si}$, Ge and Ti , and $\text{X} = \text{bidentate ligand}$.

Since the first indications were given some thirteen years ago that N.M.R. spectroscopy could provide the means of elucidating a variety of structural features, a very large quantity of work has been published. The technique is now firmly established as a means of determining molecular configuration, and is particularly useful because of its speed and (sometimes) simplicity of interpretation. Its great advantage lies in the fact that in solution state solvents ranging from carbon tetrachloride to deuterium oxide may be used. The invention of various subtleties of technique is gradually extending the range of compounds accessible to N.M.R.

(3:4) (DIPOLE MOMENTS)

When a covalent bond is formed between two atoms of different electronegativities, a separation of electric charge occurs and an electric dipole is produced. If the two atoms are separated by a distance (r) and the charges at either end of the dipole are $+\delta$ and $-\delta$, then the dipole is given by δr . Since this is a vector quantity the overall dipole moment of a molecule is given by the sum of the individual moments.

For a covalent compound the molecular dipole moment may be calculated from the effect which that compound has on the capacitance of a condenser. The dielectric constant ϵ of a material can be measured experimentally. The principal of the measurement is that the capacity of the condenser is proportional to the dielectric constant of the material between the plates; a filled condenser has the capacity $C = \epsilon_0 C^0$, where C^0 is the capacity in vacuum. For a gas of molecular weight (M) and density (d), ϵ is related to the molar total polarizability (P) by the Debye-Langevin equation:

$$P = \frac{\epsilon_0 - 1}{\epsilon_0 + 2} \frac{M}{d} = \frac{4\pi N_A}{3} \left(\bar{\alpha} + \frac{\mu^2}{3kT} \right) \quad (3:1)$$

where ϵ_0 is the dielectric constant of the gas, $\bar{\alpha}$ is the mean polarizability of the molecule and N_A is Avogadro's number.

The quantity P can be regarded as having two parts. Thus we may write

$$P = P_1 + P_0 \quad (3:2)$$

where $P_1 = \frac{4}{3} \pi N_A \bar{\alpha}$ is the molar polarizability due to the elastic displacement of charges, and $P_0 = \frac{4\pi N_A}{9k} \frac{\mu^2}{T}$ is the molar polarizability arising from the partial orientation of dipoles in the applied field.

Since ϵ_0 is a pure number and M/d is the molar volume, $P = \frac{\epsilon_0 - 1}{\epsilon_0 + 2} \frac{M}{d}$ and has the dimensions of volume (CM^3).

The Debye-Langevin equation can be written

$$P = P_1 + (P_o T)/T \quad (3:3)$$

A plot of P versus $1/T$ should be linear with slope P_o and intercept P_1 . Determination of ϵ_o over a range of temperatures therefore gives the induced molar polarizability P_1 and the permanent dipole moment μ .

In liquids and solids the situation is made more complicated by the close proximity of the dipoles. For a solution of a polar compound (A) in a non polar solvent (B) equation (3:1) is of the form

$$\frac{\epsilon_o - 1}{\epsilon_o + 2} = \frac{4\pi}{3} \left[n_B \bar{\alpha}_B + n_A \left(\bar{\alpha}_A + \frac{\mu_A^2}{3kT} \right) \right] \quad (3:4)$$

In this case $\bar{\alpha}_B$ is the mean polarizability of the solvent molecules, $\bar{\alpha}_A$ that of the solute, and n_A and n_B are the respective numbers of molecules per CM^3 . The dipole moment μ can be evaluated from a determination of ϵ_o at a single temperature provided that $\bar{\alpha}_A$ and $\bar{\alpha}_B$ are known.

The magnitude and change of dipole moment is of fundamental importance in describing the interaction of radiation with molecules. Dipole moments themselves, however, are an important field of study and when used in conjunction with other physical methods provides a powerful tool for the investigation of overall molecular shape.

The octahedral TRANS molecule is centrosymmetric and (in theory) has a zero dipole moment when all the atoms are in their equilibrium positions. In practice a TRANS isomer nearly always exhibits a small moment (of perhaps 0.1 - 0.5 D) since the centre of symmetry is rarely ideal due to vibrational phenomena. On the other hand, the CIS complex on account of its lower symmetry will possess a relatively large moment. Unfortunately, real situations are often complicated by several factors. Beattie (3) has pointed out that the formation of a six-co-ordinate TRANS adduct may result in a moment ranging from zero to quite a large value, depending on the alignment of the ligands. Further, dissociation to a

five co-ordinate species with a consequently significant moment (3) together with the possibility of the co-existence of both CIS and TRANS species in the same system, may interfere with the interpretation of the observed moment. It is therefore important that dipole moment studies should be supported by ancillary measurements. For example, the moment of $\text{SnBr}_2 \cdot 2\text{C}_4\text{H}_8\text{S}$ (8.0 D) (152) indicates a CIS configuration for the compound in solution, whereas X-ray diffraction studies have shown that the solid complex is TRANS (153).

Dipole moment measurements have been used extensively in the study of the acetyl acetate complexes, e.g. $\text{Ph}_2\text{Sn}(\text{acac})_2$ and $\text{SnCl}_2(\text{acac})_2$. Doron and Fischer (154) measured the moments of $\text{Sn}(\text{acac})\text{Cl}_2$ in benzene and found that the value was more or less constant over the temperature range (30 - 79°C) (D.M. \approx 6.7 D). They interpreted this in the light of published dipole moment (63) and spectroscopic data (63) as strong evidence for an equilibrium involving the two CIS enantiomeric forms. In a similar study of $\text{Ph}_2\text{Sn}(\text{acac})_2$, Hayes et al (123) found a value of 2.5 - 3.6 D, and decided that the complex must exist predominantly as the CIS form in benzene solution.

As an example of an octahedral complex involving monodentate ligands, $\text{SnCl}_4 \cdot 2\text{NMe}_3$ has a dipole moment (12) of 0.4 D in benzene solution, strongly suggesting a TRANS configuration. The vibrational spectrum (144) also strongly suggests a TRANS configuration.

(3:5)

MÖSSBAUER SPECTROSCOPY

The most recent addition to the range of spectroscopic techniques available to the chemist is based on the recoilless emission and resonant reabsorption of those γ rays which result from nuclear transitions from excited states having lifetimes in the range 10^{-6} - 10^{-9} secs. The effect was discovered by Rudolf Mössbauer in 1958 (155). Since then an extremely

precise technique has been evolved (Mössbauer spectroscopy) which is potentially useful for about half the elements in the periodic table. The majority of studies so far reported are concerned with iron and tin compounds.

When a nuclear transition occurs between excited (E_e) and ground (E_g) states with the emission of a photon, the conservation of momentum requires the momentum of the atom (P_m) recoiling in one direction to be exactly neutralized by the momentum of the photon P_γ reacting in the opposite direction. It can be shown that since the energies of the two moments must be equal

$$E_R = \frac{E_\gamma^2}{2Mc^2} \quad (3:5)$$

where E_R is the kinetic energy of the recoiling atom and E_γ that of the emitted photon. A consequence of equation 3:5 is that E_γ will be less than the transition energy ($E_t = E_e - E_g$) by a quantity E_R . Further, the promotion energy required to populate the excited state will be larger than E_t by the same amount E_R . The Mössbauer experiment consists of irradiating the sample with γ rays of energy appropriate to the transition under study. For example, in the case of tin compounds this energy might be provided by the 23 k.e.v. γ ray associated with the decay of ^{119m}Sn (as BaSnO_3 for which $I = 3/2$) to ^{119}Sn ($I = 1/2$). Maximum absorption of radiation by the sample occurs when the amount of energy by which the emitter and absorber are out of resonance (i.e. $2E_R$) is exactly supplied. Most experimental methods devised to provide this energy make use of the fact that a sample and emitter which have a relative velocity (V) with respect to the propagation axis of the exciting quantum, imparts to that quantum a Doppler energy E_d , such that

$$E_d = \frac{VE_\gamma}{c} \quad (3:6)$$

This velocity can be provided either mechanically or thermally. Since the width of the γ ray line is only about 10^{-12} of its energy, the magnitude of the required velocity is only about 10^{-12} of the speed of light (i.e. between 1 - 10 mm/sec). A Mössbauer spectrum consists of a γ ray count versus the instantaneous velocity of the source relative to the absorber. Conventionally, a motion towards the absorber is considered as a positive velocity; a separating motion is therefore represented by a negative velocity.

The intensity of the resonant effect, the line width, isomer shift, quadrupole splitting and magnetic hyperfine structure may all be informative (156). For stereochemical investigations, however, the most important of these parameters are the isomer shift, and in particular the quadrupole splitting.

THE ISOMER SHIFT

The isomer shift (chemical shift) depends on the fact that the magnitude of nuclear transitions are influenced by the chemical environment of the nucleus. The excited and ground states of the nucleus have slightly different radii of equivalent charge distribution ($\delta r = r_{\text{excited}} - r_{\text{ground}}$) and therefore interact to different extents with the 'S' electrons. The difference in perturbation energy between the excited and ground states is not a directly measurable quantity, and can only be evaluated for a given pair of source and absorbing atoms. To a reasonable approximation the electron density at the nucleus is significant only for 'S' electrons and can be given by $\psi_S^2(0)$. The isomer shift energy is observed in the Mössbauer experiment as a Doppler shift, which occurs at a velocity (V) given by the relationship

$$V = \frac{4\pi Ze^2 R^2}{5E} \frac{\delta R}{R} \left[\left| \psi_S^2(0) \right|_{\text{ABS}} - \left| \psi_S^2(0) \right|_{\text{SOURCE}} \right] \quad (3:7)$$

where $|\psi_S^2(0)|$ is the 'S' electron density at the absorbing and source nuclei respectively. If $\delta R/R$ is positive, a positive isomer shift corresponds to an increase in 'S' electron density at the nucleus. Conversely, if $\delta R/R$ is negative, a positive shift corresponds to a decrease in 'S' electron density at the nucleus. Shifts are usually quoted with reference to a standard absorber. For ^{119}Sn spectra Mg_2Sn or SnO_2 are frequently used as references at normal temperatures. Metallic β tin is commonly used at liquid nitrogen temperatures.

Generally speaking $\delta R/R$ is positive and a comparison of the isomer shifts observed for various absorbers, using the same source, makes it possible to estimate the relative electron density at each of the absorbing nuclei. There have been several such studies (157,135,134) of six co-ordinate halogen complexes of tin, since in complexes of this type the relationship between the isomer shift and ligand electronegativity is particularly marked. As the electronegativity of the halogen is increased the polar character of the tin-halogen bond increases, with the result that the 'S' electron density in the absorbing tin nucleus falls and the isomer shift becomes less positive (see equation 3:7). The relationship between the two parameters for the tetramethyl ammonium salts of SnX_6^{2-} ($\text{X} = \text{F}, \text{Cl}, \text{Br}, \text{I}$ including mixed species) is linear (157,135,134) each ligand making an individual contribution towards the total isomer shift. The additivity of these partial contributions, demonstrated by Herber and Cheng (135), was the first example of its kind observed for ^{119}Sn Mössbauer data. Superficially, an obvious application is the study of donor-acceptor bond strength. For example, the effectiveness of the donor atom in reducing the electron density at a tin nucleus has been found to follow the order $\text{O} > \text{N} > \text{S} > \text{P}$ for six co-ordinate complexes (94). Unfortunately, the sensitivity towards the majority of interesting ligands is greatly reduced by the presence of halogen atoms.

QUADRUPOLE SPLITTING

For a spherically symmetrical nuclear electric field, an energy level corresponding to a nuclear spin moment of odd half integrals has an $(I + \frac{1}{2})$ fold degeneracy, and the tensor describing the field gradient vanishes at the centre. When the electric field is non spherically symmetric this restriction is lifted and the nuclear level is split into $(I + \frac{1}{2})$ components symmetrically distributed about the unsplit level.

Their energies (E_Q) are given by the expression:

$$E_Q = \frac{e^2 q Q}{4I(2I-1)} \left[3m_I^2 - I(I+1) \right] \left(1 + \frac{\eta^2}{3} \right)^{\frac{1}{2}} \quad (3:8)$$

where $e.q$ is the electric field gradient, Q is the quadrupole moment of the nucleus, m_I is the magnetic quantum number and η is a parameter defining the asymmetry of the tensor describing the electric field ($\eta = 0$ for symmetric case). In the most usual case where the ground and excited states have $I = \frac{1}{2}$ and $I = \frac{3}{2}$ respectively, a simple doublet is observed.

The electric field at the nucleus of a tetrahedrally bonded Mössbauer element is symmetrical and not expected to show quadrupole splitting. On the other hand, molecules of the type $(\text{Ph})_3\text{SnX}$ and Me_2SnX_2 (113), do not have tetrahedral symmetry and in general will show resolved absorption doublets. The absence of quadrupole splitting, however, does not in itself imply cubic symmetry in the chemical sense, but only in that of the electric field (158). Indeed, compounds are known in which no quadrupole splitting is observed although the chemical symmetry is clearly less than cubic. Greenwood and Ruddick (157) drew attention to this phenomenon in octahedral tin complexes and reasoned that a mechanism involving σ and π charge transfers produced electronically cubic symmetry at the tin nucleus. In contrast, they observed clear quadrupole splitting when the molecule contained tin-carbon bonds, and concluded that splitting is to be expected when all the ligand atoms

carry filled $p\pi$ orbitals.

Fitzsimmons et al (120) have shown that as a result of the validity of Greenwood's observations, the field gradients in complexes of the types R_2SnX_2L , Ph_2SnX_2L , R_2SnL_2 , Ph_2SnL_2 (L = bidentate ligand) are controlled by the orientation of the tin-carbon bonds. Since the tin atom cannot normally distinguish between X and L it is possible to consider them (stereochemically) simply as R_2SnX_4 . Thus for complexes of this class an examination of the quadrupole splitting data is capable of providing information about the site symmetry of the molecule.

On the basis of 'point charge' arguments, Fitzsimmons et al (120) were able to predict the relative magnitudes of the quadrupole splitting for the CIS and TRANS isomers (Ratio = 1:2). Further, by direct comparison with known structures they were able to deduce values for the absolute quadrupole splitting \int CIS R_2SnX_4 , $\Delta E = 2\text{MM/sec}$, and TRANS R_2SnX_4 , $\Delta E = 4\text{MM/sec}$ \int . These predictions were verified experimentally by studying numerous complexes (R_2SnL_2 and R_2SnX_2L where $R = \text{Me, Ph, Bu}$, $X = \text{Cl, Br, I}$, and $L = \text{oxin, acac, bipy, phen}$). In nearly every case the halogen-containing compounds showed quadrupole splitting ($\Delta E \approx 4\text{MM/sec}$) and were formulated as TRANS structures, while the presence of two bidentate ligands resulted in a value of only $\Delta E = 2\text{MM/sec}$, and were assigned CIS configurations. The authors concluded that the presence of two bidentate ligands in the sphere of co-ordination is an almost (120) sufficient condition for the formation of a CIS complex. Assignments are convincingly corroborated by X-ray, N.M.R., I.R., and dipole moment results previously reported in the literature.

A similar study of the organo-tin dithiocarbamates $Ph_2Sn\sqrt{S_2}^{CMR}_2$ and $R_2Sn\sqrt{S_2}^{CMR'}_2$ (119) has indicated the apparent dependence of the stereochemistry upon the organo groups; those compounds containing phenyl groups being almost exclusively CIS (according to Mössbauer data). The

substitution of aliphatic groups gave TRANS complexes, suggesting that an electron lowering factor is conducive to a CIS stereochemistry (119). Other workers (109) have observed that the smallest quadrupole splitting for $R_2SnX_2L_2$ ($R = Ph, alkyl, L = py, \frac{1}{2} bipy$) was found for $Ph_2SnI_2 \cdot bipy$ where considerable steric crowding is expected.

Quadrupole splitting is generally very much smaller ($< 1 \text{ MM/sec}^{-1}$) in complexes formed with the simple tin IV tetrahalides. The only example known for a nitrogen donor is the partially resolved doublet in $SnCl_4 \cdot 2MeCN$ (102). With oxygen and phosphorus-containing ligands values of the order of $\Delta E = 1 \text{ MM/sec}^{-1}$ have been observed in $SnCl_4 \cdot 2POCl_3$ ($\Delta E = 1.12 \text{ MM/sec}^{-1}$) (104) which is known to be CIS octahedral, and in $SnCl_4 \cdot 2PBu_3$ (94) for which a TRANS configuration has been suggested.

Mössbauer spectroscopy is thus most effective (stereochemically) when the electronegativities of the ligands differ appreciably. X-ray data is particularly sparse for complexes formed by organo substituted acceptors and this has hindered the evaluation of the technique. In spite of this, Mössbauer spectroscopy has provided detailed information about electron densities, bonding and site symmetries, and has already taken its place with other spectroscopic methods as a powerful means of elucidating chemical structures.

CHAPTER 4

BACKGROUND TO X-RAY CRYSTALLOGRAPHIC WORK

BACKGROUND TO X-RAY CRYSTALLOGRAPHIC WORK

(4:1) In 1912 Von Laue explained his experimental observations of the diffraction of X-rays by crystals in terms of diffraction from a three dimensional grating (159), the distance between the repeat unit on a crystalline scale being of the same order as the wavelength of X-radiation. At about the same time Bragg (160) drew attention to the close similarity between the laws of ordinary reflection and the diffraction of X-rays by planes within a crystal lattice. Through a simple picture of the scattering of an incident X-ray beam by these atomic planes he deduced the familiar equation (4:1) which implies that a diffracted beam of maximum intensity results when, and only when, the angle between the normal to the incident beam and the normal to the scattering planes is such that

$$n\lambda = 2d \sin \theta \quad n = 0, 1, 2, \dots \quad (4:1)$$

where θ is the angle defined above, d the interplanar spacing and λ the wavelength of the incident radiation. This is the well known Bragg equation.

As a result of the above relationship it is possible to predict the direction in space of a reflection from any set of planes within a crystal. Conversely, by a consideration of the geometrical arrangement of the reflections produced by a large number of planes it is possible to deduce the distances and angles between the planes, and therefore between the fundamental repeating unit of the crystal structure. In other words the shape and dimensions of the unit cell may be determined.

In the derivation of Bragg's law the electron density was assumed to lie in planes. In an actual crystal, however, the electron density is distributed throughout the unit cell and does not necessarily lie in special planes. The derivation is nevertheless valid, since it

can be shown that waves scattered from various points within the unit cell can be added together to give a resultant which behaves as though it had been reflected from a single plane. It is the variation in the amplitude of the resultant from various sets of planes which accounts for the differences in intensity between one reflection and another. In practice, 'reflection' takes place from many thousands of planes, with the result that the diffraction maximum is sharp and occurs only over a very small angular range. Usually this amounts to only a small fraction of a degree, and is due mainly to the small misalignments between the mosaic building blocks. Occasionally these imperfections are not present; the crystal being near perfect. In these circumstances reflections may prove very difficult to locate and it then becomes necessary to artificially induce misalignment in the mosaic by rapidly cooling the crystal.

X-rays are scattered by electrons so that the scattering power of an isolated atom is related to its atomic number. If one assumes spherical atoms, it can be shown that this scattering power is a function only of the atom type and $\sin \theta / \lambda$. As $\sin \theta / \lambda$ increases, the scattering power decreases, since radiation scattered from an electron in one part of the atom will be increasingly out of phase with that scattered by electrons at other points in the electron cloud. The scattering power of a given atom for a particular reflection is known as its scattering factor (f_0). Its value is expressed in terms of the scattering power of an equivalent number of electrons located at the atomic nucleus. At $\sin \theta / \lambda = 0$ the value of the scattering factor is always equal to the total number of electrons in the atom.

The scattering power of the entire unit cell is the resultant of j waves scattered in the direction of a particular reflection hkl by the j atoms within the cell. Each individual wave has an amplitude proportional to f_j , the scattering factor of the atom, and a phase (δ)

with respect to a hypothetical electron scattering at the origin of the unit cell. This resultant is defined in terms of a complex quantity known as the structure factor, F_{hkl} , which requires both amplitude and phase for a complete description. Like every component comprising it, the resultant is a simple harmonic wave which may be described in terms of a point (A) moving on a circle at a constant angular velocity (Fig. 7). The projection of this point (B) on both the x and y axes executes simple harmonic motion. A plot of the linear displacement of (B) as a function of the angular displacement ϕ of the radius vector, $^2(f')$, is simply the ordinary cosine function (Fig. 7). Applying the laws of vector addition we may write the following expression for the resultant displacement in the x and y directions

$$x = f_1 \cos \delta_1 + f_2 \cos \delta_2 + f_3 \cos \delta_3 = \sum_j f_j \cos \delta_j \quad (4:2)$$

and

$$y = f_1 \sin \delta_1 + f_2 \sin \delta_2 + f_3 \sin \delta_3 = \sum_j f_j \sin \delta_j \quad (4:3)$$

where x is the projection of resultant F on x, and y is the projection of the resultant F on y. This is best shown by Fig. 8. It follows that the absolute value of the resultant F, is

$$|F| = \sqrt{x^2 + y^2} = \sqrt{(\sum_j f_j \cos \delta_j)^2 + (\sum_j f_j \sin \delta_j)^2} \quad (4:4)$$

and the phase is given by

$$\alpha = \tan^{-1} \left(\frac{\sum_j f_j \sin \delta_j}{\sum_j f_j \cos \delta_j} \right) \quad (4:5)$$

where f_j is the amplitude of each component, and δ_j is the phase of the component.

It is a consequence of Bragg's law that there is a phase difference of 2π (360°) between reflections from each of the members of a given set of hkl planes. Thus the phase differences for unit translations along each axis are $2\pi h$, $2\pi k$, and $2\pi l$ radians respectively.

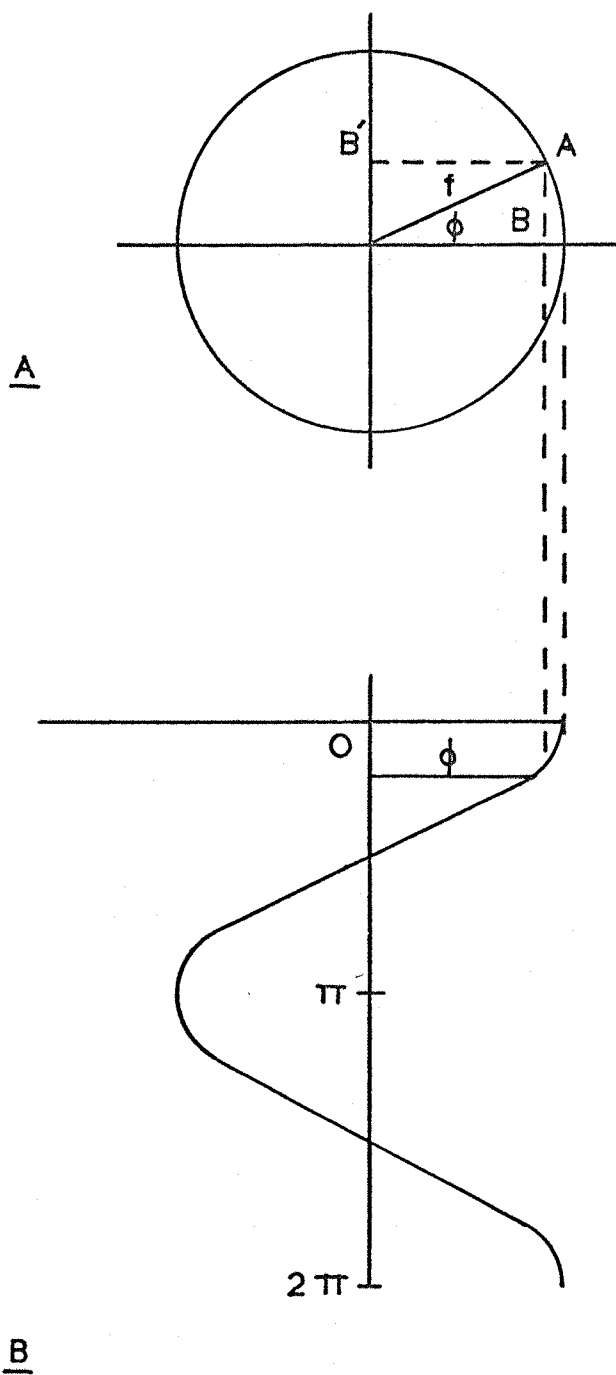


FIGURE 7 COSINE FUNCTION AS REPRESENTATION OF
SIMPLE HARMONIC MOTION

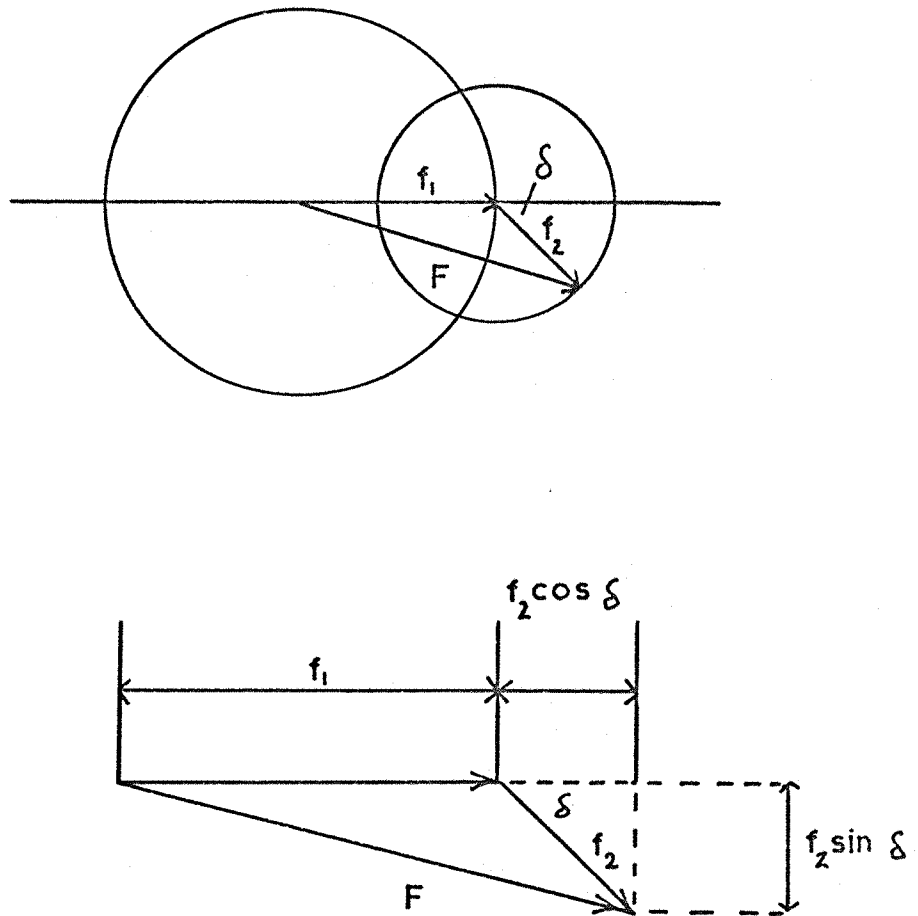


FIGURE 8 GEOMETRIC REPRESENTATION OF
SUPERPOSITION OF WAVES

The total phase difference (δ) between the origin 0,0,0, and a point u,v,w, on a specific hkl plane may then be given by

$$\delta = 2\pi (hx + ky + lz) \quad (4:6)$$

Substituting for δ in equation (4:4) gives for the magnitude of the structure factor

$$|F_{hkl}| = \sqrt{\left[\sum_j f_j \cos 2\pi(hx_j + ky_j + lz_j) \right]^2 + \left[\sum_j f_j \sin 2\pi(hx_j + ky_j + lz_j) \right]^2} \quad (4:7)$$

$$F_{hkl} = \sqrt{A_{hkl}^2 + B_{hkl}^2} \quad (4:8)$$

$$\text{where } A_{hkl} = \sum_j f_j \cos 2\pi(hx_j + ky_j + lz_j) \quad (4:9)$$

$$\text{and } B_{hkl} = \sum_j f_j \sin 2\pi(hx_j + ky_j + lz_j) \quad (4:10)$$

Similarly the phase of the resultant wave α is given by

$$\alpha_{hkl} = \frac{B_{hkl}}{A_{hkl}} \quad (4:11)$$

Calculated structure factors and their corresponding phases are normally computed from these equations.

Since the structure factor is a complex quantity consisting of real and imaginary parts, it may be concisely expressed as

$$F = A + iB \quad (4:12)$$

A wave of amplitude f and phase angle δ may therefore be expressed by the equation:

$$fe^{i\delta} = f(\cos \delta + i \sin \delta) \quad (4:13)$$

The right hand side of equation 4:13 is a complex number in polar form, and the left hand side is thus a concise way of representing the wave. It follows that the structure factor may be written down as the sum of this expression for all the wavelets scattered by the unit cell.

$$F = \sum_j f_j e^{i\delta_j} \quad (4:14)$$

Substituting for the phase difference given in equation 4:6, it is possible to give an expression for the structure factor in its exponential form:

$$F_{hkl} = \sum_j f_j e^{2\pi i(hx_j + ky_j + lz_j)} \quad (4:15)$$

Equation 4:15 is an approximation in that the distribution of the electron cloud is not centered at the nucleus of the atom, as implied by the definition of f_0 . A more precise representation is obtained by summing the wavelets scattered by each infinitesimal element of electron density in the unit cell 4:16

$$F_{hkl} = \int \rho(x,y,z) e^{2\pi i(hx + ky + lz)} dv \quad (4:16)$$

For centrosymmetric structures the B term of equations 4:8 and 4:11 is zero, with the result that the phase angle can have values only of 0 and π .

(4:2) FOURIER SYNTHESIS

Crystals, being periodic structures, are most easily described by a number of cosine and sine terms having suitable coefficients known as a Fourier series. A one dimensional Fourier series may be written as follows:

$$f(x) = a_0 + \sum_1^n (a_h \cos 2\pi hx + b_h \sin 2\pi hx) \quad (4:17)$$

where the h's are integers, a_h and b_h are constants, and x is a fraction of a period. The definition of a particular function may be increased simply by extending the number of terms in the series. In the centrosymmetric case, where $f_x = f(-x)$, the series involves only cosine terms. In complex notation we may write

$$f(x) = \sum_{-n}^n c_h e^{2\pi i hx} \quad (4:18)$$

or alternatively

$$f(x) = \sum_{-n}^n c_h (\cos 2\pi hx + i \sin 2\pi hx) \quad (4:19)$$

The electron density, ρ , at a point x, y, z in a crystal, may similarly be described by a three dimensional Fourier series in which the coefficients are the structure factors F_{hkl} :

$$\rho_{x,y,z} = \frac{1}{v} \sum_h \sum_k \sum_{l=-\infty}^{\infty} F_{hkl} e^{-2\pi i(hx + ky + lz)} \quad (4:20)$$

where v is the volume of the unit cell. A precise value for ρ_{xyz} may therefore be obtained when the structure factor is known.

If it were possible to measure the magnitude and phase of F_{hkl} directly, structure determination would be essentially a straightforward exercise in computation. Unfortunately, all that may be directly determined from the diffraction intensities are their magnitudes ($|F_{hkl}|^2$). Nothing is known of the phase; hence the term 'phase problem'. In an X-ray structural analysis, a set of phases calculated on the basis of some chemically reasonable model are combined with the observed structure factors to provide a trial electron density distribution. The resulting Fourier map shows regions of maximum electron density, which may then be compared to the assumed position of the atom, so providing the basis for an improved model. This model may similarly be used to calculate a new set of structure factors, whose calculated phases are in turn applied to the appropriate observed structure factors, to provide, hopefully, an even more accurate representation of the actual structure. The process is continued until the observed and calculated structure factors agree to the required extent with regard to both magnitude.

(4:3) THE PHASE PROBLEM

The recurring problem of X-ray crystallography is to provide the missing information, the phases, for a sufficient number of reflections to allow the construction of an approximate phasing model. Once this has been accomplished normal Fourier techniques may be applied. Various methods have been contrived to provide the phases for this first model. Which of these should be used in a particular case depends largely on the problem. The so called 'heavy atom' methods are perhaps the most reliable in straightforward structural analysis. Where a compound does not contain a heavy atom, a favourite procedure, particularly for organic molecules, is to prepare a heavy atom derivative. In recent years the so called 'direct methods' have been developed, and provide a powerful means of attacking light atom structures.

In co-ordination compounds, the central metal atom is usually much heavier than the atoms constituting the ligands, and the heavy atom approach may generally be applied. In this case the expression for the structure factor given in equation 4:15 may be written as follows:

$$F_{hkl} = f_H e^{2\pi i(hx_H + ky_H + lz_H)} + \sum_n f_L e^{2\pi i(hx_L + ky_L + lz_L)} \quad (4:21)$$

where $f_H \gg f_L$ the first term in the expression dominates. If at the same time the structure is centrosymmetric, a particularly simple situation occurs in which the sign of F_{hkl} is determined by the heavy atom. Further, it has been shown that if $\sum Z_H^2 = \sum Z_L^2$, then approximately seventy-five per cent of the phases will be correct.

Patterson (161) first drew attention to the usefulness of using $|F|^2$ as the coefficients in a Fourier synthesis. Substitution of these phaseless quantities in the calculation results in a Patterson peak at a point u, v, w , corresponding to the vectors between any pair of atoms. If the co-ordinates of these atoms are, say, x_1, y_1, z_1 , and x_2, y_2, z_2 , then

$$u = x_1 - x_2 \quad (4:22)$$

$$v = y_1 - y_2 \quad (4:23)$$

$$w = z_1 - z_2 \quad (4:24)$$

For a structure having (N) atoms in the unit cell, the Patterson map will show N^2 peaks. Of these, N correspond to vectors of zero length between the atom and itself, and fall at the origin. The remainder ($N^2 - N$) are distributed throughout the unit cell. The intensity of any peak is roughly proportional to the product of the atomic numbers of the appropriate pair. Patterson peaks are intrinsically more diffuse than those observed in a conventional Fourier map, with the result that overlapping is a frequent occurrence. However, bearing in mind appropriate atomic numbers, a comparison of the size of the more intense peaks relative to the origin, usually allows a determination of approximate heavy atom co-ordinates.

If $F_{(hkl)} = F_{(\bar{h} \bar{k} \bar{l})}$ then the value of the Patterson function is given by:

$$P_{u,v,w} = \frac{1}{v} \sum_h \sum_k \sum_l |F_{hkl}|^2 \cos 2\pi(hu + kv + lw) \quad (4:25)$$

Any pair of atoms A - B in real space gives rise to both vectors AB and BA in Patterson space. The resulting peaks are equal in magnitude but opposite in direction, so that for every peak at u,v,w, there will be a centrosymmetrically related one at -u,-v,-w. In fact all Patterson functions are centrosymmetric and by implication the symmetry elements will include a centre. The symmetry of the Patterson synthesis is derived from the normal space group by replacing translational symmetry elements by the corresponding non translational ones. It can be shown, however, that the lattice type is always the same as the space group.

Points in real space related by symmetry elements other than a centre, always have one or two identical co-ordinates. This results in unusually high concentrations of Patterson peaks on what are known as Harker lines and planes. It is through an examination of the Harker

sections that the first trial co-ordinates for the heavy atoms are frequently obtained.

Another useful form of Fourier synthesis is one in which the coefficients are the difference between the observed and calculated structure factors. This is equivalent to a point by point subtraction of the calculated electron density from the observed electron density throughout the unit cell. If the proposed model agrees in detail with the true structure, then such a calculation results in a featureless electron density map. In the case of a partially correct structure, in which there is good agreement between the observed and calculated phases, the synthesis may provide a valuable estimation as to the inadequacies of a given model, especially with regard to positions and thermal parameters. Generally, an incorrectly placed atom appears as a hole in the difference map, while a missing one results in a peak. The centre of the peak is often either sharpened or depressed depending on whether the thermal parameters have been over or under estimated. It can be shown, that for reflections which show $|F_c| \gg |F_o|$, the difference synthesis, in contrast to the normal Fourier synthesis, is extremely insensitive to phasing errors. Thus the use of an intelligently selected set of data often points immediately to errors in the calculated model. The technique may also be applied as a means of systematic refinement.

When only modest quality intensity data is available, or when the molecule contains heavy atoms, hydrogen atoms rarely appear in the Fourier synthesis as more than a distortion in the electron density distribution of the atom to which they are bonded. When, however, a structure is at a reasonable stage of refinement, and $|F_o| - |F_c| \approx 0$, additional electron density due to the observed structure is brought into relatively sharp relief, and hydrogen atoms not included in the F_c 's may appear in the ΔF map based on these F_c 's.

(4:4) REFINEMENT BASED ON THE METHOD OF LEAST SQUARES

Once a reasonably reliable model has been developed for which the reliability index (R) is of the order of 0.3 to 0.4, the refinement of the structural parameters for all the atoms may be attempted by the method of least squares.

Consider a linear function having n variables x_n . These variables may be envisaged as describing a space whose value at some point is determined by its position x_1, x_2, \dots, x_n , and by independent parameters p_1, p_2, \dots, p_n , which define the function. Thus

$$f = p_1x_1 + p_2x_2 + p_3x_3 + \dots + p_nx_n \quad (4.26)$$

According to the principle of least squares, if the function (f) is measured for m different points in space where $m > n$, the optimum values of p_1, p_2, \dots, p_n are those which minimize the sum of the appropriately weighted ΔF 's, ΔF being the difference between the observed and calculated values. It is therefore necessary to minimize the quantity D in equation 4:27

$$D = \sum_{r=1}^m W_r (f_{o_r} - f_{c_r})^2 \quad (4:27)$$

where W_r is the weight assigned to an individual of the m observations, (W_r is related to the standard deviation of the observation) and f_{o_r} and f_{c_r} are the corresponding observed and calculated quantities. This is accomplished in the usual way by differentiating the right hand side of equation 4:27 with respect to each parameter in turn and equating to zero. The result is a set of n linear equations (in practise m linear equations, where m is the number of observations) in n unknowns known as the normal equations. After rearrangement these equations may be written in the form

$$\sum_{r=1}^m w_r x_{r1}^2 p_1 + \sum_{r=1}^m w_r x_{r1} x_{r2} p_2 + \dots + \sum_{r=1}^m w_r x_{r1} x_{rn} p_n = \sum_{r=1}^m w_r f_{0r} x_{r1}$$

$$\sum_{r=1}^m w_r x_{r2} x_{r1} p_1 + \sum_{r=1}^m w_r x_{r2}^2 p_2 + \dots + \sum_{r=1}^m w_r x_{r2} x_{rn} p_n = \sum_{r=1}^m w_r f_{0r} x_{r2}$$

$$\begin{array}{ccccccc} \cdot & & \cdot & & \cdot & & \cdot \\ \cdot & & \cdot & & \cdot & & \cdot \\ \cdot & & \cdot & & \cdot & & \cdot \end{array}$$

$$\sum_{r=1}^m w_r x_{rn} x_{r1} p_1 + \sum_{r=1}^m w_r x_{rn} x_{r2} p_2 + \dots + \sum_{r=1}^m w_r x_{rn}^2 p_n = \sum_{r=1}^m w_r f_{0r} x_{rn}$$

(4:28)

The solution is straightforward, and immediately gives the optimum values for p_j in the least squares sense. Unfortunately, the situation is more complicated where the functional form of the equations is not linear, as occurs in the case of the structure factor, for in these circumstances an exact solution is not possible. In practice, however, a sufficient degree of accuracy is obtained by approximating the structure factor as a Taylor series which makes the equation essentially linear. Thus

$$\begin{aligned} f(p_1, p_2, \dots, p_n) = f(a_1, a_2, \dots, a_n) &+ \frac{\partial f(a_1, a_2, \dots, a_n)}{\partial p_1} \Delta p_1 + \dots \\ &+ \frac{\partial f(a_1, a_2, \dots, a_n)}{\partial p_n} \Delta p_n \end{aligned} \quad (4:29)$$

where the a_j 's are approximate values of p_j 's, and $\Delta p_j = (p_n - a_n)$. Terms in Δp_j of powers higher than the first are neglected.

If equation 4:29 is substituted into equation 4:27, the method of least squares may be applied to give values for Δp_j such that a'_j given by

$$a'_j = a_j + \Delta p_j \quad (4:30)$$

are better approximations to the optimum value of p_j than the initial a_j 's.

It is essential that the initial a_j 's are reasonably good approximations.

Since the value derived for the structure factor by application of a truncated Taylor series is an approximation, the calculation must be

repeated several times, updated values being used on each occasion. The iterative process is discontinued when there is no significant change in the parameters between cycles.

The normal equations discussed above may be conveniently expressed in matrix notation as

$$\begin{bmatrix} a_{11} & a_{12} & \dots & a_{1n} \\ a_{21} & a_{22} & \dots & a_{2n} \\ \cdot & & & \\ \cdot & & & \\ \cdot & & & \\ a_{n1} & a_{n2} & \dots & a_{nn} \end{bmatrix} \begin{bmatrix} x_1 \\ x_2 \\ \cdot \\ \cdot \\ \cdot \\ x_n \end{bmatrix} = \begin{bmatrix} v_1 \\ v_2 \\ \cdot \\ \cdot \\ \cdot \\ v_n \end{bmatrix} \quad (4:31)$$

$$\text{where } a_{ij} = \sum_{r=1}^m w_r \frac{\delta |F_{cr}|}{\delta p_i} \frac{\delta |F_{cr}|}{\delta p_j}$$

$$x_i = \Delta p_j$$

$$v_i = \sum_{r=1}^m w_r (\Delta F_r) \frac{\delta |F_{cr}|}{\delta p_i}$$

$$\text{or simply } \underline{AX} = \underline{V} \quad (4.32)$$

If it can be shown that for the equations 4:31 to have a solution, an inverse matrix \underline{A}^{-1} exists. It follows that

$$\begin{aligned} \underline{A}^{-1} \underline{A} \underline{X} &= \underline{A}^{-1} \underline{V} \\ \underline{X} &= \underline{A}^{-1} \underline{V} \end{aligned} \quad (4:33)$$

It has also been shown that b_{ij} , the ij^{th} element of the inverse matrix \underline{A}^{-1} , is influenced by the interdependence of parameters i and j on one another. This correlation coefficient between the i^{th} and j^{th} parameters is given by the equation

$$\delta_{ij} = b_{ij} / \sqrt{b_{ii}} \sqrt{b_{jj}} \quad (4:34)$$

In following the progress of a refinement it is often important to know the magnitude of the correlation coefficient. For this reason many modern computer programs give the correlation matrix in the output. The value

of the correlation coefficient ranges between zero and one. Where values of about 0.2 are given, little difficulty might be expected. On the other hand, a large coefficient suggests a significant interdependence between parameters, and this may seriously impair the refinement. The limiting case, where $\delta = 1$, implies complete dependence of one parameter on another, in which case one may be eliminated. When large correlation coefficients are observed it is particularly important to use the full matrix, since off-diagonal terms are important.

Several detailed texts on the theory and practice of X-ray diffraction methods are available (162-166).

CHAPTER 5

THE CRYSTAL STRUCTURE OF
TETRACHLOROTIN(IV)-BIS-ACETONITRILE

THE CRYSTAL STRUCTURE OF TETRACHLOROTIN(IV)-BIS-ACETONITRILE

(5:1) PRELIMINARY X-RAY WORK

PREPARATION AND CHARACTERIZATION OF THE CRYSTALS:

In initial attempts to grow suitable crystals solvent was slowly removed from a solution of tin tetrachloride in acetonitrile under (all glass) high vacuum conditions. Large transparent well formed crystals of $\text{SnCl}_4 \cdot x\text{MeCN}$ were obtained which when exposed to air in the dry box (< 50 p.p.m. moisture) quickly became coated with a fine white powder. This was easily removed by the addition of a drop of solvent, when the crystals again became transparent. Chloride analysis by potentiometric titration against silver nitrate were performed on approximately 100 mg samples of this material. (Found: Cl = 33.6 - 36.5%. Calculated for $\text{SnCl}_4 \cdot 2\text{MeCN}$: Cl = 41.39%, calculated for $\text{SnCl}_4 \cdot 3\text{MeCN}$: Cl = 36.96%, calculated for $\text{SnCl}_4 \cdot 4\text{MeCN}$: Cl = 33.39%). This is presumably the compound $\text{SnCl}_4 \cdot 3\text{MeCN}$ described by Groenveld et al (91). More forceful removal of the solvent by pumping or with a cold trap (-196°C) caused the crystals to fragment and slowly sublime. A plot of weight versus time during the sublimation showed that the rate of transfer was continuous, without any detectable steps indicating a change of adduct stability. Solid 1:2 complex in powder form (Found: Cl = 41.45%) was prepared by the addition of tin tetrachloride to acetonitrile using carbon tetrachloride as solvent. This material was sealed into a glass tube with excess carbon tetrachloride and slowly cooled from 100°C to room temperature, when crystallization occurred to give well formed needles. (Found: Cl = 40.04%). Small crystals were also obtained from the vapour phase by slowly cooling a sealed evacuated ampoule containing the solid 1:2 adduct alone.

The crystal density of the 1:2 adduct was determined by floatation in a solution of carbon tetrachloride in dibromomethane ($2.02 \pm 0.02 \text{ g.cm}^{-3}$).

The same density was observed for the powdered 1:2 adduct. However, the density of crystalline $\text{SnCl}_4 \cdot x\text{MeCN}$ was low (1.75 g.cm^{-3}), and increased within a few minutes to a value close to that found for the 1:2 adduct, when suspended in the pycnometer liquids, presumably due to loss of acetonitrile.

A number of small apparently well formed crystals, obtained by crystallization of the 1:2 complex from carbon tetrachloride, were mounted in sealed thin walled 'Pyrex' capillaries. These crystals were examined under the polarizing microscope for obvious sign of twinning. Several crystals were used for preliminary measurements. The best of these having overall dimensions $0.8 \times 0.3 \times 0.3 \text{ mm}$ was used for the data collection.

(5:2) X-RAY EQUIPMENT

The 'RAYMAX 60' X-ray generator used in this analysis is of the demountable continuously pumped type. For preliminary measurements, (Cu radiation) it was operated at ca 45 K.V. and 10 m.a. For all intensity measurements (Zirconium-filtered Mo - K_α radiation) the machine was run at ca. 50 K.V. and 10 m.a.

Ilford industrial X-ray films types B,G and CX, were processed at 20°C with Ilford Phenisol developer and Ilford Hypam fixer. Processing times and chemical concentrations were carefully standardized.

(5:3) UNIT CELL DIMENSIONS

Unit cell dimensions and diffraction symmetry were determined from oscillation, Weissenberg, and precession photographs. The crystal belongs to the monoclinic system and has the following cell dimensions. The needle axis is the (a) axis.

$$\begin{aligned}
 a &= 6.12 \pm (0.02) \text{ \AA} \\
 b &= 13.72 \pm (0.02) \text{ \AA} \\
 c &= 13.38 \pm (0.02) \text{ \AA} \\
 \beta &= 100.4^\circ \pm (0.3^\circ) \\
 v &= 1105 \text{ \AA}^3
 \end{aligned}$$

The following systematic absences were noted from equi-inclination Weissenberg and precession photographs.

hkl reflections : no general absences

h0l reflections : absent when $l = 2n + 1$

Ok0 reflections : absent when $k = 2n + 1$

The space group is therefore uniquely established as $P2_1/c$. (No.14)

The number of molecules in the unit cell (z) is given by the formular:

$$z = \frac{D \cdot V \cdot N}{M} \quad (5:1)$$

where D is the crystal density, V the volume of the unit cell, N is Avogadro's number and M the molecular weight of the compound. Assuming the 1:2 complex $C_4H_6Cl_4N_2Sn(SnCl_4 \cdot 2MeCN)$ $M = 343.6$, $D_M = 2.02 \pm 0.02 \text{ g.cm}^{-3}$ and $V = 1105 \times 10^{-24} \text{ c.c.}$, the calculated value for $z = 4$. On this basis the calculated value for the crystal density $D_C = 2.06 \text{ g.cm}^{-3}$.

(5:4) INTENSITY DATA COLLECTION

The linear absorbtion coefficient μ for a compound containing a fraction P of an element (n) in radiation of wavelength λ is given by the expression:

$$\mu_\lambda = D \sum P_n \left(\frac{\mu}{D} \right)_{\lambda n} \quad (5:2)$$

where D is the crystal density of the compound, and μ/D is the mass absorbtion coefficient of the element (n) at the wavelength λ . Substitution for

the appropriate values of μ/D given by the 'International Tables for X-ray Crystallography.' Vol.III (167B) gave $\mu(\text{Cu-K}_\alpha) = 275.7 \text{ cm}^{-1}$, $\text{Cu-K}_\alpha, \lambda = 1.5418 \text{ \AA}$: $\mu(\text{Mo-K}_\alpha) = 35.3 \text{ cm}^{-1}$, $\text{Mo-K}_\alpha, \lambda = 0.7107 \text{ \AA}$. The larger number of reflections available in the limiting sphere, together with the low absorption coefficient compared to that for copper radiation, made zirconium filtered Mo-K_α radiation the obvious choice for all intensity measurements.

Fortunately, not all the reciprocal lattice points defined by the molybdenum sphere represent independent observations, since the symmetry of the lattice dictates that reflections having indices related in certain ways have the same intensity. Assuming the validity of Friedel's law, the intensity weighted reciprocal lattice of a monoclinic crystal always has symmetry $2/m$, and reflections with the same absolute values of h , k and l , have equivalences related by $I_{hkl} = I_{\bar{h}kl}$ and $I_{hkl} = I_{h\bar{k}l}$. When intensity data is taken from Weissenberg photographs with the crystal rotated about the (a) axis, some care is required in setting the crystal so that all the unique data available on a particular level appears on the same film. The zero level Weissenberg presents little difficulty since the unique data consists of only the block with both indices positive. The upper levels, however, require more care, and the present crystal was set so that the unique (kl) and (k \bar{l}) reflections could be measured from a single film without having to resort to the use of equivalent reflections. Measurements were made to maximum indices of $h = 5$, $k = 18$, $l = 16$.

A multiple film technique was employed so that reflections of widely differing intensities could be brought within a range to which the eye is accustomed. A pack containing three films of different speeds (Ilford G, B, CX), were used for each exposure and processed together. Measurements made on different films were scaled from common reflections and previously determined speed factors. The intensity of each reflection

was measured by visual comparison with an optical wedge consisting of 25 spots made by photographing one of the most prominent reflections with the Weissenberg camera. In this wedge an intensity factor of two between one spot and the next was produced by doubling the number of 5° oscillations about the standard reflection for each exposure. The intensities of 1699 reflections were measured, of which 557 were considered unobserved. Unobserved reflections were assigned an intensity equal to one half the minimum observable. Level to level scaling of the Weissenberg photographs was established approximately from h0l precession photographs.

(5:5) TREATMENT OF DATA

All calculations and data processing were carried out using the X-ray 63 system of crystallographic programs, in conjunction with the computing facilities of the Atlas Computing Laboratories and Imperial College.

Atomic scattering factors for chlorine, nitrogen and carbon were taken from the values tabulated in 'International Tables for X-ray Crystallography' Vol.III (167B), while those of Thomas and Umeda (168) were used for tin.

Individual intensities were corrected for Lorentz and polarization factors in the usual way. Dispersion corrections for tin and chlorine in Mo-K $_{\alpha}$ radiation were small (167B), and bearing in mind the accuracy of the intensity data were not included. There was little evidence of spots having uneven intensity, or of hollow spots on any of the photographs. Further, since the crystal dimensions as seen by the X-ray beam were all of the same order of magnitude, and the crystal was in any case enclosed in glass, it was decided not to apply an absorption correction.

(5:6) DETERMINATION OF THE POSITIONS OF THE TIN AND CHLORINE ATOMS

Tin and chlorine together represent 76% of the scattering material in the unit cell. It is therefore reasonable to expect that a correct determination of their positions should enable a large number of phases to be determined; thereby allowing a preliminary Fourier synthesis to be carried out.

Successive application of the symmetry elements of the space group P_{2_1}/c (monoclinic, centrosymmetric, with a twofold axis parallel to b and a c glide perpendicular to it) to some general point within the unit cell, gives rise to four generally equivalent positions. On the other hand, a centrosymmetrical object placed at the origin $(0,0,0)$ gives rise to only one equivalent position at $(0, \frac{1}{2}, \frac{1}{2})$, nevertheless satisfying the symmetry requirements of the space group because of its special position. Since in the present case there are four molecules in the unit cell, the tin must necessarily fall in a general position (x,y,z) . (i). Symmetry dictates that the positions (ii) $\bar{x}, \bar{y}, \bar{z}$. (iii) $\bar{x}, \frac{1}{2} + y, \frac{1}{2} - z$ (iv) $x, \frac{1}{2} - y, \frac{1}{2} + z$ are equivalent to (i). For any pair of atoms in equivalent positions, a peak is expected in the Patterson function at a position whose co-ordinates are the difference between the co-ordinates defining real space. Thus atoms in equivalent positions give rise to Patterson peaks having the co-ordinates shown in Table 4. Bearing these co-ordinates in mind, it should therefore be possible to assign positions for the tin and chlorine atoms on the basis of a three dimensional Patterson synthesis. Accordingly, the Patterson function was calculated in units of $x = 30^{\text{th}}$, $y = 40^{\text{th}}$, $z = 40^{\text{th}}$ over $\frac{1}{4}$ of the unit cell using the complete data set. The resulting map showed a number of peaks, the more prominent of which are listed in Table 5 together with their relative peak heights.

A vector between two atoms i and j may be expected to give rise to a peak having a height approximately proportional to the product of the

TABLE 4

Equiv.Pos	x,y,z	$\overline{x} \ \overline{y} \ \overline{z}$	$\overline{x}, \frac{1}{2}+y, \frac{1}{2}-z$	$x, \frac{1}{2}-y, \frac{1}{2}+z$
x,y,z	0,0,0	-2x,-2y,-2z	-2x, $\frac{1}{2}, \frac{1}{2}-2z$	0, $\frac{1}{2}-2y, \frac{1}{2}$
$\overline{x}, \overline{y}, \overline{z}$	2x, 2y, 2z	0,0,0	0, $\frac{1}{2}+2y, \frac{1}{2}$	2x, $\frac{1}{2}, \frac{1}{2}+2z$
$\overline{x}, \frac{1}{2}+y, \frac{1}{2}-z$	2x, $\frac{1}{2}, 2z-\frac{1}{2}$	0,-2y, $-\frac{1}{2}, -\frac{1}{2}$	0,0,0	2x,-2y,+2z
$x, \frac{1}{2}-y, \frac{1}{2}+z$	0,2y, $-\frac{1}{2}, -\frac{1}{2}$	-2x, $-\frac{1}{2}, -2z-\frac{1}{2}$	-2x,2y,-2z	0,0,0

TABLE 4 INTERATOMIC VECTORS (POSITION OF PATTERSON PEAK) BETWEEN
ATOMS IN EQUIVALENT POSITIONS

	$x, y, z,$
FOUR FOLD	$\overline{x}, \overline{y}, \overline{z},$
GENERAL EQUIVALENT	$\overline{x}, \frac{1}{2} + y, \frac{1}{2} - z$
POSITIONS FOR P2, _{/c}	$x, \frac{1}{2} - y, \frac{1}{2} + z$

TABLE 5

PROMINENT PEAKS IN THREE DIMENSIONAL PATTERSON FUNCTION

Originating Atom Pair	No	x 30 th	y 40 th	z 40 th	Relative Peak Height
Origin Peak	1	0	0	0	660
Sn-Sn x 2	2	0	8	20	350
	3	2	15	4	150
	4	1.5	20	5	160
(Sn-Cl 2.3A)	5	7	5	2.7	190
Sn-Sn x 1	6	5	12	19	160
	7	4	8	14	110
	8	4.5	20	0	200
	9	18.5	20	6.5	140
Sn-Cl	10	25.5	0	6	210
Sn-Sn x 2	11	25	20	1	330
	12	23	13	17	110
	13	23.5	3	17.5	110

atomic numbers. If the intensity of the origin peak is H_{ii} , the relative peak height H_{ij} is given by:

$$H_{ij} = m \frac{H_{ii}}{\sum_i Z_i^2} Z_i Z_j \quad (5.3)$$

where Z_i and Z_j are the appropriate atomic numbers and m is the vector multiplicity.

To place the heavy atom in the unit cell it is necessary to locate it with respect to the symmetry elements of the cell, and to know the relationship these bear to the origin. The fact that translational symmetry elements give rise to Harker sections was mentioned earlier. Since the screw axis and glide planes in $P2_1/c$ are displaced from the origin and therefore the centre of symmetry, the Harker peaks fall at positions which are not simply twice the atomic co-ordinates. Instead, while the vector relating two screw related atoms ($1 \rightarrow 3$) occurs predictably in the $u, \frac{1}{2}, w$ plane, it is located at $-2x, \frac{1}{2}, -2z$. Similarly, the reverse vector ($3 \rightarrow 1$) gives rise to another Harker peak at $2x, -\frac{1}{2}, 2z$ and since $\vec{v} = \frac{1}{2}$ and $\vec{v} = -\frac{1}{2}$ lie in the same plane, the two peaks are related by a centre of symmetry in the $u, \frac{1}{2}, w$ plane. The second pair of screw related atoms have vectors which coincide with those of the first pair, so that instead of producing more Harker peaks they merely serve to reinforce the other. Because of the centre of symmetry only half the Harker plane is unique and a Fourier calculated over the asymmetric unit shows only a single peak. This may be arbitrarily considered to represent either vector, so that the x and z co-ordinates for the tin atom may be deduced from it.

The c glide similarly results in a Harker line $0, v, \frac{1}{2}$ and allows the y co-ordinate to be calculated. An examination of the general peak u, v, w , occurring at $2x, 2y, 2z$, (also found at positions related by the

Patterson symmetry) provided confirmation of the values obtained by the method outlined above. Vectors having the correct relative intensity lying approximately 2.3 \AA from the origin (peaks 5 and 10, Table 5) were assumed to be Sn - Cl vectors. The symmetry of the Patterson gave an octahedral arrangement of these vectors about the origin. The six vectors arise from four Sn - Cl distances in real space. It was not possible at this stage to make a clear cut choice of four chlorine atoms. On the basis of equations 4:22,23,24, atomic co-ordinates were calculated for all six possible chlorine positions.

A structure factor calculation and Fourier synthesis phased on one tin and six chlorine atoms gave peaks in the Fourier of weights 983, 922, 828, 716, 588, 537. A second structure factor calculation using one tin and four chlorines (the four largest peaks) gave $R = 0.168$ after two cycles of least squares refinement.^x Confidence in the choice of these four chlorine atoms was enhanced by the dramatic improvement in the overall definition of the Fourier map, the only anomaly being a rather streaky peak of very low intensity. Its co-ordinates, however, ruled out the possible presence of other atoms, and the peak was explained as being due to diffraction ripples resulting from termination of series errors. The temperature factors, which had previously been rather large, attained much more realistic values.

A Fourier synthesis based on the new co-ordinates (one tin and four chlorines) revealed a number of peaks, of which six indicated the positions of two acetonitrile ligands in a CIS orientation around the octahedrally co-ordinated tin atom.

Scattering factor curves are normally calculated on the assumption that the electron distribution is that expected of a stationary atom.

^x Orfls link of X-ray 63 program.

The atoms in a crystal are, of course, always vibrating about their rest positions with an amplitude dependent on the temperature, the mass of the atom, and on the way it is bonded. The effect of this thermal motion is to modify the volume and shape of the electron cloud, causing the scattering power of the real atom to decrease as a function of $\sin \theta / \lambda$ even more rapidly than in the idealized model. Additional terms are therefore required in the temperature factor expression to define the effect of the vibrational displacement in various directions. A more accurate description of the scattering power is given by the expression

$$e^{-B(\sin^2 \theta) / \lambda^2} = e^{-B/4d^2} \quad (5:4)$$

where $B (=8\pi^2 \bar{u}^2)$ is related to the mean square amplitude (\bar{u}^2) of the atomic vibration, and d is the interplanar spacing. The scattering factor for a real atom at normal temperatures may then be represented by combining equation 5:4 with the scattering factor f_0 .

$$f = f_0 e^{-B(\sin^2 \theta) / \lambda^2} \quad (5:5)$$

The approximation used for the shapes of the vibrational boundaries may be taken to various degrees of sophistication. In the first instance it is usual to assume that all atoms vibrate with equal amplitude in a spherically symmetrical fashion. This so called 'overall isotropic' temperature factor is naturally an over simplification of reality. The 'individual isotropic' assumption allows the assignment of temperature factors to each atom, at the same time retaining spherical symmetry. This provides a distinct improvement over the overall temperature factor. In most structural analysis carried out today, the final stages of refinement includes individual anisotropic approximations which no longer assume spherical symmetry. This requires six parameters to define the dimensions and orientation of the resulting vibrational ellipsoid. The expression for this general case is

$$T = \exp \left[-\frac{1}{2} (B_{11} h^2 a^{*2} + B_{22} k^2 b^{*2} + B_{33} l^2 c^{*2} + 2B_{12} hka^{*}b^{*} + 2B_{13} hla^{*}c^{*} + 2B_{23} klb^{*}c^{*}) \right] \quad (5:6)$$

where the B_{ij} 's are the thermal parameters having units identical with the conventional isotropic thermal parameter B . a^*, b^*, c^* are the usual reciprocal lattice parameters.

Two cycles of full matrix least squares refinement[†] with all atoms (except the hydrogens) varying individual isotropic temperature factors, scale factors and positional parameters, gave a conventional weighted residual R of 0.128

[†] Orfls link of X-ray 63.

(5:7) WEIGHTING SCHEME^{*}

The correct weight to be assigned an observation is equal to the reciprocal of the variance of that observation. Unfortunately, it is not practicable in routine analysis to make a sufficiently large number of measurements on each reflection in order to calculate its standard deviation. Instead, it is usual to make an estimate based on a set of reflections having representative magnitudes and $\sin \theta$ values. In practice weights for photographic data can be obtained towards the end of the refinement by plotting $|\Delta \bar{F}|$ versus $|\bar{F}_0|$. The weight applied to any F is proportional to $1/|\Delta \bar{F}|^2$, where ΔF is given approximately by the equation

$$\Delta F = A + BF_0 + CF_0^2 + DF_0 \Delta F + EF_0 \quad (5:7)$$

Values of $|\Delta \bar{F}|$ and \bar{F}_0 were calculated for seven groups of reflections covering ranges of magnitude $F = 0 - 250$. In order to reduce the amount of calculation a representative sample of 447 reflections was used (see Table 6 and Fig. 9). Figure 9 may be approximated by three straight lines,

^{*} WT - Delcon X-Ray 63.

FIGURE 9

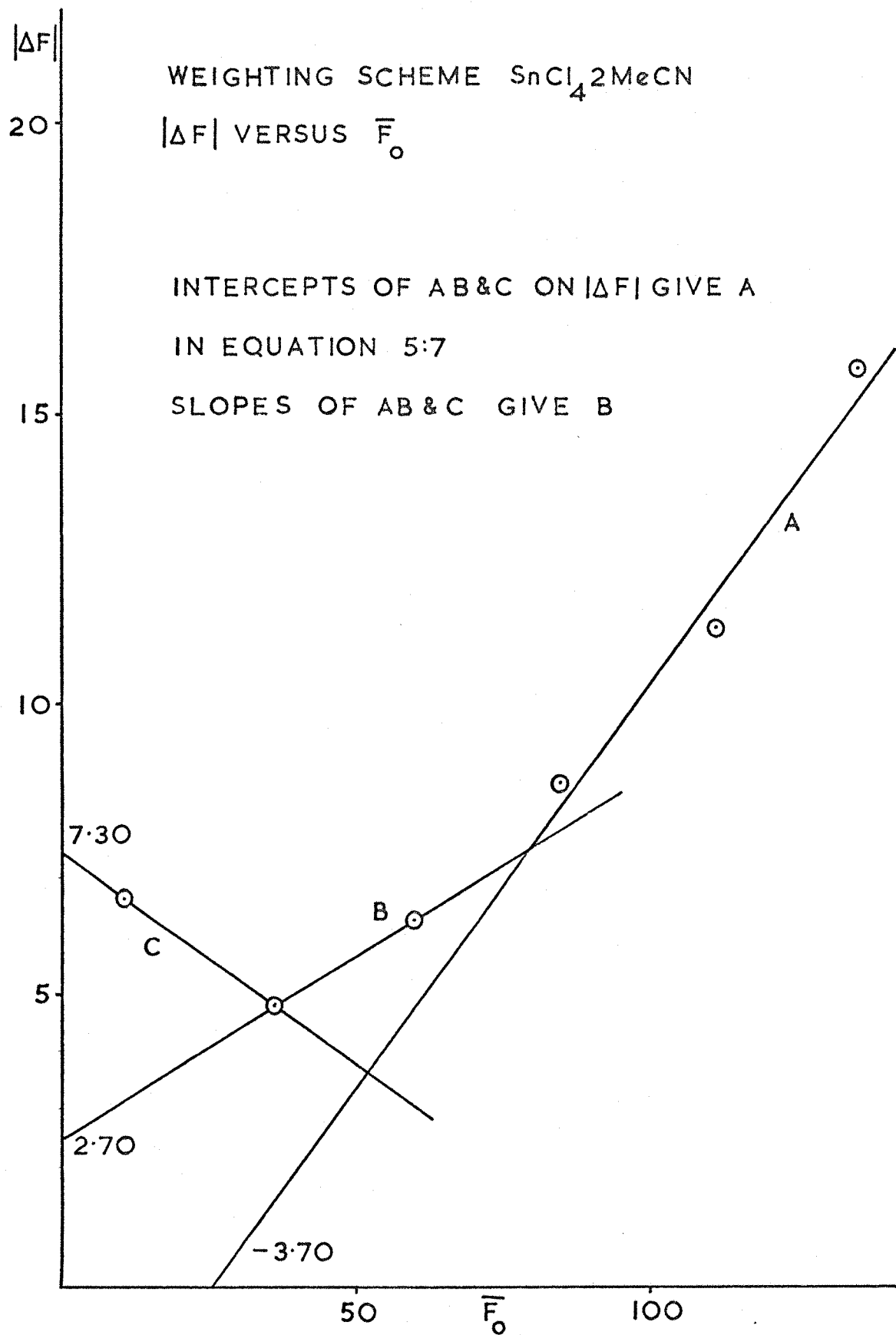


TABLE 6

WEIGHTING SCHEME

A. Distribution of $|F_o|$ in various ranges of selected data.

F_o (range)	$\sum F_o $	n	$ \bar{F}_o $	$\sum \Delta F $	$ \Delta \bar{F} $
0 - 25	1071	98	11	635	6.6
25 - 50	3394	94	36	450	4.8
50 - 75	4598	77	60	480	6.2
75 - 100	6711	79	85	679	8.6
100 - 125	6680	60	111	681	11.3
125 - 150	3244	24	135	379	15.8
150	2682	15	179	329	21.9

B. Coefficient A and $B^{\#}$ applied to equation $\Delta F = A + BF_o$ (123)

Coefficient A	Coefficient B	Lower Limit	Upper Limit	
7.30	- 0.0722	0	37	(Range 1)
2.70	0.0580	37	78	(Range 2)
- 3.70	0.1409	78	245	(Range 3)

so that over the specified ranges of F_o , (A, B and C) equation 5:7 reduces to

$$\Delta F = A + BF_o \quad (5:8)$$

The coefficients A and B for equation 5:8 were obtained graphically from Fig.9. The limits over which this equation was applied are given in Table 6.

A new structure factor calculation based on the weighted data, followed by further least square refinement including anisotropic temperature factors for the tin and chlorine atoms gave a residual of $R = 0.110$.

Finally intramolecular distances and angles were calculated[¶].
(Table 9).

(5:8) SUMMARY OF STRUCTURAL INFORMATION

The final structural information is summarized in Tables 7,8,9 and Figures 10 and 11. Final observed and calculated structure factors will be found in Appendix B. A molecular structure containing CIS $\text{SnCl}_4 \cdot 2\text{MeCN}$ molecules is established in agreement with earlier spectroscopic conclusions (12-22). A similar complex, $\text{SnCl}_4 \cdot \text{NC}(\text{CH}_2)_3\text{CN}$ in which glutaronitrile acts as a bridging ligand between two SnCl_4 units, has also been shown to be CIS octahedral with Sn-Cl distances of 2.35 Å (130). In CIS $\text{SnCl}_4 \cdot 2\text{POCl}_3$ (169) and CIS $\text{SnCl}_4(\text{OSeCl}_4)_2$ (170) Sn-Cl distances of 2.31, 2.36 Å and 2.36, 2.41 Å have been observed. These values are to be compared with 2.34, 2.36 Å observed in the present analysis. The Sn-N distances 2.33, 2.34 Å are close to the value of 2.29 Å found in the glutaronitrile complex (130). Differences in the values determined for Sn-Cl and Sn-N bond lengths, in the same molecule, are not statistically significant. Small distortions are observed from formal octahedral geometry (Table 9) which presumably minimize the Cl-Cl repulsions. Distortions of similar magnitudes are observed in both the closely related compound $\text{TaBr}_4 \cdot 2\text{MeCN}$ (171) and in $\text{SnCl}_4 \cdot (\text{g.n.})$ (130). The structures of several acetonitrile -containing complexes are known (172). The present work shows no significant changes in ligand geometry. Thus C = N and C-C distances of 1.09, 1.11 Å and 1.43, 1.45 Å are to be compared with 1.13 and 1.44 Å in BF_3MeCN (172) and with 1.18 and 1.42 Å in SbCl_5MeCN (173).

[¶] Bondla link of X-ray 63

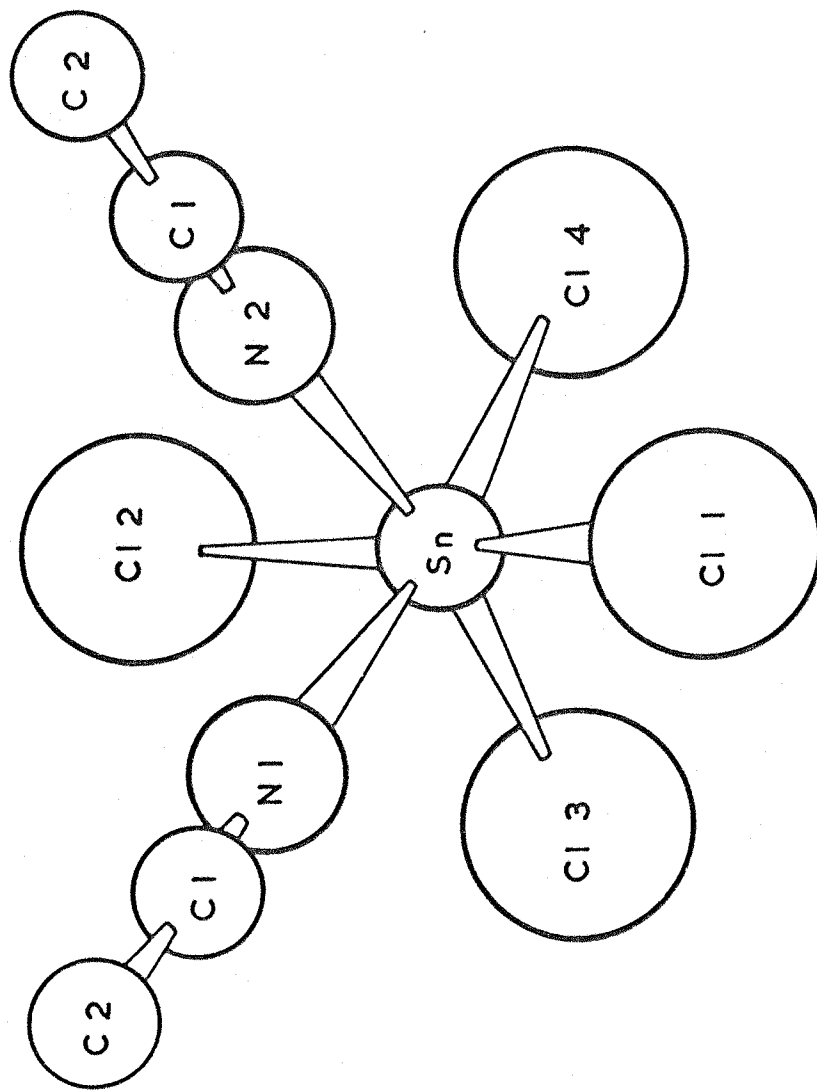


FIGURE 10 STEREOCHEMISTRY OF AN ISOLATED $\text{SnCl}_4 \cdot 2\text{MeCN}$ MOLECULE VIEWED DOWN

THE X DIRECTION

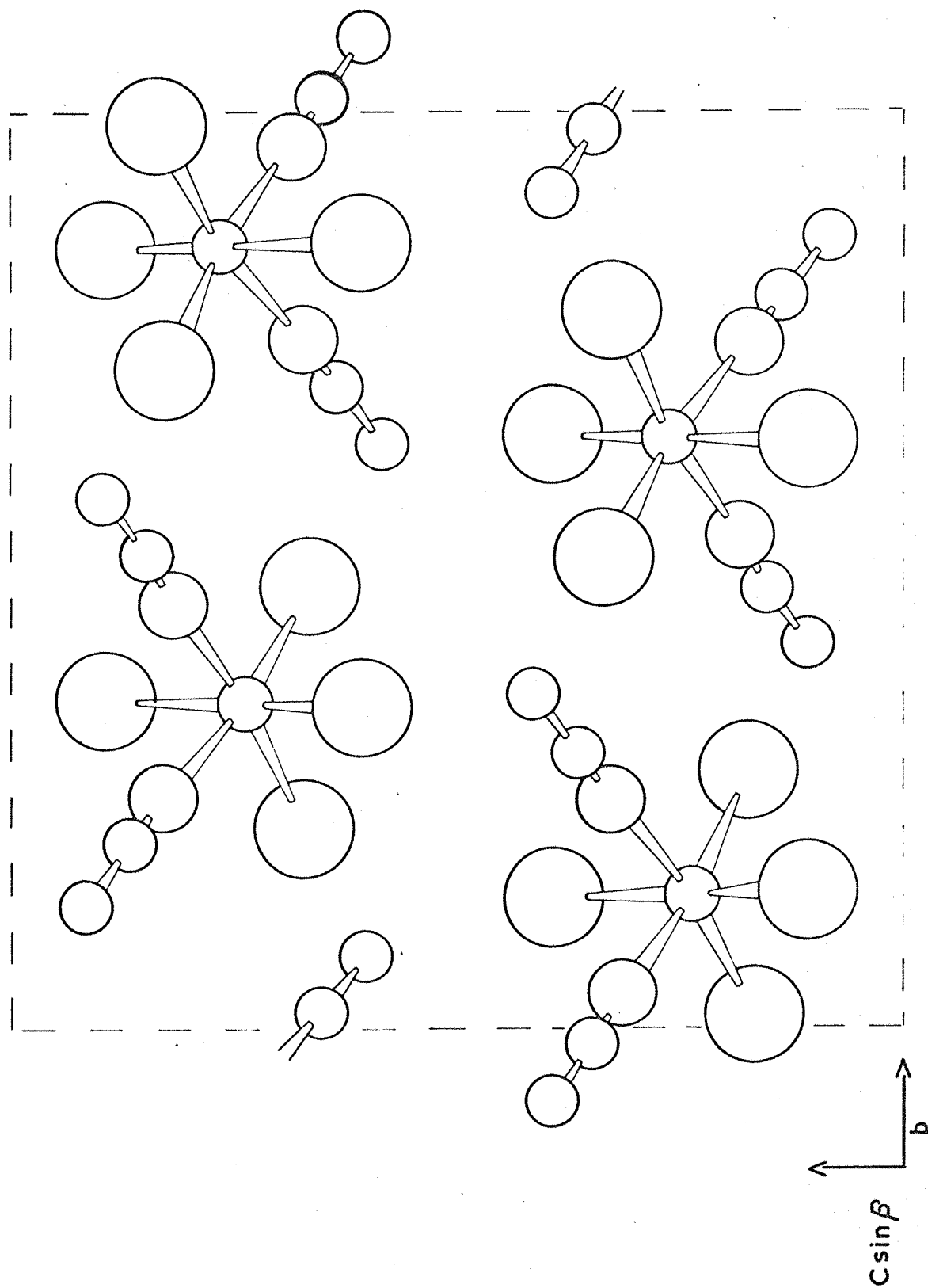


FIGURE 11 THE CRYSTAL PACKING ARRANGEMENT $\text{SnCl}_4 \cdot 2\text{MeCN}$ DOWN X DIRECTION

TABLE 7

FINAL POSITIONAL AND ISOTROPIC THERMAL PARAMETERS
WITH STANDARD DEVIATIONS IN PARENTHESIS

	x/a	y/b	z/c	$B(\text{\AA}^2)$
Sn	0.5835 (3)	0.1460 (1)	0.2362 (1)	
Cl (1)	0.7929 (15)	0.1495 (6)	0.1063 (6)	
Cl (2)	0.4578 (12)	0.1421 (6)	0.3923 (5)	
Cl (3)	0.3646 (13)	0.0145 (5)	0.1658 (5)	
Cl (4)	0.3648 (13)	0.2816 (5)	0.1731 (6)	
N (1) [*]	0.8545 (41)	0.0378 (16)	0.3161 (17)	3.07
N (2) [†]	0.8505 (42)	0.2484 (19)	0.3273 (18)	3.49
C (1) [*]	0.9731 (47)	-0.0179 (18)	0.3483 (18)	2.58
C (2) [*]	1.1529 (55)	-0.0808 (22)	0.3950 (23)	3.78
C (1) [†]	0.9798 (52)	0.2997 (20)	0.3651 (21)	3.12
C (2) [†]	1.1491 (54)	0.3640 (23)	0.4150 (22)	3.69

* Denote atoms belonging to one ligand

† Denote atoms belonging to second ligand

TABLE 8

HEAVY-ATOM ANISOTROPIC TEMPERATURE FACTORS (\AA^2)^{*}

	B_{11}	B_{22}	B_{33}	B_{12}	B_{13}	B_{23}
Sn	1.898	1.656	2.147	0.198	-0.253	0.000
Cl (1)	4.855	3.765	3.879	0.132	1.077	0.072
Cl (2)	3.362	4.442	2.771	0.892	0.032	0.000
Cl (3)	3.493	2.485	3.602	-0.529	-0.475	-0.289
Cl (4)	3.522	2.635	4.156	0.859	0.063	0.506

* In the form:

$$T = \exp \left[-\frac{1}{4} (B_{11} h^2 a^{*2} + B_{22} k^2 b^{*2} + B_{33} l^2 c^{*2} + 2B_{12} hka^*b^* + 2B_{13} hla^*c^* + 2B_{23} klb^*c^*) \right]$$

TABLE 9
INTRAMOLECULAR DISTANCES (\AA) AND ANGLES
WITH STANDARD DEVIATIONS IN PARENTHESES

<u>Interatomic Distances</u>			
Atoms	Distance (\AA)	Atoms	Distance (\AA)
Sn - Cl (1)	2.339 (08)	Sn - N (2)	2.326 (25)
Sn - Cl (2)	2.355 (07)	N (1) - C (11)	1.088 (35)
Sn - Cl (3)	2.341 (07)	C (11) - C (12)	1.449 (41)
Sn - Cl (4)	2.356 (07)	N (2) - C (21)	1.111 (39)
Sn - N (1)	2.336 (23)	C (21) - C (22)	1.430 (43)

<u>Intramolecular Angles</u>			
Atoms	Angle (deg)	Atoms	Angle (deg)
Cl(1) - Sn - Cl(2)	166.14 (28)	Cl(3) - Sn - Cl(4)	102.57 (25)
Cl(1) - Sn - Cl(3)	93.86 (28)	Cl(3) - Sn - N (1)	90.10 (58)
Cl(1) - Sn - Cl(4)	93.99 (29)	Cl(3) - Sn - N (2)	166.68 (64)
Cl(1) - Sn - N (1)	85.07 (62)	Cl(4) - Sn - N (1)	167.34 (60)
Cl(1) - Sn - N (2)	87.11 (65)	Cl(4) - Sn - N (2)	90.61 (65)
Cl(2) - Sn - Cl(3)	94.85 (26)	N (1) - Sn - N (2)	76.74 (84)
Cl(2) - Sn - Cl(4)	94.61 (26)	Sn - N (1) - C (11)	174.51 (2.21)
Cl(2) - Sn - N (1)	84.16 (61)	Sn - N (2) - C (21)	175.57 (2.41)
Cl(2) - Sn - N (2)	81.94 (65)	N (1) - C(11) - C(12)	171.93 (3.03)
		N(2) - C(21) - C(22)	178.73 (3.26)

CHAPTER 6

THE CRYSTAL STRUCTURE OF BIS(TRIMETHYLPHOSPHINE)TETRACHLORO
SILICON IV

THE CRYSTAL STRUCTURE OF BIS(TRIMETHYLPHOSPHINE)TETRACHLORO SILICON IV

(6:1) PRELIMINARY X-RAY WORK

Suitable crystals of $\text{SiCl}_4 \cdot 2\text{PMe}_3$ were obtained by cooling a benzene solution prepared under high vacuum conditions in an all glass vacuum system. A number of crystals selected from a sample kindly provided by Dr. G.A. Ozin were mounted in thin walled pyrex capillaries with the aid of a dry box. The best of these, chosen according to its size and optical properties under polarized light, was mounted on a eucentric goniometer head and used for all measurements. This crystal had overall dimensions of (0.8 x 0.2 x 0.2 mm).

Rotation, Weissenberg and precession photographs using Zr. filtered Mo radiation gave approximate cell dimensions and space group. The monoclinic crystal of $\text{C}_6\text{H}_{18}\text{Cl}_4\text{P}_2\text{Si}$ ($M = 322.1$) gave $a = 6.63$, $b = 8.26$, $c = 13.13$, $\beta = 101.8^\circ$. Unique determination of space group $\text{P}2_1/c$ was possible from systematic absences hkl : $h0l$ for $l = 2n + 1$ and $0k0$ for $k = 2n + 1$.

The crystal was transferred to a General Electric XRD.5 Manual Diffractometer and set by established methods (174) so that ω , 2θ , and ψ were concentric. A set of refined cell parameters were obtained on the basis of prominent axial reflections in the $h0l$ net. Preliminary cell parameters were used as an aid to locating the reflections, and fixed time counts (100 secs) at intervals of 0.01° in 2θ then used to determine the exact position of the maximum for $(k_{a_1} + k_{a_2})$. The measurements also gave a more accurate value for β . The refined cell parameters obtained in this way together with derived parameters are:

$$\begin{aligned}
 a &= 6.65 \text{ \AA} \\
 b &= 8.26 \text{ \AA} \\
 c &= 13.10 \text{ \AA} \\
 \beta &= 101.8^\circ
 \end{aligned}$$

$$\begin{aligned}
 \text{Calculated density } D_{\text{calc}} &= 1.57 \text{ g.cm}^{-3} \\
 V &= 703.495 \text{ \AA}^3
 \end{aligned}$$

The observed density measured by floatation in a solution of chlorobenzene in carbon tetrachloride was $D_M = 1.50 \text{ g.cm}^{-3} \pm 0.03$. Thus assuming $M = 322.1$ the number of molecules in the unit cell $z = 2$.

(6:2) DATA COLLECTION

Angular settings for χ , ϕ and 2θ , together with the appropriate scanning ranges were calculated on the basis of the above parameters using the setting program DIFSET (175) in conjunction with the University computer (I.C.L.1970). All other calculations were carried out using the X-ray 63 system of programs and the facilities of the Atlas Computer Laboratory.

Intensity data was collected using Zr filtered Mo radiation with a scintillation tube detector and employing the moving crystal-moving counter technique. The X-ray source was a General Electric CA-8-S/Mo small focal spot tube operated at 45 K.V. - 15 M.A. The stability of the primary beam was checked by successive fixed time counts on the 004 and 200 reflections at $\chi = 90^\circ$

The intensity of the standard reflections (004 and 200) were determined before and after each period of data collection (approximately 3 hr). The overall time taken to collect the data was about two weeks. A plot of standard intensity versus time showed a slow though approximately linear decrease in scattering efficiency, presumably due to radiation

damage in the crystal. Accordingly, the final data were scaled using a factor which varied between 0 and 1.2. The intensity of 507 non zero reflections were determined using a scan of 40 seconds. Background was measured either side of the maximum (20 secs x 2) at values of 2θ determined by the setting program. Halving the background count (20 secs instead of 40 secs) greatly reduced the time involved in collecting data, without significantly affecting the precision of individual measurements. Intensity was defined as $P_c - B_1 - B_2$, where P_c is the peak count and B_1 , B_2 are the background counts. The minimum observable intensity was defined as $P_c / (B_1 + B_2) = 3$.

At larger values of 2θ the calculated settings failed to exactly coincide with those providing the maximum counting rate. This it was felt was probably due to the crystal being mounted in a glass tube. As a consequence, it was necessary to maximize each reflection using the ϕ and ω adjustments. The ϕ setting was most sensitive, particularly at $\chi = 0$, while ω became increasingly effective as the value of χ approached 90° .

Scattering factors for silicon, chlorine, phosphorus and carbon were taken from the 'International Tables for X-ray Crystallography' (167B). All intensities were corrected for Lorentz and polarization factors in the usual way, but no corrections for dispersion or absorption were applied. (Linear coefficient of absorption $\text{MoK}_\alpha = 11.1 \text{ cm}^{-1}$).

(6:3) DETERMINATION OF SILICON, CHLORINE AND PHOSPHORUS POSITIONS

The presence of two molecules in the unit cell requires the silicon atoms to be at centres of symmetry and therefore in the twofold special positions $0,0,0$ and $0, \frac{1}{2}, \frac{1}{2}$ for $P2_1/C$. It follows that the asymmetric unit must itself be centrosymmetric thus dictating a TRANS stereochemistry for $\text{SiCl}_4 \cdot 2\text{PMe}_3$.

A three dimensional Patterson synthesis in units of $x = 20^{\text{ths}}$, $y = 25^{\text{ths}}$, $z = 40^{\text{ths}}$ over quarter of the unit cell, and based on the complete data set, showed only two peaks having the correct relative intensity for Si-Cl/Si-P vectors at reasonable distances (2.3 \AA) from the origin. The symmetry of the Patterson map generated an octahedral arrangement of these peaks around a central silicon. An examination of the Harker line $0, V, \frac{1}{2}$, and the Harker section $u, \frac{1}{2}, W$, allowed the determination of real space co-ordinates for the heavy atoms. Approximate calculations (163) of bond lengths and angles indicated a somewhat distorted octahedron (Cl-Si-Cl, $93^\circ, 86, 95^\circ$) with sensible bond lengths (2.3 \AA).

Since the scattering powers of chlorine ($z = 17$) and phosphorus ($z = 15$) are so similar, the initial structure factor calculation and electron density synthesis were phased on one silicon and three chlorines, in the hope that the carbon atoms appearing in a Fourier synthesis would establish the position of the phosphorus atoms. Unfortunately, it was impossible to distinguish between chlorine and phosphorus atoms in this way. Nevertheless, several additional peaks of much lower intensity appeared. The most reasonable of these in terms of possible C-P distances were assumed to be carbon atoms, but their inclusion in a further structure factor calculation had negligible effect on the residual. The least squares refinement of positional parameters showed large correlation effects due to a pseudo mirror plane in the molecule (P mirrored to Cl). Two cycles of refinement gave $R = 0.34$.

The roughly symmetrical distribution of scattering material around the silicon atom produces an approximate A-faced centering condition in the data in which reflections of the type $(hkl: k + l = 2n + 1)$ are weak. To a good approximation these reflections are contributed to by only three carbon atoms, and the difference between a ^{CHLORINE} ~~carbon~~ and a phosphorus ($\Delta Z = 2$). On the other hand, $(k + l = 2n)$ type reflections

are almost entirely dependent on the large mass of material symmetrically distributed about the special positions (the octahedra) which in themselves represent 72% of the total scattering power of the unit cell. As a result of this, calculations based on the complete data set were very insensitive to positional errors of the carbon atoms. A difference electron density synthesis provided little further information.

A disordered structure seemed a distinct possibility at this stage. However, assuming that this was not the case, it seemed reasonable to expect that a single set of carbon atom co-ordinates should provide the optimum phasing model. Since such atoms might be expected to lie on a circle perpendicular to the Si-P vector, it seemed feasible to fix their positions by plotting the residual R for successive structure factor calculations against the rotational displacement of the PMe_3 group. Possible carbon co-ordinates were obtained from a scale model (1 ins = 1\AA) of the Si - P \angle grouping which was constructed in accordance with P-C distances (1.83\AA) and C-P-C angles (100°) reported in the literature (176). In this model a brass tube proportional in length to the Si-P distance (2.3\AA) was inclined at 45° to a base representing the h0l plane and intersecting β . The tube acted as a bearing for a rotor representing the PMe group; a protractor and locking screw allowing it to be fixed in any desired orientation. The appropriate co-ordinates were read directly from the projection of the rotor on the marked base board. Co-ordinates were found for each of the three carbon atoms in thirteen (10°) rotational increments.

A structure factor calculation was carried out phased on the octahedron of heavy atoms, ($R = .34$) and the resulting F_c 's were used as a fixed atom contribution in thirteen successive calculations including the carbon atoms. A plot of R versus the angle of displacement of the rotor from its initial position showed a well defined minimum for a

particular conformation (Fig.12) thus defining the optimum carbon atom co-ordinates. An identical series of calculations on the mirror image of this model ($y \rightarrow \bar{y}$) gave a similar result. This can be explained by a consideration of the structure factor. The general expression for the structure factor (equation 4:15) can be simplified to include explicitly the effects of the symmetry elements of the space group. It can be shown (165) that in $P2_1/c$ equation 4:15 reduces to

$$F_{hkl} = \sum_n f_n (4 \cos 2\pi(hx + lz) \cos 2\pi ky) \quad (6:1)$$

for $k + l$ even

$$\text{and} \quad F_{hkl} = \sum_n f_n (-4 \sin 2\pi(hx + lz) \sin 2\pi ky) \quad (6:2)$$

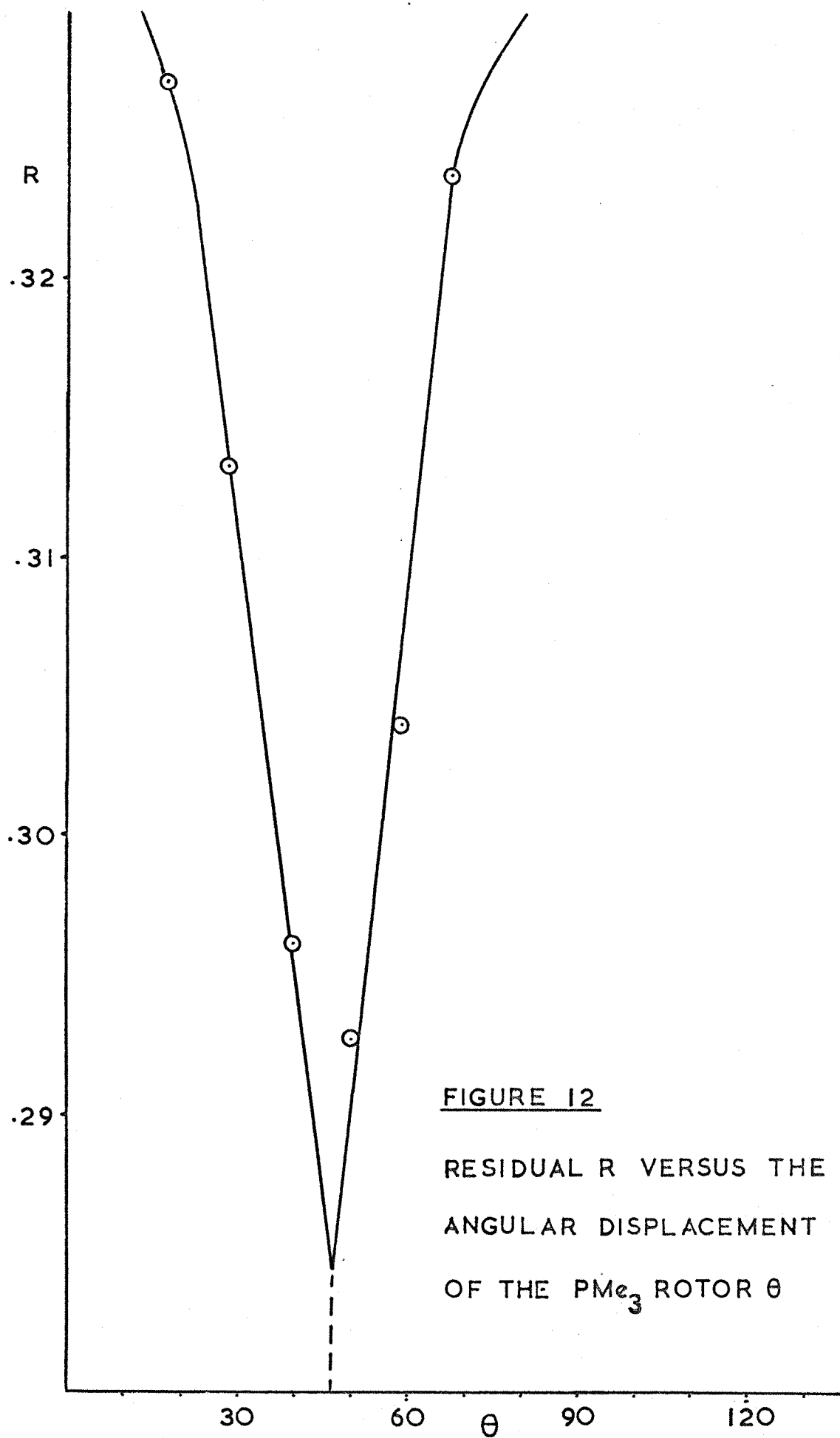
for $k + l$ odd, where f_n are the scattering factors of the n unique atoms in the asymmetric unit. Inspection of these expressions shows that for models related by a mirror, ($y \rightarrow \bar{y}$), the magnitudes of the structure factors must remain unaltered, even though their signs may change. Since the residual R is dependent only on the structure factor magnitudes, the two models will give indistinguishable results.

(6:4) REFINEMENT

Two cycles of full matrix least squares refinement varying the positional parameters of Si, Cl₁, Cl₂, P and C, with an overall temperature factor, gave a residual $R = 0.29$.

Seven equal scale factors (=1), arbitrarily spaced throughout the data set, were then refined together with all positional parameters, individual isotropic temperature^{FACTORS} being applied to the heavy atoms. Two cycles resulted in a reduction of the residual to $R = 0.24$.

A survey of the data showed that although agreement between F_o 's and F_c 's was acceptable for the majority of reflections, a certain number,



apparently randomly spaced throughout the reciprocal lattice, had large ΔF 's. A large majority of these showed $|F_o| \gg |F_c|$. A total of 48 such reflections were rejected on the grounds that the diffractometer settings were known to be inaccurate and that minor changes in the scale settings could easily result in a peak being missed or only partially scanned through.

The weighting scheme^F described in Chapter 5 was applied over a single range of intensities (0-120) (Table 10, Fig.13). Continued refinement gave a residual $R = 0.16$. Least squares refinement was concluded by three cycles varying all positional parameters. Individual anisotropic temperature factors were applied to the heavy atoms, (Si was shut off) while individual isotropic temperature factors were used for the carbon atoms. Scale factors were not refined in this calculation. A total of 52 parameters were varied. (Total number of reflection/number of ^{VARIABLES} ~~variables~~ = $459/52 \approx 10$). The final conventional weighted residual $R = 0.142$, with shifts less than the least squares standard deviation. (Average value shift/error = 0.233). Bond lengths and angles were calculated using the Bondla link of the X-ray 63 system of programs.

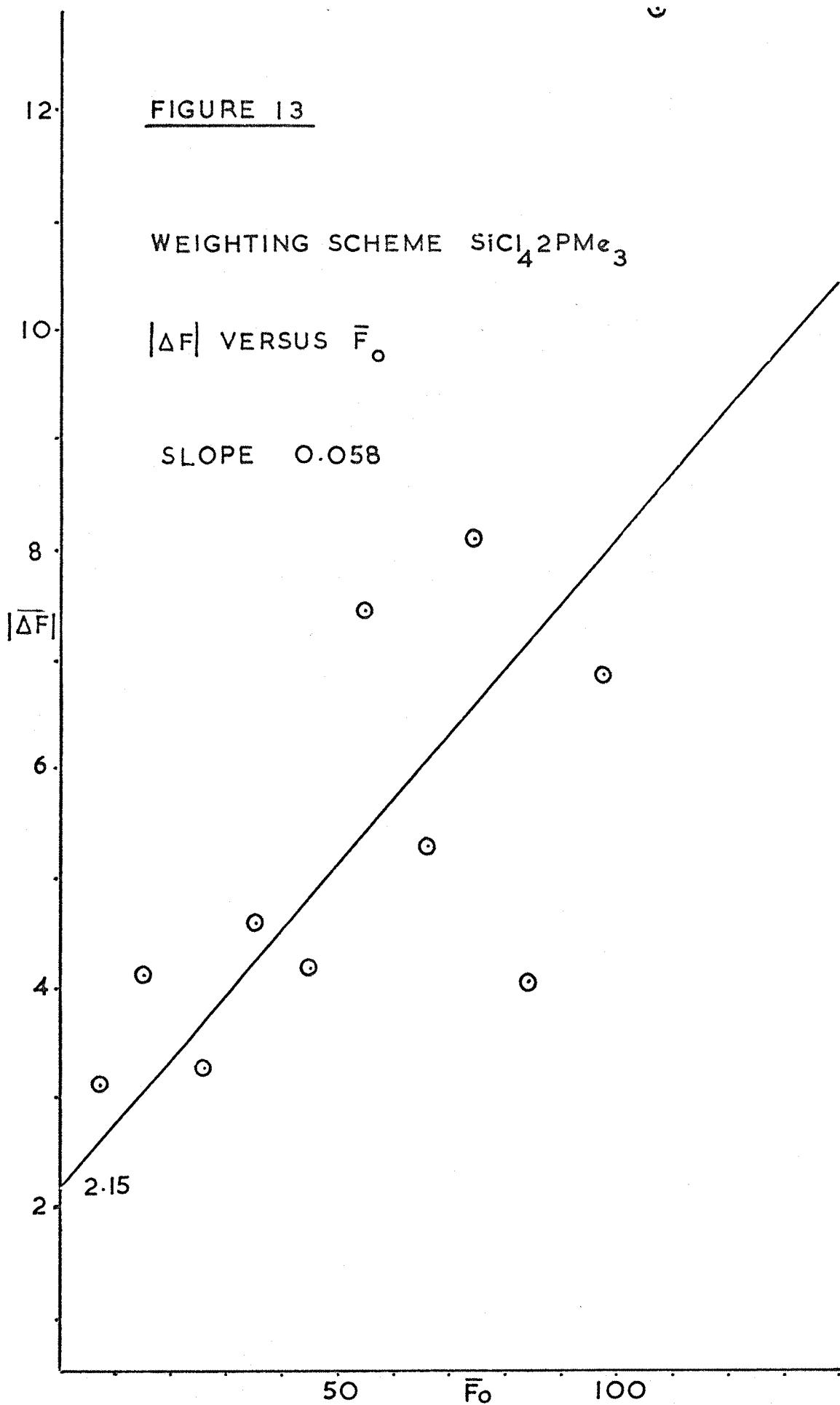
^F

WT - Delcon links of X-ray 63 system

TABLE 10

Range F_o	$\sum F_o $	No. of Ref in Range (n)	$\sum F_o /n$	$\sum \{ F_o - F_c \}$	$\overline{\Delta F}$
0 - 10	747.9	112	6.67	337.00	3.0
10 - 20	1660.3	115	14.44	474.75	4.0
20 - 30	2268.2	90	25.20	287.40	3.2
30 - 40	1856.7	54	34.38	250.25	4.6
40 - 50	1505.3	34	44.27	140.73	4.1
50 - 60	7575.3	14	54.11	103.36	7.4
60 - 70	7152.8	11	65.03	57.49	5.2
70 - 80	6627.5	9	73.64	80.47	8.1
80 - 90	5814.3	7	83.06	28.12	4.0
90 - 100	2908.8	3	96.96	20.41	6.8
100 —	4280.0	4	107.00	51.46	12.9

WEIGHTING SCHEME — F_o STATISTICS (SEE FIG.13)



(6:5) SUMMARY OF STRUCTURAL INFORMATION

Figures 14 and 15 show respectively the disposition of the atoms in a single molecule and the crystal packing arrangement as viewed down the y axis. Refined parameters are listed in Tables, 11, 12 and 13. Final observed and calculated structure factors will be found in Appendix B. The structure consists of discrete centrosymmetric TRANS $\text{SiCl}_4 \cdot 2\text{PMe}_3$ molecules with angles around the central silicon showing only small ($< 5^\circ$) deviations from 90° . Si - Cl and Si - P bond lengths have not previously been available, except in unpublished work on TRANS $\text{SiCl}_4 \cdot 2\text{py}$ (52). Predictably, Si - Cl distances shown at the present state of refinement are longer than those generally found in the chlorosilanes (177) (approx. 2.02 \AA). Again as might be expected, there is statistically no significant difference between individual Si-Cl ($\text{Si-Cl}_1 = 2.30$, $\text{Si-Cl}_2 = 2.20 \text{ \AA}$) bond lengths, or between Si-Cl and Si-P (2.26 \AA) distances. The distances and angles between bonded carbon and phosphorus atoms compare favourably with those reported in the literature (176) (P - C bond length 1.83 \AA and C-P-C angles 100°).

An interesting feature of the model (Fig.14) is that the orientation of the PMe_3 groups are such that each carbon atom is at the apex of a roughly equilateral triangle whose base is the line joining the two nearest chlorine atoms. The distance between an individual carbon atom and each of the nearest chlorines is similar, though not identical (3.3 and 3.8 \AA). Presumably such a configuration minimizes the C-Cl interactions and defines the only way in which co-axial groups having four (SiCl_4 residue) and three fold (PMe_3) axes may attain a minimum of potential energy.

It is unlikely that the present model could be further improved using existing data, which is of modest quality due to a poor crystal, its mounting in glass, and to radiation damage.

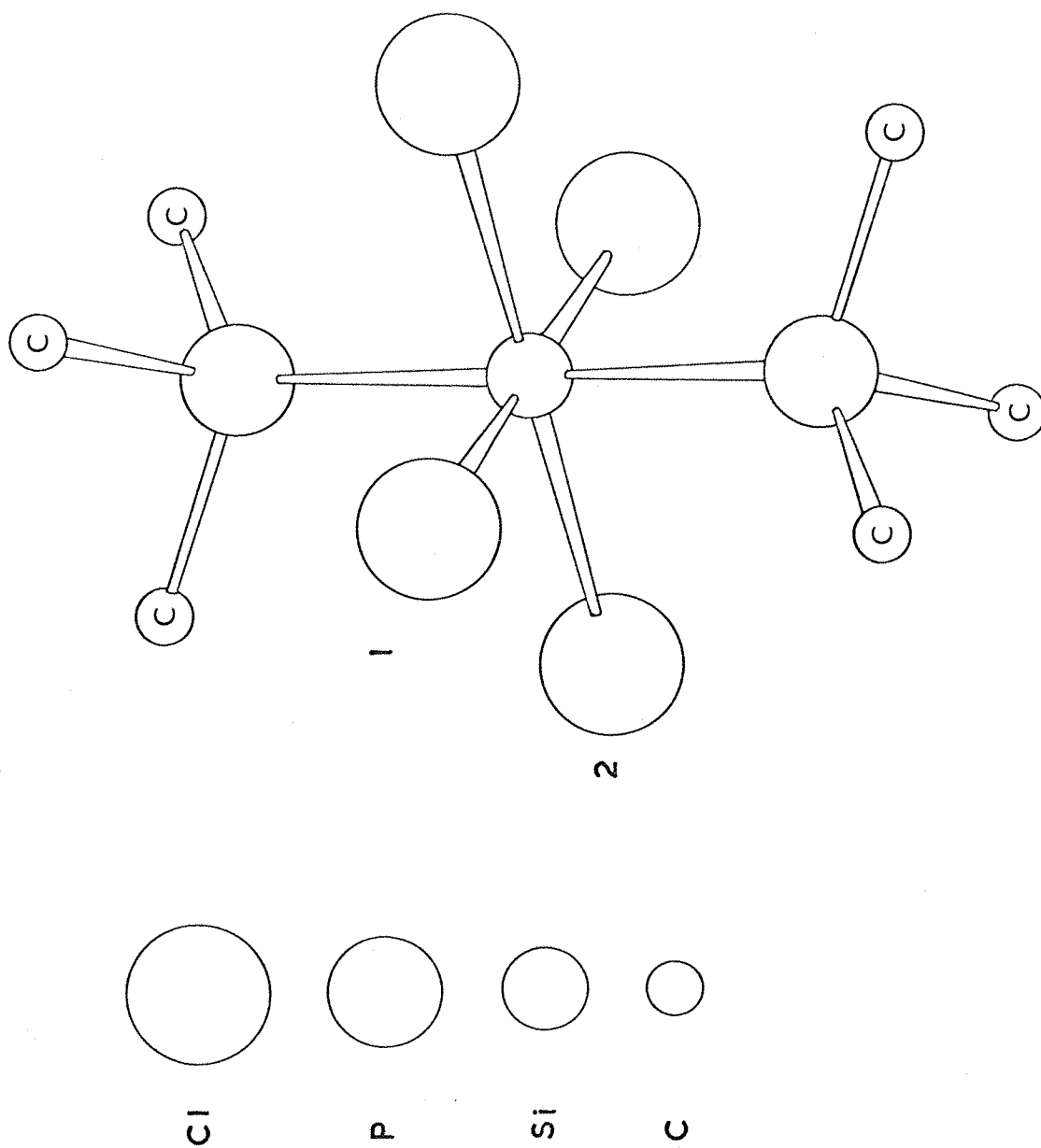


FIGURE 14 STEREOCHEMISTRY OF AN ISOLATED $\text{SiCl}_4 \cdot 2\text{PMe}_3$ MOLECULE

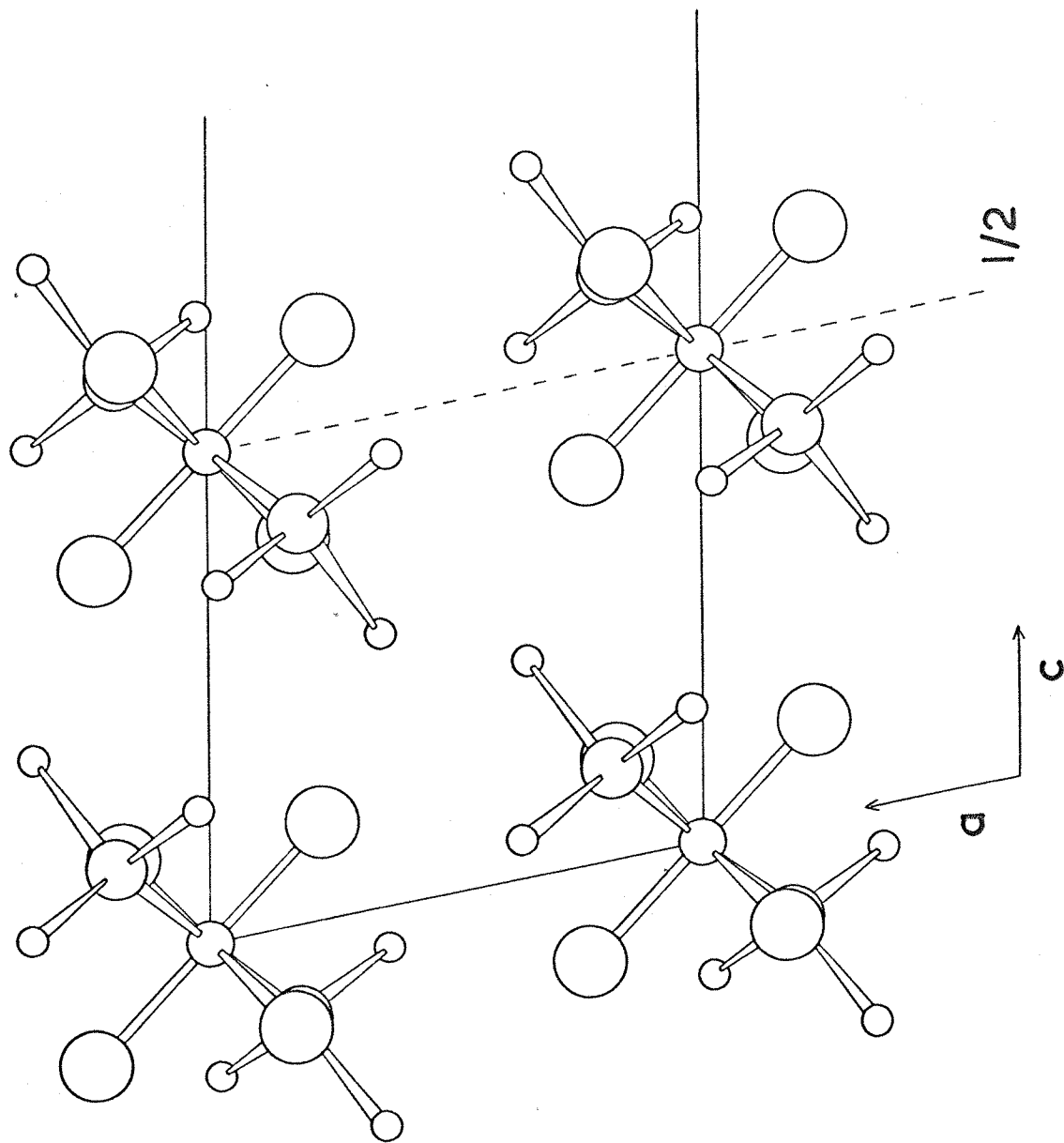


FIGURE 15 THE CRYSTAL PACKING ARRANGEMENT $\text{SiCl}_4 \cdot 2\text{PMc}_3$ [$1/2$ CELL] DOWN Y DIRECTION

TABLE 11
FINAL POSITIONAL AND ISOTROPIC THERMAL PARAMETERS,
WITH STANDARD DEVIATIONS IN PARENTHESES

Atom	x/a	y/b	z/c	B(Å ²)
Si	0.0000 (0)	0.0000 (0)	0.0000 (0)	
Cl ₁	0.1747 (9)	-0.2014 (8)	0.1033 (6)	
Cl ₂	-0.2262 (10)	-0.0105 (11)	0.1002 (6)	
P	0.1831 (14)	0.1999 (12)	0.0951 (9)	
C ₁	0.0169 (56)	0.3546 (45)	0.1377 (35)	4.99
C ₂	0.3623 (49)	0.3218 (43)	0.0392 (29)	4.28
C ₃	0.3501 (53)	0.1308 (46)	0.2230 (32)	4.65

TABLE 12
HEAVY-ATOM ANISOTROPIC TEMPERATURE FACTORS (Å)² *

	B ₁₁	B ₂₂	B ₃₃	B ₁₂	B ₁₃	B ₂₃
Si	2.130	1.078	2.073	0.000	0.475	0.000
Cl ₁	1.743	1.078	2.021	0.000	-2.678	0.000
Cl ₂	3.040	2.235	2.644	0.000	4.801	0.000
P	4.151	3.057	2.854	0.000	2.393	0.000

* In the form:

$$T = \exp \left[-\frac{1}{2} (B_{11} h^2 a^{*2} + B_{22} k^2 b^{*2} + B_{33} l^2 c^{*2} + 2B_{12} hka^* b^* + 2B_{13} hla^* c^* + 2B_{23} klb^* c^*) \right]$$

TABLE 13
MOLECULAR GEOMETRY

A. INTRAMOLECULAR DISTANCES

Distances are between 0.500 - 3.000 Å inclusively

<u>ATOMS</u>	<u>DISTANCE</u> (Å)	<u>ATOMS</u>	<u>DISTANCE</u> (Å)
Si - Cl ₁	2.299 (6)	C ₁ - C ₂	2.874 (58)
Si - Cl ₂	2.196 (7)	C ₁ - C ₃	2.922 (50)
Si - P	2.263 (9)	C ₂ - C ₃	2.895 (56)
P - C ₁	1.851 (42)		
P - C ₂	1.827 (39)		
P - C ₃	1.893 (38)		

B. INTRAMOLECULAR ANGLES

<u>ATOMS</u> ^a	<u>ANGLE</u> (deg)	<u>ATOMS</u>	<u>ANGLE</u> (deg)
Cl ₁ - Si - Cl ₂	86.82 (27)	P - C ₁ - C ₂	38.33 (1.16)
Cl ₁ - Si - P	93.26 (29)	P - C ₁ - C ₃	39.23 (1.14)
Cl ₂ - Si - P	93.25 (35)	C ₂ - C ₁ - C ₃	59.92 (1.32)
Si - P - C ₁	112.55 (1.18)	P - C ₂ - C ₁	38.91 (1.11)
Si - P - C ₂	120.15 (1.27)	P - C ₂ - C ₃	39.75 (1.05)
Si - P - C ₃	114.53 (1.23)	C ₁ - C ₂ - C ₃	60.86 (1.33)
C ₁ - P - C ₂	102.76 (1.75)	P - C ₃ - C ₁	38.18 (1.18)
C ₁ - P - C ₃	102.58 (1.86)	P - C ₃ - C ₂	38.12 (1.05)
C ₂ - P - C ₃	102.13 (1.60)	C ₁ - C ₃ - C ₂	59.22 (1.35)

^a The central atom of the triad is the apex atom.

PART II

CHAPTER 7

CALORIMETRY OF MX₄.2Py COMPLEXES

CALORIMETRIC STUDIES OF SOME MX₄.2py COMPLEXES

(7:1) STABILITY AND DONOR-ACCEPTOR STRENGTH

The term 'stability' when applied to the formation of complexes is often used rather loosely. For example, in studies concerned with the formation of complex ions in solution, the 'thermodynamic stability' is a quantitative measure of the extent to which one species has been converted into another at equilibrium, and under precisely defined conditions.

'Kinetic stability' on the other hand, is taken to apply to the rate at which such changes take place. The majority of stability constant studies refer to aqueous solutions in which the reaction observed is the displacement of water from the sphere of co-ordination by a new ligand. In non-aqueous, non-co-ordinating solvents, a species usually displays its normal symmetry; tetrahedral for the Group IV tetrahalides. When an octahedral complex is formed the halide increases its co-ordination number so that a reorganization energy is involved. This makes it rather difficult to predict relative stabilities. Ideally a quantitative study would involve some means of directly measuring the heat of dissociation of the M-L bond. This, however, is rarely possible and in practise it is usual to arrive at the quantity indirectly. One way of doing this is to measure the heat of reaction of the donor and acceptor in solution and then to compute the required energy from a knowledge of the heats of vapourization, solution and sublimation. These quantities may not of course be available.

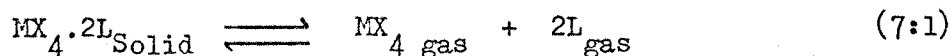
Tensiometric studies of solid complexes may be complicated by incomplete dissociation in the gas phase, thermal decomposition, the formation of solid solutions (3) or in the case of compounds of high stability, by very low vapour pressures.

In some ways spectroscopic methods offer an attractive method of studying trends in stability, both from the point of view of speed and

because they may be conveniently applied to the solid state. For example, the relative change in the infra-red active carbonyl frequency of ethyl acetate has been interpreted in terms of the stability of the adducts formed with SiCl_4 , GeCl_4 , SnCl_4 and SnBr_4 (178). In other studies (12,20) the position of the skeletal M-Cl stretching vibrations of $\text{MCl}_4 \cdot 2\text{L}$ complexes have been taken as an indicator of the M-L bond strength, assuming D_{4h} symmetry. P.M.R. spectroscopy has been used extensively to study the acceptor orders of the boron trihalides towards NMe_3 (179a) and MeCN (179b) by observing the chemical shifts of the methyl protons relative to tetramethylsilane. Mössbauer spectroscopy is potentially capable of giving at least a rough guide to the 'stability' of complexes with a given acceptor, through a comparison of the observed isomer shifts with those of a suitable reference (see Chapter 3). However, although spectroscopic investigations have provided useful results (notably in Group III studies) none of the methods provides a universally useful approach to the question of stability in Group IV. Vibrational spectroscopy is often ambiguous and difficult to interpret; for example, although the formation enthalpies of $\text{SbCl}_5 \cdot \text{Me}_3\text{PO}$ and $\text{SbCl}_3 \cdot \text{Me}_3\text{PO}$ are very different, the P-O stretching frequencies occur at similar positions in the infra-red spectrum (180). N.M.R. spectroscopy is useful only for the more soluble complexes. Mössbauer spectroscopy is both insensitive and cannot be applied to silicon complexes.

Assuming complete dissociation in the gas phase, the stability of a solid complex may be related to its vapour pressure at a particular temperature. The complex may be considered to have measureable stability if the partial pressures of its components at equilibrium are each less than their vapour pressures in the free state at the same temperature. Consider as an example the complex $\text{MX}_4 \cdot 2\text{L}$ dissociating according to equation (7:1). If the vapour pressure above such a complex is measured

as a function of temperature, then in the absence of complicating effects (3), it is possible to determine the equilibrium constant K_p at a number of temperatures. By plotting $\log_e K_p$ against $1/T$ it is possible to evaluate the left hand side of equation 7:3, and therefore to arrive at the enthalpy change ΔH in equation 7:1.



L = Unidentate Ligand

$$K_p = p_{\text{MX}_4} \cdot p_L^2 = \frac{1}{3} P_{\text{obs}} \left(\frac{2}{3} P_{\text{obs}} \right)^2 = 4/27 P_{\text{obs}}^3 \quad (7:2)$$

$$\frac{d \log_e K_p}{d(1/T)} = - \frac{\Delta H}{R} \quad (7:3)$$

$$\text{OR} \quad \Delta H = -R \frac{d \log_e K_p}{d(1/T)} \quad (7:4)$$

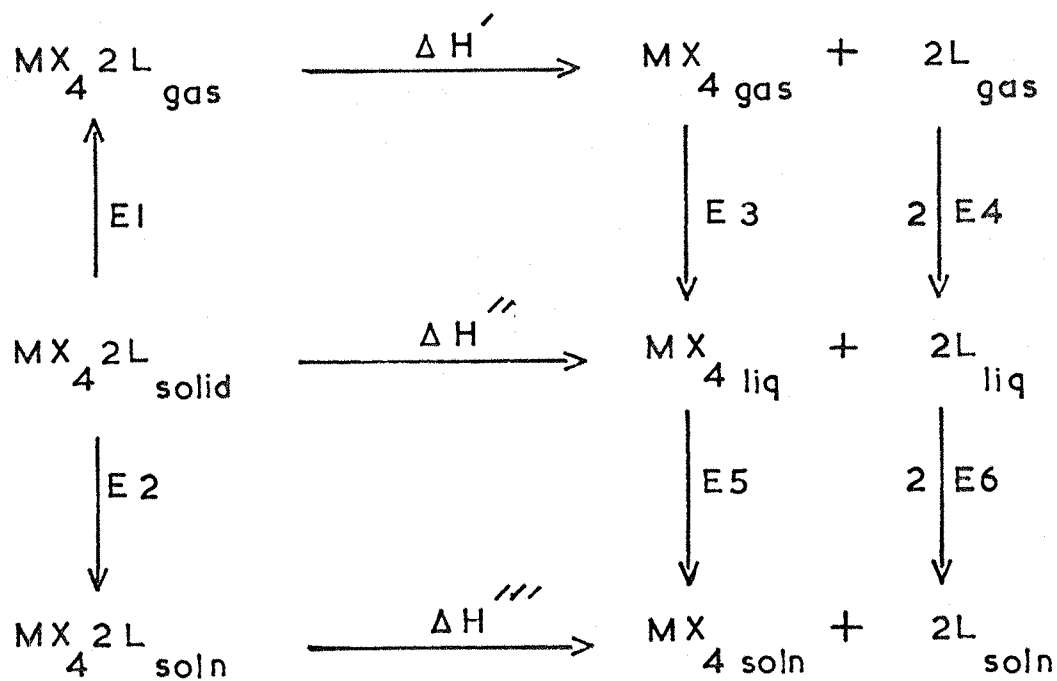
where $R = 1.98733 \text{ cal.deg}^{-1} \text{ mole}^{-1}$

and $T = \text{the absolute temperature } ^\circ\text{K}$

This approach was used by Beattie and Leigh (9) to calculate the formation enthalpy of $\text{SiCl}_4 \cdot 2\text{py}$. The initially reported value of $-11.2 \text{ K.cal.mole}^{-1}$ (9) was found to be in error, but a recalculation has shown the true value to be $-62 \text{ K. cal.mole}^{-1}$, which corresponds to about $-35.6 \text{ K Cal.mole}^{-1}$ in the liquid/solid states. This corrected value, however, is still questionable since the reaction appeared to be incompletely reversible. Unfortunately, it is not possible to measure the lattice energy term E_1 (Fig.16) for complexes which are completely dissociated in the gas phase. Nevertheless, if it is assumed that E_1 is more or less constant for a closely related series of adducts, then it should be possible to make at least qualitative comparisons of donor-acceptor strengths by the method, especially in the presence of adequate structural evidence. Tensiometric studies of the 1:1 and 1:2 complexes of SiX_4 with NMe_3 and PMe_3 have

recently been carried out by Beattie and Ozin (24). Some interesting anomalies are indicated. In particular, the stability sequences $\text{SiF}_4 \ll \text{SiCl}_4 \approx \text{SiBr}_4$ towards PMe_3 , and $\text{SiF}_4 > \text{SiCl}_4 > \text{SiBr}_4$ towards NMe_3 , suggest that steric effects greatly influence the relative donor powers of the two ligands.

Calorimetric measurements of the heats of reaction of Lewis acids with Lewis bases to form molecular addition compounds offer one of the most suitable methods of studying relative donor-acceptor bond strengths. A simple cycle (Fig.16) will show that if the reaction takes place entirely in solution (ΔH^{lll} being determined) the only quantity which cannot be measured experimentally is the lattice energy E_1 ; thus precluding comparisons in terms of ΔH^{l} . By way of compromise, the heats of formation of a related series of complexes must therefore be compared by determining ΔH^{lll} in each case. If the complexes are all very insoluble, comparisons in terms of ΔH^{lll} and ΔH^{lll} are no longer straightforward. They become meaningful, however, if the constancy of the lattice energy term E_1 for the series is again assumed. It has been argued (10,11) that for the Group III halide adducts with pyridine, the heats of sublimation are very close to one another. This sort of assumption certainly seems reasonable for boron trihalide adducts since the sequence of relative acceptor powers derived from the formation enthalpies of the crystalline adducts is identical whether determined by calorimetric, spectroscopic, dipole moment, or N.M.R. measurements. (179a,179b,68). It seems particularly reasonable to suppose that similar assumptions may be applied to the $\text{MX}_4 \cdot 2\text{py}$ species of Group IV, since these are now thought to be isostructural on the basis of X-ray analysis (see Chapter 2). Further, preliminary experiments have suggested that the heats of solution of crystalline $\text{MX}_4 \cdot 2\text{PMe}_3$ adducts in benzene (which include lattice energy terms) are probably all within the range 1.5 - 3.0 K.cal.mole⁻¹.



$$\Delta H' = -E_3 - 2E_4 + \Delta H'' - E_1$$

FIGURE 16 ENTHALPY CYCLE

The literature relating to stability studies in Group IVB is summarized in Table 14. It is immediately apparent that by comparison with other groups very little systematic work has been carried out. Until recently extremely few calorimetric studies concerning the MX_4 acceptors have been available. Apart from one or two studies on the heats of dissociation of MX_4L (181) and $\text{MF}_4\cdot 2\text{L}$ (182) species, most workers seem to have concentrated on the relative donor powers of a variety of ligands towards specific tetrahalides. Notable exceptions in which the acceptor is varied with respect to a single unidentate donor include the work of Onyszchuk et al (68,69^{*},183) and Wannagat (67). Onyszchuk (68) recorded the heats of reaction of the tetrahalides (except SnBr_4) [$\text{M} = \text{Si}, \text{Ge}, \text{Sn}$, $\text{X} = \text{F}, \text{Cl}, \text{Br}$] with pyridine and isoquinoline. Soon after this work was published, Wannagat (67) reported formation enthalpies for $\text{SiF}_4\cdot 2\text{py}$, $\text{SiCl}_4\cdot 2\text{py}$ and $\text{SiBr}_4\cdot 2\text{py}$. These results differed substantially from those of Miller and Onyszchuk and three distinct anomalies subsequently came to light, none of which were satisfactorily explained. Firstly, the formation enthalpies of the isoquinoline adducts were reported as being twice as great as those of the corresponding pyridine complexes. This is surprising because pyridine and isoquinoline are expected to show similar basicities towards the Group IV tetrahalides. Secondly, the formation enthalpies of $\text{SiCl}_4\cdot 2\text{py}$ and $\text{SiBr}_4\cdot 2\text{py}$ were nearly twice that of $\text{SiF}_4\cdot 2\text{py}$. At the time this was explained by the fact that both $\text{SiCl}_4\cdot 2\text{py}$ and $\text{SiBr}_4\cdot 2\text{py}$ were thought to be CIS; $\text{SiCl}_4\cdot 2\text{py}$ at least is now known to be TRANS. Finally, the formation enthalpy of $\text{SnCl}_4\cdot 2\text{py}$ ($-52.9 \text{ K.cal.mole}^{-1}$) obtained by the direct reaction of SnCl_4 with excess pyridine, was substantially greater than the value obtained by Zenchelsky and Segatto (184) in benzene solution. Miller and Onyszchuk (68,69) do not mention their method of purification for SnCl_4 , while Zenchelsky and Segatto used a commercially available sample without further purification. It is well

* Published Dec. 1970

TABLE 14

ACCEPTOR PROPERTIES GROUP IVB TETRAHALIDES

Complex	Method of Study	Information	Ref.
$\text{MX}_4 \cdot \text{ETAC}$	IR	$\text{Sn} > \text{Ge} > \text{Si}, \text{Cl} > \text{Br}$	178
$\text{MX}_4 \cdot \text{NMe}_3$	Heat Dissociation	$\text{GeF}_4 > \text{SiF}_4$ and $\text{GeCl}_4 > \text{SiCl}_4$	181
$\text{MF}_4 \cdot 2 \text{ Ether}$	Heat Dissociation	$\text{GeF}_4 > \text{SiF}_4$ $\text{SnCl}_4 > \text{SnBr}_4 > \text{SnI}_4$	182 185
$\text{SnCl}_4 \cdot 2\text{L}$	Calorimetry	$\text{L} = \text{Variety of donors}$	186
$\text{SnCl}_4 \cdot 2\text{L}$	Calorimetry		187
$\text{SnCl}_4 \cdot 2\text{L}$	Calorimetry	$\text{L} = \text{Various cyclic ethers}$	188
$\text{SnCl}_4 \cdot 2\text{L}$	Calorimetry	$\text{L} = \text{T.H.F., py}$	184
$\text{SnCl}_4 \cdot \text{L}'$	Calorimetry	$\text{L}' = 1,4\text{-dioxane, morpholine}$	184
Various	Various	Weak oxygen donors $\text{Sn} > \text{Ge} > \text{Si}$	3
$\text{SiF}_4 \cdot 2\text{NH}_3$	Heat Dissociation	$\Delta H = -18.2 \text{ K.cal.mole}$	189
$\text{MX}_4 \cdot 2 \text{ Ether}$	VP/IR	$\text{GeF}_4 > \text{SiF}_4$	54/190
$\text{SiX}_4 / \text{NMe}_3 / \text{PMe}_3$	V.P.	$\text{SiF}_4 \ll \text{SiCl}_4, \text{SiBr}_4$ towards PMe_3 and $\text{SiF}_4 > \text{SiCl}_4 > \text{SiBr}_4$ towards NMe_3	24
$\text{SnX}_4 \cdot 2\text{L}$	Calorimetry IR	$\text{SnCl}_4 > \text{SnBr}_4$ $\text{L} = \text{naphthaldehyde}$	106
Various	IR	$\Delta V(\text{OH}) \text{Methanol}, \Delta V(\text{NH}) \text{Pyrrole}$ $\text{Sn} > \text{Ge} > \text{Si}$	191
$\text{MX}_4 / \text{Amine}$	V.P.	$\text{Si, Ge, Ti}, \text{SiCl}_4 \cdot 2\text{py}$ ΔH formation $= -11.2 \text{ K.cal.mole (corrected)}$ -62 K.cal.mole	9
$\text{MX}_4 / \text{Dioxane}$	D.M.	$\text{Sn} \gg \text{Ge} > \text{Si}$ in solution	192
SnX_4 / L	IR	$\text{SnCl}_4 \approx \text{SnBr}_4$ towards Xanthrone	193
$\text{MX}_4 \cdot 2\text{L}$	Calorimetry	Preliminary investigation (see Ref.68)	183
$\text{MX}_4 \cdot 2\text{L}$	Calorimetry	$\text{M} = \text{Si, Ge, Sn}, \text{X} = \text{F, Cl, Br.}$ $\text{L} = \text{Py, isoquinoline}$ <div style="display: flex; align-items: center;"> <div style="margin-right: 10px;"> $\left. \begin{array}{l} 1) \text{SiF}_4 > \text{SiCl}_4 > \text{SiBr}_4 \\ 2) \text{GeF}_4 > \text{GeCl}_4 > \text{GeBr}_4 \\ 3) \text{GeF}_4 > \text{SiF}_4 \\ 4) \text{SnCl}_4 > \text{GeCl}_4 > \text{SiCl}_4 \\ 5) \text{GeBr}_4 > \text{SiBr}_4 \\ 6) \text{GeF}_4 > \text{GeCl}_4 > \text{GeBr}_4 \\ 7) \text{SnCl}_4 > \text{GeCl}_4 \end{array} \right\}$ </div> <div> Towards Iso- quinoline Towards Pyridine </div> </div>	68

TABLE 14 (Continued)

Complex	Method of Study	Information	Ref.
$\text{MX}_4 \cdot 2\text{py}$	Calorimetry	$\text{SiF}_4 < \text{SiCl}_4 \sim \text{SiBr}_4 > \text{SiI}_4 (?)$	67
$\text{MX}_4 \cdot 2\text{L}$	Calorimetry	L = py, isoquinoline M = Si, Ge, Sn $\text{GeF}_4 \cdot 2\text{L} > \text{SiF}_4 \cdot 2\text{L}$	69
$\text{MX}_4 \cdot 2\text{py}$	u.v.	M = Si, Ge. X = F, Cl, Br $\text{SiBr}_4 > \text{SiCl}_4 > \text{GeCl}_4 > \text{SiF}_4$	194

known that both pyridine and the tetrahalides readily absorb moisture.

The development work described in this chapter was initiated with a view to carrying out several extended calorimetric studies on various oxygen and/or moisture sensitive $\text{MX}_4 \cdot n\text{L}$ systems. However, the contrasting results mentioned above suggested the necessity for a re-examination of the relative stabilities of the $\text{MX}_4 \cdot 2\text{py}$ species, especially since these complexes represent such a unique and important series. Their formation enthalpies (M = Si, Ge, Sn. X = Cl, Br) have been determined using a small scale calorimeter. The development of the calorimetric system is reported first. However, when this work was just completed Vandrish and Onyszchuk (69) published a paper repeating their earlier work. As a result discussion naturally centres largely around a comparison of these two sets of results.

(7:2) CALORIMETRY

The energy changes which accompany changes of state and chemical reactions form the subject matter of thermodynamics. The direct evaluation of these energy changes is the aim of the various methods of calorimetry. Calorimetric measurements are particularly useful in that they can ideally

allow a study of the entire course of a chemical reaction, its rate and equilibrium.

There are many types of reaction calorimeters reported in the literature, the design varying according to the physical states of the reaction studied. Solution calorimeters are generally of two main types; constant temperature environment and adiabatic. In the first case the temperature of the surroundings is kept constant and the temperature of the calorimeter either varies or is prevented from changing. If the calorimeter temperature varies there will be a heat exchange between the calorimeter and the environment, and a correction must be made for the net heat change during the course of the experiment. If the calorimeter temperature is kept constant, by the controlled withdrawal or input of heat, we have an isothermal and thus automatically adiabatic system, and no heat exchange occurs between the calorimeter and its surroundings. If the temperature of the surroundings is made to follow the temperature of the calorimeter then we have a non-isothermal or adiabatic system. In this case there will be no heat exchange between the calorimeter and its surroundings and no correction will be needed. For fast reactions (< 1 min) it is usual to use the isothermal type.

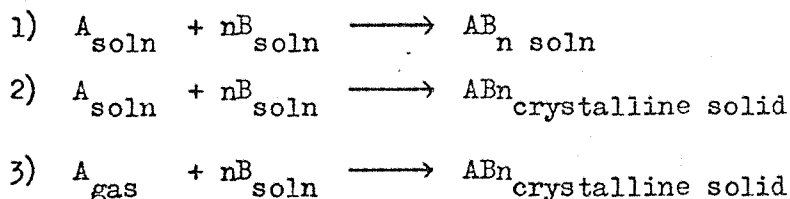
One of the most important devices used by modern precision calorimetry involves, essentially, the measuring of the amount of electrical energy required to duplicate (or nullify, in the case of an endothermic process) the thermal effect accompanying the reaction being studied. The more sophisticated systems are designed to enable a very precise comparison to be made between the actual reaction and the electrical experiment (calibration). Temperature is usually measured very accurately as a function of time and the experimental conditions are chosen so as to provide as identical a temperature change as possible in both experiments. By knowing the amount of electrical energy added in the calibration run,

the precise temperature changes in the two experiments, and by taking the amount of the reactants and stoichiometry into account, a precise value for the energy change may be calculated.

(7:3) REQUIREMENTS OF THE CALORIMETER

The variety of chemical reactions makes it very difficult to design an efficient and universally useful reaction calorimeter. It is generally better and more convenient to construct the apparatus with a specific type of reaction in mind. Several microcalorimeters are now commercially available^x based on design features already reported in the literature (195-199). Such instruments are potentially capable of giving very precise results ($< 0.1\%$) for many reactions in solution.

The types of reaction to be considered for the formation of Group IVB complexes are in general threefold:



In many cases these systems are both oxygen and/or moisture sensitive. Enthalpies of formation are typically 20-60 K.cal.mole⁻¹. Since moisture free solvents and reactants are very difficult to obtain in large quantities, an important design requirement is that the effective volume of the calorimeter should be reduced to a minimum. Reactions of type (2), of which the formation of $\text{MX}_4 \cdot 2\text{py}$ is typical, introduce a second essential requirement; that the resulting heterogeneous reaction mixture should be very efficiently stirred. It is particularly difficult on a small scale to provide for reactions involving gaseous components, so that reactions

^x L.K.B. Instruments Ltd., LKB House, 232, Addington Road,
S. Croydon, Surrey, England. CR2 8YD

of type (3) (e.g. the formation of $\text{SiF}_4 \cdot 2\text{py}$) are referred to a separate design. (To be described in a later study). A consideration of these and related requirements indicates that the following limiting features might be expected to define the optimum design for the study of reactions (1) and (2).

- a) The total effective volume should be not greater than 25-30 mls with overall volume of perhaps 60 mls.
- b) The total amount of energy evolved should be less than 100 cal. If $\Delta H \approx -50 \text{ K.cal.mole}^{-1}$ only 2 millimoles of the complex need be formed. Such a quantity probably represents the limit for accurate weight measurements.
- c) It should be possible to maintain strictly anhydrous conditions during the entire course of the experiment.
- d) It should be possible to stir both homogeneous and heterogeneous reaction mixtures efficiently.
- e) Accuracy and precision should be better than 1%.

The reaction rate is fast (typically < 30 secs) so that two further requirements follow:

- f) The thermal lag of the calorimeter should be less than 2 mins.
- g) The overall time required to supply electrical energy during the calibration should be of the same order as the reaction period (i.e. < 30 secs).

(7:4) DESIGN CONSIDERATIONS

(i) ELECTRICAL MEASUREMENTS

Procedures for the determination of temperature as a function of thermistor resistance are well established. Using modern equipment only very small errors in electrical measurements are expected provided

the heater is correctly designed. Time may be measured to within 0.1% even when manual switching is employed. Since the required precision is only about 1%, errors arising from these sources are very small in comparison to those induced by the calorimeter and impurities in the reagents. For the present discussion precision in these measurements is therefore assumed.

(ii) EXCLUSION OF MOISTURE

Since calorimetric experiments concerning complex formation in solution generally involve the formation of only small quantities of the complex in comparatively large quantities of liquid, it is vitally important to ensure that moisture is excluded. This requires that all reagents have been rigorously dried. It must be remembered that if only 2 millimoles. of a complex are formed in 30 mls of solvent then only a few parts per million moisture in that solvent are required to produce a significant mole ratio complex:water. Several studies have been carried out using calorimeters having volumes in excess of 100 mls. It is reasonable to suppose that this volume might be reduced to 25-30 mls without greatly affecting the reproducibility.

Several precision calorimeters have been used to study moisture sensitive systems outside the dry box, but these are not ideally suited for use in the dry box. Reduced size renders the dual function of the stirrer/breaker a necessity, and simplicity of design is in itself important in reducing errors due to adsorbed moisture. Preliminary experiments have shown that conventional rotary stirrers are incapable of providing efficient mixing for heterogeneous systems in a small volume. As far as is known, no microcalorimeter has yet been constructed which combines reciprocal stirring with the ampoule breaking mechanism, and at the same time is capable of being used under normal conditions. However, bearing

in mind that a precision of only about 1% is required (compared to 0.01 - 0.1% in precision work) it is reasonable to expect the most meaningful results to be obtained by carrying out the entire experiment inside the dry box. This makes it impracticable to use conventional thermostat baths. Nevertheless, providing reasonable temperature control ($\pm 0.5^{\circ}\text{C}$) is provided, the advantages of being able to combine simplicity of design with reciprocal stirring and ultra dry conditions should outweigh the disadvantages of not having precise ambient temperature control[‡] ($\pm 0.001^{\circ}\text{C}$).

(iii) MATERIALS

The masses and types of materials used to construct an isothermal calorimeter may greatly affect its efficiency. In their extended study of isothermal calorimeters Sumner and Wadso (196) drew attention to the fact that "Any construction which creates an indetermined boundary of the calorimeter system towards the surroundings leads to slow equilibration". This means that an insulating material used to slow down the rate of heat transfer may introduce an appreciable thermal lag. This in turn results in the slow attainment of the normal cooling curve and decreases the accuracy of extrapolation.

The heat capacity of the calorimeter itself automatically introduces a degree of thermal lag. The effect becomes increasingly noticeable as the size of the apparatus is reduced, since it is difficult to make corresponding reductions in the relative masses of the components. Heat losses resulting from electrical connections and the stirring mechanism are also magnified by reduced scale. As a general rule, therefore, it is better to use good conductors of minimal mass (suitably isolated

[‡] This is not true for slow reactions.

from the surroundings) than to attempt to prevent heat losses by using insulation in direct contact with the contents of the calorimeter.

Electrical connections in more or less direct contact with the contents must be of the finest possible gauge; a point particularly relevant to heater design.

(iv) STIRRING AND AMPOULE-BREAKING MECHANISM

Efficient stirring is known to be one of the most difficult things to achieve in precision calorimetry. The combination of stirring and ampoule-breaking mechanism is a now well established device (196), but no satisfactory reciprocal ampoule-breaking mechanism has yet been devised. Ideally, provision should be made for complete and instantaneous mixing of the reactants with only a small and yet predictable heat of rupture. Errors due to inconsistencies in the strength of the sample bulbs have been shown to be significant for very precise work (196). Perhaps more important, however, is the difficulty of preventing small quantities of unreacted material being trapped in the neck of the bulb by the formation of the solid complex. This is to be expected particularly when ampoules are sealed under vacuum or when the diameter of the neck is small enough to provide appreciable capillary action. Ideally, the ampoule-breaking pin should be designed to completely displace the reacting materials from the neck.

The rapid response of the thermistor compared to thermocouple devices, has if anything increased the need for efficient stirring. A high stirring efficiency is essential for the study of a series of heavy crystalline complexes because differences in the density and ageing characteristics of the precipitates may cause problems of reproducibility. The first problem in the present study was therefore to develop a simple reciprocating stirrer and combined ampoule breaker.

(v) ACCURACY AND PRECISION

If accuracy in the reacting quantities, electrical measurements and time are assumed, by far the largest errors arise from the fact that the determination is a comparative procedure. This is particularly so for fast reactions since it is impossible to supply electrical energy at a suitably high rate. The efficiency of a calorimeter is therefore highly dependent on two factors; a) thermal lag, b) the gradient of the cooling curve (i.e. the time taken to reach equilibrium). It is required to extrapolate the normal cooling curve through an interval which is half the time taken to dissipate the net reaction or calibration energies (Fig.22). It follows that whereas the total interval requiring correction for the reaction may be $2\frac{1}{2}$ mins.; correction for the calibration may involve an uncertainty of up to 4 mins. Acceptable results will be obtained only if the thermal lag and the slope of the cooling curve are both small.

(7:5) THE FINAL CALORIMETER

Figure 17 and plate 1 show the essential features of the isothermal solution and reaction calorimeter at its present stage of development. The design is based on the best features of several previously reported instruments (195,196,200-202) and is intended to be used entirely in a dry box atmosphere at a fixed temperature within a range of approximately 15°C - 40°C . Figure 18 is a block diagram of the calorimetric system as a whole. Figure 19 shows the temperature control, drive mechanism and the disposition of the instrument in the dry box.

The calorimeter proper consists of a thin walled Pyrex glass reaction Dewar based on a standard B.34 socket and evacuated to approximately 10^{-4} mm Hg. A B.34 Teflon sleeved brass cone serves as a support for a 2000 OHM thermistor, a 50 OHM calibration heater, and as a bearing

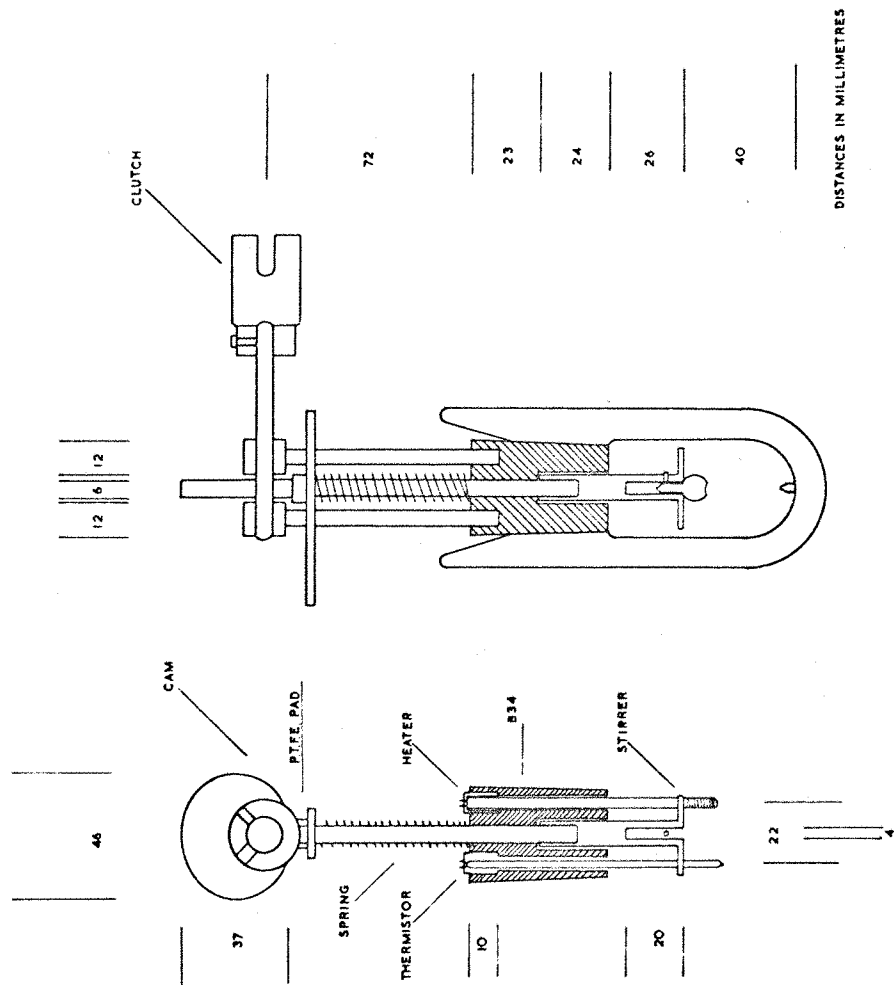


FIG.17 SOLUTION AND REACTION CALORIMETER

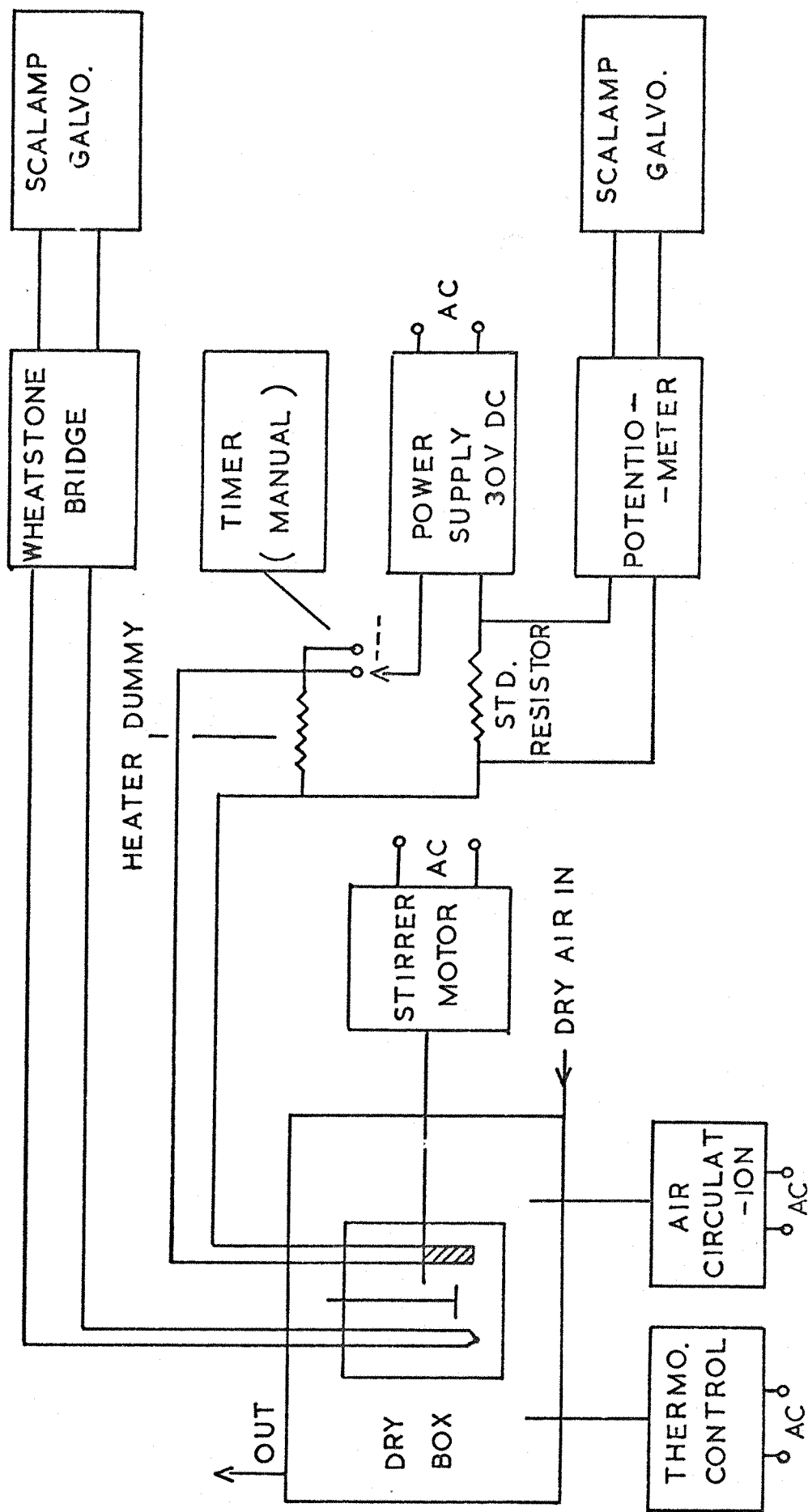


FIGURE 18 SCHEMATIC DIAGRAM OF CALORIMETRY SYSTEM

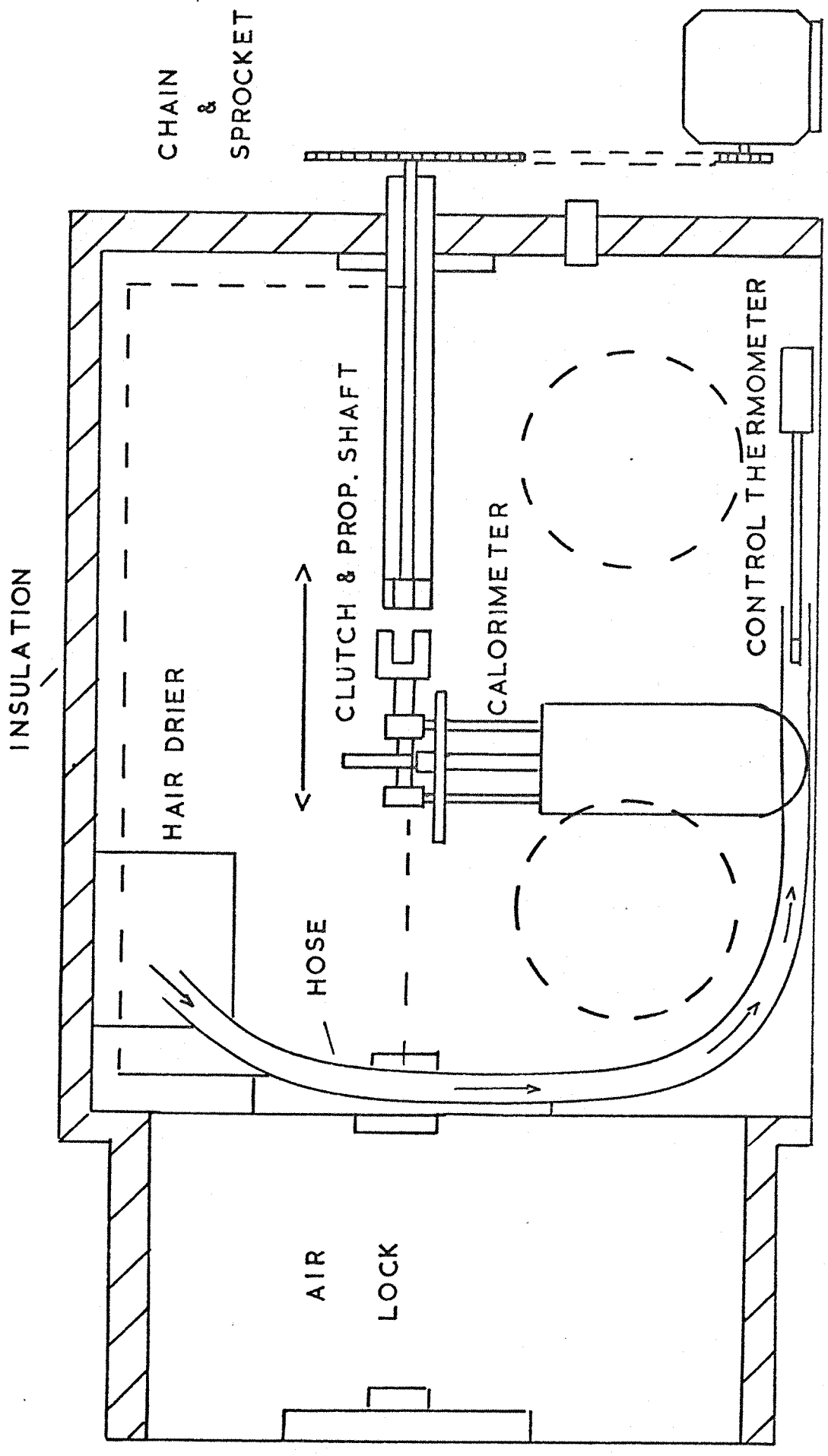


FIGURE 19 DRY BOX LAYOUT AND AMBIENT TEMPERATURE CONTROL SYSTEM

for a simple overhead cam operated reciprocal stirring mechanism. The calorimeter is remotely driven by an electric motor situated outside the dry box. The Teflon^{*} stirrer is machined to a minimum thickness and also serves as a holder for a cylindrical 1 ml Pyrex glass sample ampoule, (blown from 4 mm tubing). Holes in the paddle allow for clearance of the thermistor and heater.

When operating, the stirrer and attached ampoule reciprocate through a distance of 2.5 cms at 120 cycles per min. This allows for a clearance of approximately 2 mm between the sample ampoule and the glass spike. The ampoule is ruptured against the spike by depressing the entire stirring assembly through a distance of 1 cm beyond that provided by the cam. The dimensions of the spike are such that it penetrates the ampoule neck to a distance of a few millimetres.

^{*} Should ideally be gold or other noble metal.

DRIVE MECHANISM

The stirring mechanism is driven by an electric motor (see page 100 for details of all auxiliary equipment), situated outside the dry box and geared in a ratio 1:5 using 'Meccano' chain and sprockets. The remotely situated (Fig.19) calorimeter is connected to the motor by way of a simple 'dog tooth' clutch and propeller shaft.

TEMPERATURE DETECTION

The thermistor forms one arm of a conventional D.C. Wheatstone bridge network. A sensitive galvanometer allows a temperature change of approximately $1.10^{-4}^{\circ}\text{C}$ to be detected. The thermistor's glass extension probe and leads are isolated from the calorimeter head by a machined Teflon insert.

ELECTRICAL CALIBRATION

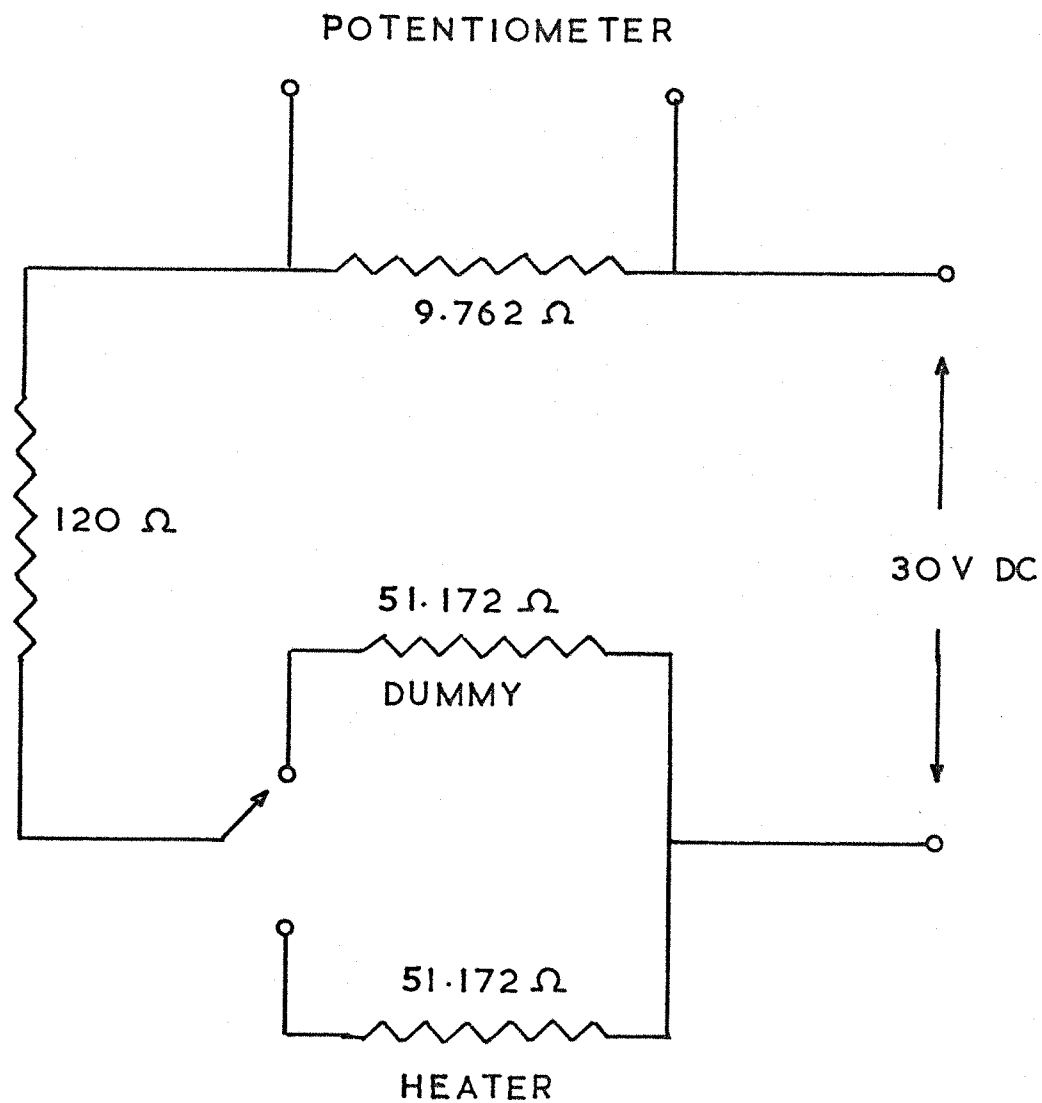
The calibration heater is used to release a known quantity of electrical energy which is determined by the current through the heater circuit, the heater resistance (measured using a potentiometer), and the time which is measured with a chronometer. Figure 20 gives a schematic diagram of the electrical calibration circuit. Power for the heater is supplied by a stabilized 30 V.DC source. Current through the heater is determined by measuring the voltage drop across a series standard resistor (9.762 OHMS) with a vernier potentiometer. A matched ballast resistor is used to stabilize the DC supply prior to calibration. A single pole double throw switch is used manually to disconnect the ballast and to connect the heater for the required time. All heat quantities are given in calories. (1 normal calorie = 4.1840 Joules (203)).

CALIBRATION HEATER

The heater consists of a Nichrome wire (42 s.w.g.) 50 OHM coil wound on to a hollow bakelite former (4.5 mm diameter x 10 mm). The leads are spot welded (1 cm from the coil) to insulated low resistance Nichrome wires (20 s.w.g.). This coil is encapsulated in a 5 mm (OD) precision thin walled Pyrex tube (N.M.R. tube). Thermal conductivity between the windings and the glass tube is ensured by adding a single drop of dry Nujol. A machined Teflon cap provides support and isolates the heater from the calorimeter head (see Fig.21).

(7:6) TEMPERATURE CONTROL OF DRY BOX

A temperature of $30^{\circ}\text{C} \pm 0.25^{\circ}\text{C}$ is maintained by a 100 watt carbon filament heater (lamp) used in conjunction with a conventional control thermometer. Electrical power (AC) is switched on and off as required by a 9 amp relay. Dry (< 50 p.p.m. moisture) air circulation



RESISTORS PRECISION WIRE WOUND

FIGURE 20 CALIBRATION CIRCUIT

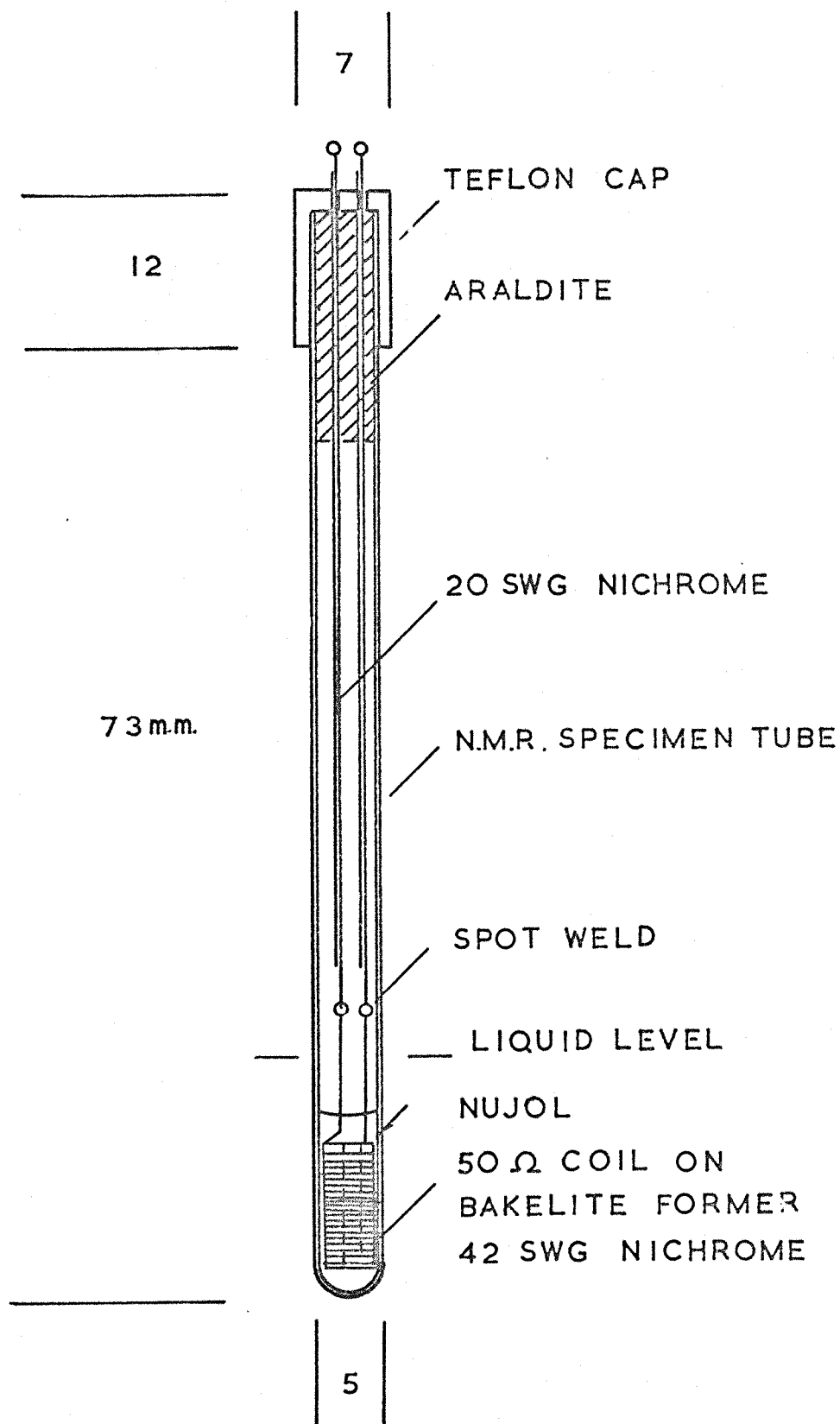


FIGURE 21 CALIBRATION HEATER

is provided by a hair drier fitted with a flexible hose, positioned so that air at the ceiling of the box is continuously returned to the floor. The control thermometer is situated inside the flexible hose. The exterior of the dry box is insulated with expanded polystyrene and blistered transparent polythene (over the window) (See Fig.19).

(7:7) DETAILS OF AUXILIARY EQUIPMENT

(CALORIMETER)

-THERMISTOR

S.T.C. Type F. Code No.F23D

Nominal resistance $R_{20} = 2k$

$R_{25} = 1.7k$, $k = 0.85 \text{ m.w./}^{\circ}\text{C}$

-CALIBRATION HEATER

51.172 Ω , 20°C

-DRIVE MOTOR

Citenco Type 29.

Torque 8 oz/in at 350 R.P.M.

Gear ratio 5:1 using 'Meccano' chain and sprockets.

ELECTRICAL

Wheatstone Bridge

D.C. Conventional

Standard Resistors (Bridge)

Precision Wire Wound Type (Muirhead

1 k $\pm 0.1\%$

Standard Resistor (Heater
Circuit)

9.762 OHMS

Variable Resistance

Decade Box. H.W. Sullivan type AC 1013

Galvanometers

Pye Scalamp

Power (Bridge and Pot)

Lead accumulators 2V (Exide type DHG)

Standard Cell

Cadmium cell. 1.01859 V at 20°C

Cambridge Instruments.

Potentiometer

Tinsley Type 4363E-auto.

Power (Calibration Heater)

30V.DC Mullard type L280 stabilized
source.

TEMPERATURE CONTROL

Heater (Dry box)	100 watt Carbon filament lamp (covered with aluminium foil)
Control Thermometer	Shandon 5.62
Relay	Sunvic F 102/4 9 amp.
Air Circulation	Hair drier (Morphy Richards) (synchronous motor) fitted with flexible hose.

(7:8) TESTING THE FINAL CALORIMETER

The heat of neutralization of dilute solutions of hydrochloric acid and sodium hydroxide (69) and the heat of solution of potassium chloride (196) are frequently used standards for solution calorimetry. The latter quantity is very accurately known[‡]. However, the enthalpy change is endothermic (KCl_{soln} , $\Delta H = + 4.194 \pm .003 \text{ K.cal.mole}^{-1}$) and although it provides a reliable check of systematic and random errors due to the calorimeter (used in the constant temperature sense) it provides little information about the overall performance for exothermic reactions. The heat of neutralization of HCl/NaOH is conveniently exothermic ($\Delta H = -13.37 \text{ K.cal.mole}^{-1}$ at infinite dilution). Unfortunately, the precise value is a function of the acid-base (or salt) molality. $\text{KCl}(\text{molal} = 0)$ $\Delta H = -13.37 \text{ K.cal.mole}^{-1}$, $\text{KCl}(\text{molal} = 0.4955)$ $\Delta H = -13.75 \text{ K.cal.mole}^{-1}$ (204). This concentration dependence, together with the number of measurements required to define the reacting quantities, makes the reaction a rather inconvenient standard for precise work. It nevertheless provides a useful check on performance for exothermic reactions and has the distinct advantage of not being moisture sensitive. The exothermic solution

[‡]For a discussion of the use of KCl as a standard see ref.196.

enthalpies of dilute mineral acids are rather too small to act as a useful comparison ($\approx -5\text{K.cal.mole}^{-1}$).

The reliability of the present calorimeter was checked with reference to both the heat of neutralization of HCl/NaOH and the heat of solution of KCl . A sample of pure (Analar) KCl was pulverized, carefully dried at 105°C for 2 hours and stored in vacuum over phosphorus pentoxide. About 400 m.g. were weighed out corresponding to a mole ratio $\text{KCl}:\text{H}_2\text{O}$ of approximately 1:400. Sample ampoules were loaded in the dry box. Solution enthalpies were determined by the constant temperature method. A series of five determinations gave an average value of $\Delta H = + 4.362 \pm .030$ K.cal.mole^{-1} compared to the accepted value $\Delta H = + 4.194 \pm .003$ K.cal.mole^{-1} (196) (see table 15). The average heat of neutralization of 5N HCl (1-4 millimoles determined by WT/SG methods) in 30 mls N. NaOH was $\Delta H = -13.5 \pm 0.1$ K.cal.mole^{-1} . This agrees favourably with the literature value $\Delta H = -13.48$ K.cal.mole^{-1} (204) for the salt molality used (i.e. $\text{KCl} \approx 0.15$ molal).

The heat of rupture of waterfilled ampoules in water was just detectable, but varied little between samples. The thermal effect was thought to be insignificant with regard to the precision of the present experiments.

Overall thermal lag as determined from typical cooling curves (Fig.22) is 2 minutes.

Stirring efficiency with reference to a sand/water mixture was found to be completely satisfactory at 120 cycles min.^{-1} . Thermal effects of stirring are negligible.

The self-heating effect of the thermistor produces a continuous change of resistance of 0.05 OHMS.min^{-1} at 30°C .

TABLE 15

HEAT SOLUTION POTASSIUM CHLORIDE 25.0°C *

Wt. KCl Gms	Millimoles KCl	P.D. over Standard Resistor (V)	Current in Heater (A) $\times 10^{-1}$	Time Current Passed (secs)	Electrical Calories Delivered	Heat Soln. KCl K.cal. Mole ⁻¹	Deviation from Mean
.3204	4.2972	.77757	.79653	240	18.763	4.366	+ .004
.2996	4.0182	.77364	.79250	226	17.491	4.352	- .010
.3379	4.5319	.77620	.79512	252	19.632	4.332	- .030
.4637	6.2192	.76939	.78815	357	27.327	4.394	+ .032
.4367	5.8570	.76843	.78716	335	25.579	4.367	+ .005
Mean =						(4.362)	

* Literature value 4.194 K.cals.mole⁻¹ (196)

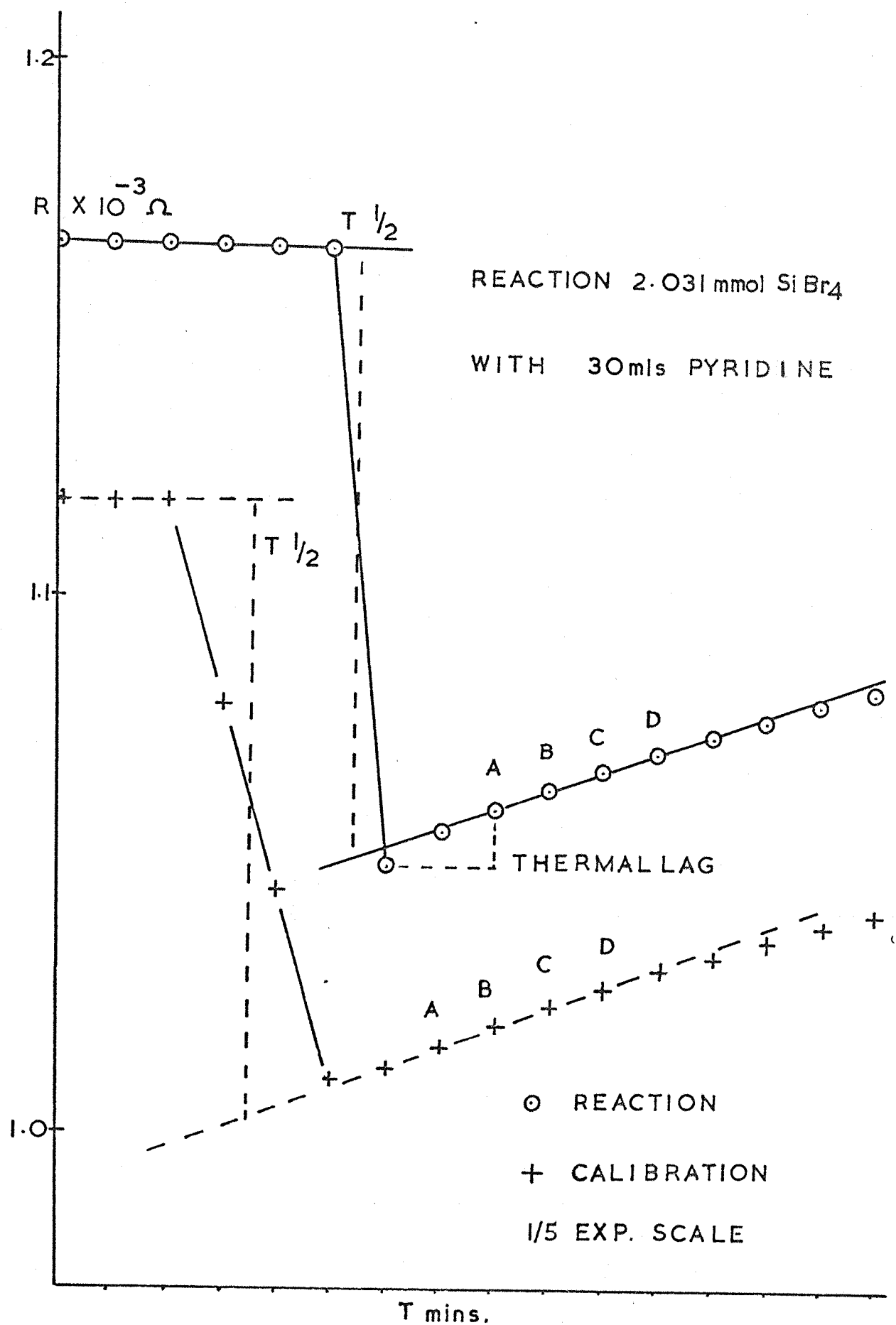


FIGURE 22 RESISTANCE V:S TIME PLOTS

(7:9) THE DETERMINATION OF THE FORMATION ENTHALPIES OF CRYSTALLINE
 $\text{MX}_4 \cdot 2\text{py}$ COMPLEXES

(1) PREPARATION OF REAGENTS

Pyridine was dried by standing it over $\text{SiCl}_4 \cdot 2\text{py}$ (9) (prepared in situ.) for a period of two weeks. The dry material was then distilled several times in an all glass vacuum system. During the final distillation the pure pyridine was sealed into individual 40 ml bulbs. A fresh bulb was opened for each experiment.

The tetrahalides MX_4 ($\text{M} = \text{Si}, \text{Ge}, \text{Sn}$, and $\text{X} = \text{Cl}, \text{Br}$) were dried by standing them over acridine for two weeks. The dry material was then degassed, vacuum distilled, and finally sealed into fragile break-seal ampoules. Accurately weighed sample ampoules were connected to the vacuum line using polythene tubing and filled by distillation with 1-4 m.moles of the tetrahalide. Ampoules were sealed off 1 cm above the bulb.

EXPERIMENTAL PROCEDURE

The reactions were carried out by rupturing the tetrahalide ampoules under 30 mls of neat pyridine. The routine outlined below was strictly followed for each experimental run.

- (1) The dismantled calorimeter and samples were allowed to stand in the dry box overnight prior to the experiment.
- (2) A fresh bulb of pyridine was opened and 30 mls pipetted into the reaction Dewar. The ampoule containing the tetrahalide was attached to the stirrer and the instrument immediately reassembled.
- (3) All electrical systems were allowed to run at their normal settings for a period of 2 hours before starting the reaction.
- (4) Temperature was recorded for periods of 15 mins. before and after the start of the reaction or calibration by plotting thermistor resistance as a function of time at 1 min. intervals.

(5) The calorimeter was allowed to cool for one hour with the thermistor switched off, and then to re-equilibrate for 2 hours prior to the calibration. As far as possible all calibration procedures were identical with those of the reaction. The time during which current was passed through the calibration heater was varied (2 - 4 mins) so that the temperature changes duplicated as closely as possible those produced by the reaction.

(6) Heating and cooling curves were approximated by straight lines (Fig.22). The precise slope of the cooling curves were routinely defined by the 3rd, 4th, 5th and 6th measurements (A - D Fig.22) following the reaction or calibration. The first two measurements are affected by the thermal lag of the calorimeter. Straight lines were extrapolated to $T = \frac{1}{2}$ of the energy input period to give the initial and final resistances.

(7) The stirrer and reaction vessel were removed from the dry box and washed with detergent and water. After rinsing with acetone they were returned to the dry box for overnight drying. Moving parts were cleaned without removing them from the box using dry chloroform.

(8) Bearing surfaces were lightly lubricated before each run using specially dried machine oil.

(9) The heats of reaction ΔH K.cal.mole⁻¹ were determined from the following relationships:

$$\text{Heat evolved by reaction } h = Q.r$$

$$\text{where } r^* = \frac{\log \frac{\text{Initial resistance}}{\text{Final resistance}} \quad (\text{Reaction})}{\log \frac{\text{Initial resistance}}{\text{Final resistance}} \quad (\text{Calibration})}$$

$$\text{and } Q = \frac{I^2 RT}{J} = \text{heat supplied electrically}$$

where I = current in the heater (amps)

R = heater resistance (OHMS) = (51.172)

T = Time (secs)

J = Mechanical equivalent of heat defined by

$$1 \text{ normal cal.} = 4.1840 \text{ Joules } (203)$$

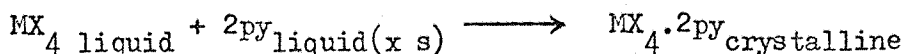
* Exponential response of thermistor

$$\text{Heat of reaction } H = \frac{1000 Q_r}{m} \text{ K.cal.mole}^{-1}$$

where m is the quantity of complex formed in millimoles.

(7:10) RESULTS AND DISCUSSION

Table 16 gives the heats of formation of crystalline $MX_4 \cdot 2py$ complexes ($M = Si, Ge, Sn$ and $X = Cl, Br$) from the pure constituents according to the reaction



For comparison, enthalpies are given for $SiCl_4 \cdot 2py$ determined using pyridine dried $SiCl_4^{\text{I}}$, and for $SnCl_4 \cdot 2py^{\text{II}}$ using $SnCl_4$ purified by vacuum distillation alone (i.e. without the use of acridine). The differences between these new results and those of Miller and Onyszchuk (68) vary by between 1-22 K.cal.mole⁻¹. Values for $SiCl_4 \cdot 2py$ and $SiBr_4 \cdot 2py$ are in quite good agreement with those of Wannagat et al (67) and with the recent results of Vandrish and Onyszchuk (69). They are somewhat lower than the corrected value obtained for $SiCl_4 \cdot 2py$ ($\Delta H = -35$ K.cal.mole⁻¹) obtained from vapour pressure measurements by Beattie and Leigh (9). Apart from the value for $SnCl_4 \cdot 2py$, results for the series as a whole are in broad agreement with Vandrish and Onyszchuk (69). In this particular case, however, the discrepancy is large (-13 K.cal.mole⁻¹) the present value being almost identical with that obtained in earlier work (68). A similar discrepancy is shown with the value obtained by Zenchelsky and Segatto (184) in benzene solution. The fact that the most recently published results are in all cases comparable with values for isoquinoline (68,69) suggests that the value for $SnCl_4 \cdot 2py$ obtained in the present study is in error. Further evidence to this effect is found in the fact that preliminary experiments using $SnCl_4$ which had been only vacuum

^I with subsequent vacuum distillation

TABLE 16

HEATS OF FORMATION OF CRYSTALLINE $\text{MX}_4 \cdot 2\text{py}$

$\text{SiCl}_4 \cdot 2\text{py}$		$\text{SiBr}_4 \cdot 2\text{py}$		$\text{GeCl}_4 \cdot 2\text{py}$		$\text{GeBr}_4 \cdot 2\text{py}$		$\text{SnCl}_4 \cdot 2\text{py}$		$\text{SnBr}_4 \cdot 2\text{py}$	
$-\Delta H_f$	DEV^\times	$-\Delta H_f$	DEV^\times	$-\Delta H_f$	DEV^\times	$-\Delta H_f$	DEV^\times	$-\Delta H_f$	DEV^\times	$-\Delta H_f$	DEV^\times
30.28	+ 0.15	29.93	+ 0.20	33.16	- 0.49	27.92	+ 1.56	50.36	- 1.62	39.85	- 1.34
30.56	+ 0.43	29.76	+ 0.03	33.92	+ 0.27	24.80	- 1.56	53.46	+ 1.48	42.08	+ 0.89
30.45	+ 0.32	29.60	- 0.13	33.96	+ 0.31	27.84	+ 1.48	52.44	+ 0.46	43.94	+ 2.75
29.58	- 0.55	29.63	- 0.10	33.56	- 0.09	26.95	+ 0.59	52.85	+ 0.87	37.86	- 3.33
29.77	- 0.36					25.82	- 0.54	51.98	0.00	42.24	+ 1.05
Mean						25.05	- 1.31	50.81	- 1.17		
(30.13)	(0.36)	(29.73)	(0.12)	(33.65)	(0.29)	(26.36)	(1.03)	(51.98)	(0.93)	(41.19)	(1.87)
py dried SiCl_4		$\text{SnCl}_4 \cdot 2\text{py}^\times$									
31.49		41.0									
28.28		46.1									
29.81		42.8									
(29.86)		40.1									
		46.9									
		40.7									
		41.9									
		(42.8)									

$-\Delta H_f$ = Heat reaction MX_4 in neat pyridine. K.cal.mole⁻¹
 (ΔH_f) = Mean value
 DEV^\times = Deviation from the mean
 (DEV^\times) = Mean deviation
 $\text{SnCl}_4 \cdot 2\text{py}^\times$ (Preliminary Results)

distilled (without the use of ^{ACRIDINE}~~acidine~~) gave an average result ($\Delta H = -42.8 \text{ K.cal.mole}^{-1}$) nearer to that of Vandrish and ^{ONYSZCHUK,}~~Onyszchuk~~. Unfortunately, the latter workers do not specify the exact procedure used to dry their SnCl_4 . Of all the halides this is the most likely to be hydrated. The complex $\text{SnCl}_4 \cdot 2\text{H}_2\text{O}$ distills quite easily under vacuum (205). A possible, though admittedly speculative, explanation for the present high result is that the smaller value results from ligand substitution involving water and pyridine. Obviously, the present $\text{SnCl}_4 \cdot 2\text{py}$ values require further investigation. However, it is interesting to note that the ratio of the enthalpies $\text{SnCl}_4 \cdot 2\text{py} : \text{SnBr}_4 \cdot 2\text{py}$ (51.98 : 41.19) is almost identical with that observed for the analogous naphthaldehyde complexes (29.6 : 22.8) (106).

On the basis of the results shown in Table 16 it is tempting to suggest the following sequences of acceptor strengths:

- (1) $\text{SnCl}_4 \gg \text{GeCl}_4 > \text{SiCl}_4$
- (2) $\text{SnBr}_4 \gg \text{SiBr}_4 > \text{GeBr}_4$
- (3) $\text{Cl} > \text{Br}$

Apart from $\text{SiBr}_4 > \text{GeBr}_4$ such an order is in agreement with the most frequently occurring trends shown by the literature collected in Table 14. As has already been mentioned, however, the interpretation of relative acceptor powers for a series of tetrahalides on the basis of the condensed phase enthalpies, must take into consideration the solution $E_{2,5,6}$ and the crystal lattice energies (E_1) (Fig.16). These parameters were originally thought to be comparable throughout the series. With the exception of the tin complexes which show a (suspect) difference of $\sim 10 \text{ K.cal.mole}^{-1}$, differences between the others are not sufficiently large to allow any confident predictions to be made, since crystal lattice energies, even assuming the complete dominance of one isomer, may vary by $\pm 3 \text{ K.cal.mole}^{-1}$. It is therefore difficult to decide whether the

formation enthalpy of $\text{SiBr}_4 \cdot 2\text{py}$ is abnormally high or that of $\text{GeBr}_4 \cdot 2\text{py}$ abnormally low. Ironically these are the only two members of the series whose structures have not been defined by X-ray diffraction methods. If $\text{SiBr}_4 \cdot 2\text{py}$ is CIS it would have a higher dipole moment than the TRANS isomer and as a result would have a larger crystal lattice energy. This might easily account for the $\sim 3.4 \text{ K.cal.mole}^{-1}$ by which the $\text{SiBr}_4 \cdot 2\text{py}$ result appears to be high. However, it must be pointed out that enthalpies reported for $\text{SiF}_4 \cdot 2\text{py}$ ($-34.3 \text{ K.cal.mole}^{-1}$) and $\text{SiCl}_4 \cdot 2\text{py}$ ($-29.4 \text{ K.cal.mole}^{-1}$) (69) show a difference ($\Delta = 4.9 \text{ K.cal.mole}^{-1}$) which is only slightly greater, and these are both known to be TRANS. Even so, the closeness of the observed enthalpies suggests that the X-ray powder photographs of $\text{SiCl}_4 \cdot 2\text{py}$ and $\text{SiBr}_4 \cdot 2\text{py}$, together with their germanium analogues, should be examined in order to make sure that all the complexes are TRANS. Unfortunately, the dipole moments cannot be measured because the complexes are insoluble. An abnormally low enthalpy for $\text{GeBr}_4 \cdot 2\text{py}$ is less easy to account for, unless it results from an abnormally low 'TRANS' lattice energy.

The calorimetric system as a whole proved to be a convenient and satisfactory instrument for the study of moisture sensitive complexes. Long equilibrium times make it difficult to carry out more than one accurate experiment per day. The precision (1%) in the $\text{Si} \rightarrow \text{Ge}$ portion of the series studied was felt to be entirely satisfactory. The decreasing precision (5%) on passing from $\text{GeCl}_4 \rightarrow \text{SnBr}_4$ is not easy to explain. There are two probable explanations. Firstly, several of the precipitated complexes ($\text{SnBr}_4 \cdot 2\text{py}$, $\text{SnCl}_4 \cdot 2\text{py}$, and $\text{GeBr}_4 \cdot 2\text{py}$) appeared to age rather more quickly than the others with respect to their crystallite size during the period between the reaction and the calibration. Aging depends on several factors, one of which is the number of nuclei available for initial crystallization. This, of course, depends on the degree of

cleanliness within the calorimeter; something which is very difficult to control under dry box conditions. If the degree of sedimentation (a little always occurs) varies for different experiments, errors resulting from incomplete mixing are likely to occur. Such an effect would be expected to be most noticable for the heavier precipitates.

Another possibility is that since the volume of tetrahalide required to produce a given amount of heat becomes smaller with increasing exothermicity, errors due to material being trapped in the ampoule neck become increasingly significant.

Any further increases in the performance of the system are likely to result from attention to the following points:

- (1) The use of a stirrer having a high thermal conductivity.
 - (2) A more precise method of controlling the ambient temperature is required.
 - (3) The addition of an automatic timing mechanism for calibration.
 - (4) The use of an improved sample ampoule is indicated.
-

APPENDIX

- (A) EXPERIMENTAL (X-RAY SECTION)
- (B) OBSERVED AND CALCULATED STRUCTURE FACTORS
- (C) REFERENCES

A. EXPERIMENTAL (X-ray Section)

All manipulations were performed either in a dry box (moisture content < 50 pp.m.) or using an all glass vacuum system. Purified reagents were introduced into the vacuum system using the 'fragile glass seal' technique.

PURIFICATION OF REAGENTS

Silicon tetrachloride (9), tin tetrachloride (20) and acetonitrile (56) (used in X-ray studies) were purified according to methods reported in the literature.

Carbon tetrachloride, dibromomethane, and chlorobenzene (pycnometer liquids) were dried over calcium hydride and distilled.

Carbon tetrachloride and benzene used as solvents were dried by refluxing for 24 hours over calcium hydride and purified by distillation under high vacuum.

ANALYSIS

Chloride analyses were performed on approximately 100 m.g. samples of material ($\text{SnCl}_4 \cdot 2\text{MeCN}$) after hydrolysis, by potentiometric titration against 0.1 M silver nitrate solution.

The complex $\text{SiCl}_4 \cdot 2\text{PMe}_3$ was prepared and characterized by Dr. G.A. Ozin (23,24).

CHEMICAL SUPPLIERS

Silicon tetrachloride	B.D.H.
Silicon tetrabromide	Alfa Inorganics, Ventrom. Beverly, Mass.
Germanium tetrachloride	B.D.H.
Germanium ^{TETRABROMIDE} tetrachloride	Koch-Light Labs.Ltd., Colnbrook, Bucks. Eng.
Tin tetrachloride	B.D.H.
Tin tetrabromide	B.D.H.
All other chemicals	B.D.H.

APPENDIX B

OBSERVED AND CALCULATED STRUCTURE FACTORS

APPENDIX B F_O AND F_C $SnCl_4 \cdot 2MeCN [\times 10]$

[illegible]

AN ASTERISK INDICATES A LESS THAN THE MINIMUM
OBSERVED INTENSITY

I	F ₀	F _c	I	F ₀	F _c	I	F ₀	F _c	I	F ₀	F _c	I	F ₀	F _c
-1	552	-521							-1	536	-629	-1	223	123
-2	501	-502							-2	163*	-65	-2	223*	9
-3	664	732							-3	714	906	-3	318	337
-4	568	545							-4	170*	77	-4	227*	130
-5	630	-652							-5	631	-741	-5	484	-455
-6	254	-298							-6	183*	-107			
-7	261	240							-7	566	651			
-8	190*	140							-8	199*	122			
-9	371	-313							-9	687	-732			
-10	338	-339							-10	218*	-57			
-11	477	508							-11	478	466			
-12	361	361							-12	238*	-12			
-13	317	-325												
	2,12.L													
0	177*	-86							0	176*	-51			
1	697	684							1	174*	-113			
2	180*	29							2	183*	-3			
3	717	-750							3	267	186			
4	146*	106							4	197*	-27			
5	512	557							5	387	374			
6	197*	-39							6	353	339			
7	421	-421							7	652	-696			
8	205*	-76							8	383	-401			
9	356	376							9	452	467			
10	217*	24							10	426*	196			
11	378	-396							-1	177*	23			
12	335*	33							-2	176*	-127			
13	403	418							-3	176*	-234			
14	245	1							-4	182*	89			
15	361	-339							-5	187*	131			
-1	337	-264							-6	193*	-6			
-2	176*	-24							-7	200*	-60			
-3	177*	-80							-8	208*	224			
-4	181*	-1							-9	281	300			
-5	184*	119							-10	428	-354			
-6	146*	108							-11	697	-649			
	2,13.L								-12	244*	204			
0	392	348							0	373	357			
1	558	-376							1	363	-317			
2	480	-434							2	1002	-1150			
3	486	494							3	456	441			
4	276	225							4	467	1048			
-1	392	401							5	493	-367			
-2	315	-256							6	461	-418			
-3	477	-319							-1	267	263			
-4	437	396							-2	476	-329			
-5	574	617							-3	269	-292			
-6	374	-396							-4	636	808			
-7	381	-369							-5	198*	196			
-8	291	246							-6	317	-348			
-9	298	247							-7	410*	-162			
-10	306	-266							-8	412	406			
-11	317	-323							-9	318	236			
-12	227*	259							-10	332	-470			
-13	438*	254												
	2,14.L													
0	329	320							0	382	449			
1	197*	20							1	287	197			
2	281	-203							2	391	-301			
3	201*	34							3	210*	-101			
4	287	254							4	216*	85			
5	208*	-116							5	222*	4			
6	357	-382							-1	199*	-65			
7	217*	134							-2	200*	166			
8	466	506							-3	202*	-82			
9	227*	-157							-4	606	-629			
10	497	-300							-5	208*	82			
11	247*	117							-6	406	397			
12	382	362							-7	219*	-82			
-1	196*	101							-8	379	-292			
-2	417	-416							-9	234*	140			
-3	196*	-151							-10	457	406			
-4	334	257							-11	250*	-99			
-5	202*	14							-12	367	-310			
-6	277*	-30												
	2,15.L													
0	286*	-201												
1	406*	-152							0	610	-533			
2	437	436							1	542	-526			
3	297	187							2	364	372			
4	447	-426							3	464	516			
5	210*	-94							4	320	-281			
6	312	297							5	386	-359			
7	227*	63							-1	628	724			
-1	207*	121							-2	629	717			
-2	291	284							-3	702	-799			
-3	207*	-219							-4	580	-528			
-4	261	-646							-5	590	450			
-5	211*	210							-6	224*	162			
-6	243	606												
-7	216*	-124							0	224*	-37			
-8	372	-351							1	319	-302			
-9	227*	133												
-10	326	304												

I	Fo	Fc	I	Fo	Fc	I	Fo	Fc	I	Fo	Fc	I	Fo	Fc	
	4,3,L		-1	421	435					4,15,L		4	202	207	
			-2	621	695		4,10,L					2	2/2	297	
			-3	660	-744							0	311	-257	
0	427	-303	-4	513	-250	0	227	185	0	468	-416	7	143	-139	
1	701	663	-5	204	341	1	137	36	1	248	-175				
2	350	257	-6	240	242	2	140	-93	2	526	537				
3	600	-504	-7	304	-277	3	143	-11	3	253	210		5,7,L		
4	348	-260	-8	493	-417	4	394	318	4	540	-479				
5	729	693	-9	510	513	5	151	12	5	189	-168	0	112	73	
6	362	277	-10	544	592	6	176	-131	6	396	349	1	598	654	
7	920	-923	-11	593	-336	7	101	43	7	192	110	2	119	-127	
8	453	-337	-12	217	-270	8	238	-164				3	643	-731	
9	810	646	-13	227	187	9	175	-125		4,10,L		4	129	28	
10	413	298	-14	237	206	10	525	-533				5	308	322	
11	531	-524	-15	240	-266	11	135	83		182	155	6	141	-10	
12	169	-156	-16	250	-220	12	490	443				7	147	-243	
13	251	228				13	139	12		5,8,L		8	154	64	
14	185	90		4,7,L		14	382	-383				9	367	478	
-1	638	-693				15	146	107				10	167	-58	
-2	353	391	0	254	-153	16	587	594		2	387	-317	11	366	-471
-3	694	915	1	1044	-1051	17	155	-214		4	103	76	12	101	55
-4	347	-361	2	260	250	18	528	-524		6	229	-273	13	315	345
-5	534	-640	3	1044	1160					8	314	291			
-6	259	228	4	180	-100		4,11,L			10	292	-261		5,6,L	
-7	265	194	5	972	-636					12	169	180			
			6	139	80	0	425	350					0	323	319
			7	477	503	1	369	372		0	312	359	1	404	-341
			8	152	-52	2	208	-186		1	420	427	2	126	-67
			9	362	-371	3	315	-310		2	642	-656	3	130	114
0	142	-52	10	160	39	4	217	185		3	431	-474		5,9,L	
1	242	158	11	394	382	5	399	347		4	474	214			
2	256	148	12	180	-76	6	436	-371		5	257	224	0	260	241
3	146	126	13	426	-364	7	496	-457		6	397	-31	1	218	-184
4	613	527	-1	473	482	8	463	432		7	217	-231	2	397	-473
5	447	-346	-2	110	7	9	478	471		8	349	399	3	137	179
6	490	-393	-3	157	-189	10	349	-308		9	369	410	4	301	427
7	133	87	-4	113	32	11	360	-336		10	523	-464	5	146	-115
8	295	-211	-5	314	341	12	196	179		11	307	-374	6	319	323
9	146	109	-6	121	60	13	423	-451		12	284	344	7	157	162
10	327	246	-7	410	-367	14	423	-395		13	251	240	8	343	382
11	163	-117	-8	132	-60	15	513	537					9	165	-137
12	287	-202	-9	349	259	16	368	331					10	369	-445
13	179	167	-10	144	-7	17	436	-447					11	182	122
14	350	321	-11	213	-146								12	310	355
-1	32	145					4,12,L			0	227	-210			
-2	527	-600				0	151	-1		1	204	-443		5,10,L	
-3	393	-421	0	363	-270	1	152	60		2	85	113			
-4	603	612	1	401	327	2	154	30		3	389	386	0	450	-413
-5	346	366	2	170	25	3	263	237		4	106	-152	1	136	-29
-6	665	-673	3	182	-180	4	160	-18		5	280	-640	2	297	303
-7	478	-516	4	133	-20	5	416	-349		6	200	146	3	144	20
-8	749	945	5	130	17	6	168	25		7	331	320	4	338	-430
-9	572	546	6	144	-70	7	173	15		8	139	-29	5	152	-102
-10	607	-623	7	310	291	8	178	-63					6	399	414
			8	262	170	9	260	206					7	163	68
			9	273	-202	10	189	47		0	70	-8			
			10	169	-29	11	275	-201		1	252	-229		5,11,L	
			11	175	-25	12	200	-9		2	212	-211	0	143	11
			12	143	3	13	150	174		3	647	634	1	145	-78
			-1	723	-807	14	150	-5		4	270	282	2	146	139
			-2	430	459	15	496	-510		5	240	-250	3	317	328
			-3	697	769	16	152	-14		6	177	-199	4	219	-197
			-4	203	-200	17	414	446		7	437	560	5	334	-368
			-5	124	-151	18	157	37		8	199	229	6	274	262
			-6	128	80	19	475	-457		9	441	-639	7	320	379
			-7	168	164	20	164	-67		10	221	-274	8	291	-342
			-8	314	-262	21	552	522		11	344	422	9	340	-393
			-9	559	-555	22	172	39		12	172	173	10	261	262
			-10	401	312	23	297	-301					11	190	256
			-11	461	467	24	183	15					12	196	-124
			-12	229	-198										
			-13	238	-292		4,13,L			0	277	-220		5,12,L	
			-14	248	158	0	224	182		1	351	326			
			-15	258	209	1	405	-351		2	290	344	0	151	4
						2	340	-320		3	498	-410	1	387	426
				4,9,L		3	442	410		4	684	-693	2	155	-51
			0	863	-675	4	450	417		5	374	422	3	400	-430
			1	365	323	5	460	-436		6	213	253	4	161	49
			2	706	661	6	333	-302		7	192	-172	5	347	404
			3	365	-248	7	377	385					6	170	-35
			4	646	-628	8	261	225						5,13,L	
			5	275	235	9	268	-304		0	284	-263			
			6	493	441	10	260	287		1	100	-42	0	224	-159
			7	220	-243	11	267	-222		2	247	241	1	227	237
			8	409	-419	12	264	-233		3	111	106	2	230	209
			9	237	202	13	265	-233		4	507	-540	3	276	-480
			10	467	481	14	268	232		5	125	-137	4	236	-235
			11	180	-147	15	271	226		6	508	506	5	243	235
			12	393	-344	16	164	-161		7	139	90	6	249	218
			13	194	113					8	434	-500			
			-1	320	-291		4,14,L			9	153	-15		5,14,L	
			-2	641	687	0	349	-274		10	432	540			
			-3	127	127	1	352	115		11	168	10			
			-4	425	-405	2	169	85		12	248	-343	0	379	431
			-5	132	-63	3	230	-146		13	183	-24		5,15,L	
			-6	191	160	4	492	468		14	269	261			
			-7	139	77	5	166	133					0	246	257
			-8	204	-165	6	280	-317							
			-9			7	169	-52							
						8				0	429	594			
						9				1	422	4262			

APPENDIX C

REFERENCES.

REFERENCES

1. J.J. Park, D.M. Collins and J.L. Hoard, J. Amer. Chem. Soc., 1970 92, 12, 3636.
2. E.L. Muetterties and C.M. Wright, J. Amer. Chem. Soc., 1964, 86, 5132.
3. I.R. Beattie, Quart. Rev. Chem. Soc., 1963, 17, 382.
4. D.S. Dyer and R.O. Ragsdale, Inorg. Chem., 1969, 8, 1116.
5. C.E. Michelson, D.S. Dyer and R.O. Ragsdale, J. Chem. Soc., (A) 1970, 2296.
6. R. West, R.H. Baney and D.L. Powell, J. Amer. Chem. Soc., 1960, 82, 6269.
7. R.O. Ragsdale and B.B. Stewart, Proc. Chem. Soc., 1964, 194.
8. R.O. Ragsdale and B.B. Stewart, Inorg. Chem., 1963, 1002.
9. I.R. Beattie and G.J. Leigh, J. Inorg. Nuc. Chem., 1961, 23, 55.
10. N.N. Greenwood and T.S. Srivastava, J. Chem. Soc. (A), 1966, 267.
11. M.F. Lappert and J.K. Smith, J. Chem. Soc., 1965, 5826.
12. H.A. Brune and W. Zeil, Z. Phys. Chem., 1962, 32, 384.
13. H.A. Brune and W. Zeil, Z. Naturforsch., 1961, 16a, 1251.
14. A. Werner and P. Pfeiffer, Z. Anorg. Chem., 1898, 17, 82.
15. P. Pfeiffer and O. Halperin, Z. Anorg. Chem., 1914, 87, 335.
16. H.J. Coerver and C. Curran, J. Amer. Chem. Soc., 1958, 80, 3522.
17. Y.N. Terenin, W. Filimonov and D. Bystrov, Z. Elektro. Chem., 1958, 62, 180.
18. T.L. Brown and M. Kubota, J. Amer. Chem. Soc., 1961, 83, 4175.
19. I.R. Beattie and L. Rule, J. Chem. Soc., 1965, 2995.
20. I.R. Beattie, G.P. McQuillan, L. Rule and M. Webster, J. Chem. Soc., 1963, 1514.
21. M.F. Farona and J.R. Grasselli, Inorg. Chem., 1967, 6, 1675.
22. J. Masaguer and V. Coto, Anales de Quim., 1965, 61, B, 905.
23. I.R. Beattie and G.A. Ozin, J. Chem. Soc. (A), 1970, 370.
24. I.R. Beattie and G.A. Ozin, J. Chem. Soc. (A), 1969, 2267.

25. M. Gielen and N. Sprecher, *Organometal. Chem. Rev.*, 1966, 1, 455.
26. B.J. Aylett, "The Stereochemistry of Main Group IV Elements" in "Progress in Stereochemistry", 1968, 4, P213. Eds. B.J. Aylett and M.M. Harris. Butterworths, London.
27. A.A. Lavigne and J.M. Tancrede, *Coord. Chem. Rev.*, 1968, 3, 497-508.
28. M. Webster, Ph.D. Thesis, London 1962.
29. L. Rule, Ph.D. Thesis, London 1964.
30. D.S. Brown, F.W.B. Einstein and D.G. Tuck, *Inorg. Chem.*, 1969, 8, 1, 14.
31. S.R. Leone, B. Swanson, D.F. Shriver, *Inorg. Chem.*, 1970, 9, 9, 2189.
32. D.F. Shriver and I. Wharf, *Inorg. Chem.*, 1969, 8, 2167.
33. R.F. Bryan, *J. Amer. Chem. Soc.*, 1964, 86, 733.
34. I.R. Beattie, T. Gilson, K. Livingston, V. Fawcett and G.A. Ozin, *J. Chem. Soc. (A)*, 1967, 712.
35. F.W.B. Einstein, B.R. Penfold, *Chem. Comm.*, 1966, 780.
36. I.R. Beattie and T. Gilson, *J. Chem. Soc.*, 1965, 6595.
37. D.I. Cook, R. Fields, M. Green, R.N. ^{HASZELDINE}~~Hazeldine~~, B.R. Iles, A. Jones and M.J. Newlands, *J. Chem. Soc. (A)*, 1966, 887.
38. H.C. Clark, P.W.R. Corfield, K.R. Dixon and J.A. Ibers, *J. Amer. Chem. Soc.*, 1967, 89, 3360.
39. H.C. Clark and K.R. Dixon, *Chem. Comm.*, 1967, 717.
40. J.Y. Corey and R. West, *J. Amer. Chem. Soc.*, 1963, 85, 4034.
41. B.J. Aylett and J.M. Campbell, *Chem. Comm.*, 1967, 159
42. R. Rudham, W.C. Hamilton, S. Novick and T.D. Goldfarb, *J. Amer. Chem. Soc.*, 1967, 89, 5157.
43. H.J. Campbell-Fergusson and E.A.V. Ebsworth, *J. Chem. Soc. (A)*, 1967, 5, 705.
44. I.R. Beattie and F.W. Parrett, *J. Chem. Soc. (A)*, 1966, 1784.
45. F. Klanberg and E.L. Muetterties, *Inorg. Chem.*, 1968, 7155.
46. I.R. Beattie, T.R. Gilson and G.A. Ozin, *J. Chem. Soc. (A)*, 1968, 1092.

47. G.A. Ozin, Chem. Comm., 1969, 3, 104.
48. T.J. Pinnavia, W.J. Collins and J.J. Howe, J. Amer. Chem. Soc., 1970, 29, 15, 4544.
49. T. Ito and N. Tanaka, Inorg. Nucl. Chem. Lett. 1969, 5, 781.
50. I.R. Beattie, T. Gilson, M. Webster and in part G.P. McQuillan, J. Chem. Soc., 1964, 238.
51. I.R. Beattie, T. Gilson and G.A. Ozin, J. Chem. Soc. (A), 1968, 2772.
52. V.A. Bain, R.C.G. Killeen and M. Webster, Acta. Cryst. B.25, 1969, 1, 156.
53. H.E. Blayden and M. Webster, Inorg. Nucl. Chem. Lett., 1970, 6, 703.
54. G.P. Guertin and M. Onyszchuk, Can. J. Chem., 1969, 47, 1275.
55. T. Tanaka, G. Matsubayashi and A. Shimizu, Inorg. Nucl. Chem. Lett., 1967, 3, 8, 275.
56. I.R. Beattie, P.J. Jones and M. Webster, J. Chem. Soc. (A), 1969, 218.
57. T. Tanaka, G. Matsubayashi, A. Shimizu and S. Matsuo, Inorg. Chim. Acta., 1969, 3, 2, 187.
58. D. Kummer, H. Koester and M. Speck, Angew. Chem. (Int. Ed.) 1969, 8, 8, 599.
59. I.R. Beattie and G.A. Ozin, J. Chem. Soc. (A), 1968, 2373.
60. D.W. Thompson, Inorg. Chem., 1969, 8, 9, 2015.
61. W.H. Nelson, Inorg. Chem., 1967, 6, 1509.
62. J.A.S. Smith and E.J. Wilkins, Chem. Comm., 1965, 381.
63. J.W. Faller and A. Davison, Inorg. Chem., 1967, 6, 182.
64. P.A.W. Dean and D.F. Evans, J. Chem. Soc. (A), 1970, 2569.
65. P.A.W. Dean and D.F. Evans, J. Chem. Soc. (A), 1968, 1154.
66. A.D. Adley, D.F.R. Gilson and M. Onyszchuk, Chem. Comm., 1968, 813.
67. V. Wannagat, F. Vielberg, H. Voss, K. Henson and W. Sarholz, Monatsh. Chem., 1969, 100, 4, 1127.
68. J.M. Miller and M. Onyszchuk, J. Chem. Soc. (A), 1967, 1132.
69. G. Vandrish and M. Onyszchuk, J. Chem. Soc. (A), 1970, 3327.

70. A.A. Ennan, B.M. Kats, U.N. Anisimov and E.I. Yur'eva, Zh. Neorg. Khim., 1969, 14, 11, 3172.
71. J. Bleidelis, A. Kemme, L.O. Atovmjan and R.P. Shibaeva, Khim. Geterotsikl. Soedin., 1968, (1), 184, (Russ.) (C.A. 100650e).
72. J.E. Fergusson, W.R. Roper and C.J. Wilkins, J. Chem. Soc., 1965, 3716.
73. S. Craddock, P.W. Harland and J.C.J. Thynne, Inorg. Nucl. Chem. Lett. 1970, 6, 425.
74. R. Hulme, G.J. Leigh and I.R. Beattie, J. Chem. Soc., 1960, 366.
75. V.A. Nazarenko, N.U. Lebedeva and L.I. Vinarova, Zh. Neorg. Khim, 1970, 15, 3, 330.
76. W.B. Vincent and J.L. Hoard, J. Amer. Chem. Soc., 1942, 64, 1233.
77. A.W. Laubengayer, O.B. Billings and A.E. Newkirk, J. Amer. Chem. Soc. 1940, 62, 546.
78. M. Cox, R.J.H. Clark and H.J. Milledge, Nature, 1966, 212, 1357.
79. N. Serpone and R.C. Fay, Inorg. Chem. 1969, 8, 2379.
80. J.A.S. Smith and E.J. Wilkins, J. Chem. Soc. (A), 1966, 1749.
81. T.J. Pinnavia, L.J. Matienzo, Y.A. Peters, Inorg. Chem., 1970, 9, 4, 993.
82. K. Furue, T. Kimura, M. Yasuoka, N. Kasai and M. Kakudo, Bull. Chem. Soc. Jap., 1970, 43, 1661.
83. M. Honda, M. Komura, Y. Kawasaki, T. Tanaka and R. Okawara, J. Inorg. Nucl. Chem., 1968, 30, 3231.
84. T. Kamitani and T. Tanaka, J. Inorg. Nucl. Chem. Lett., 1970, 6, 91.
85. K.M. Harmon, L. Hesse, L.P. Klemann, C.W. Kochler, S.V. McKinley and A.E. Young, Inorg. Chem., 1969, 8, 1054.
86. G.J.D. Peddle and G. Redl, J. Amer. Chem. Soc., 1970, 92, 2, 365.
87. M. Komura, T. Tanaka and R. Okawara, Inorg. Chem. Acta., 1968, 2, (3), 321 (Eng).
88. S.C. Jain and R. Rivest, J. Inorg. Nucl. Chem., 1970, 32, 1579.
89. R. Rivest, S. Singh and C. Abraham, Can. J. Chem., 1967, 45, 3137.
90. M. Webster and H.E. Blayden, J. Chem. Soc. (A), 1969, 2443.

91. J. Reedijk and W.L. Groenveld, *Rec. Trav. Chim.*, 1967, 86, 1103: 1968, 87, 552.
92. A.J. Carty, T. Hinsperger, L. Mihichuk and H.D. Sharma, *Inorg. Chem.*, 1970, 9, 11, 2573.
93. T. Tanaka and T. Kamitani, *Inorg. Chim. Acta.*, 1968, 2, 2, 175.
94. J. Philip, M.A. Mullins and C. Curran, *Inorg. Chem.*, 1968, 7, 9, 1895.
95. S.H. Hunter, V.M. Langford, G.A. Rodley and C.J. Wilkins, *J. Chem. Soc. (A)*, 1968, 2, 305.
96. I.R. Beattie, M. Milne, M. Webster and in part H.E. Blayden, P.J. Jones, R.C.G. Killeen and J.L. Lawrence, *J. Chem. Soc. (A)*, 1969, 3, 482.
97. C.E. Michelson, D.S. Dyer and R.O. Ragsdale, *J. Inorg. Nucl. Chem.* 1970, 32, 3, 833.
98. T. Tanaka, Y. Matsumura, R. Okawara, Y. Musya and S. Kinumaki, *Bull. Chem. Soc., Jap.*, 1968, 41, 7, 1497.
99. K.G. Huggins, F.W. Parrett and H.A. Patel, *J. Inorg. Nucl. Chem.*, 1969, 31, 1209.
100. E.A. Kravchenko, Yu.K. Maksyutin, E.N. Gur'yanova and G.K. Semin, *Izv. Akad. Nauk, S.S.S.R. Ser. Khim.*, 1968, 6, 1271.
101. M.T. Rogers and J.A. Ryan, *J. Phys. Chem.*, 1968, 72, 4, 1340.
102. S. Ichiba, M. Mishima, H. Sakai and H. Negita, *Bull. Chem. Soc., Jap.*, 1968, 41, 49.
103. S. Ichiba, M. Mishima and H. Negita, *Bull. Chem. Soc., Jap.*, 1969, 42, 6, 1486.
104. P.A. Yeats, J.R. Sams and F. Aubke, *Inorg. Chem.*, 1970, 9, 740.
105. Z. Iqbal and T.C. Waddington, *J. Chem. Soc. (A)*, 1968, 8, 1745.
106. R.C. Paul, H.C. Singal and S.L. Chadha, *J. Inorg. Nucl. Chem.*, 1970, 32, 3205.
107. R.C. Paul, P. Singh, S.L. Chadha and H.S. Makhani, *J. Inorg. Nucl. Chem.*, 1970, 32, 2141.
108. B.W. Fitzsimmons, *J. Chem. Soc. (A)*, 1970, 3235.

109. R.C. Poller, J.N.R. Ruddick, M. Thevarasa and W.R. McWhinnie, J. Chem. Soc. (A), 1969, 16, 2327.
110. R.C. Poller, J.N.R. Ruddick, B. Taylor and D.L.B. Toley, J. Organometal. Chem., 1970, 24, 2, 341.
111. R.V. Parish and R.H. Platt, J. Chem. Soc. (A), 1969, 2145.
112. A.G. Davies, L. Smith and P.J. Smith, J. Organometal. Chem., 1970, 23, 135.
113. A.G. Davies, H.J. Milledge, D.C. Puxley and P.J. Smith, J. Chem. Soc. (A), 1970, 2862.
114. N.W. Isaacs and C.H.L. Kennard, J. Chem. Soc. (A), 1970, 8, 1257.
115. E.A. Blom, B.R. Penfold and W.T. Robinson, J. Chem. Soc. (A), 1969, 6, 913.
116. E.V. Van Den Berghe, L. Verdonck and G.P. Van Der Kelen, J. Organometal. Chem., 1969, 16, 497.
117. K.L. Jaura, K. Chander and K.K. Sharma, Z. Anorg. Allg. Chem., 1970, 1, 107.
118. R.W.J. Wedd and J.R. Sams, Can. J. Chem., 1970, 48, 1, 71.
119. B.W. Fitzsimmons, A.A. Owusu, N.J. Seeley and A.W. Smith, J. Chem. Soc. (A), 1970, 6, 935.
120. B.W. Fitzsimmons, N.J. Seeley and A.W. Smith, J. Chem. Soc. (A), 1969, 143.
121. T. Kamitani, H. Yamamoto and T. Tanaka, J. Inorg. Nucl. Chem., 1970, 32, 8, 2621.
122. T.V. Malysheva, O.M. Petrukhin, V.A. Dolgopov and Yu.A. Zolotou, Zh. Neorg. Khim., 1970, 15, 6, 1699.
123. J.W. Hayes, R.J. Le Fèvre and D.V. Radford, Inorg. Chem., 1970, 9, 2, 400.
124. Y. Kawasaki, T. Tanaka and R. Okawara, Bull. Chem. Soc., Jap., 1967, 40, 1562.
125. D. Petridis, F.P. Mullins and C. Curran, Inorg. Chem., 1970, 9, 5, 1270.
126. A. Van den Bergen, R.J. Cozens and K.S. Murray, J. Chem. Soc. (A), 1970, 3060.

127. R.J.H. Clark, A.G. Davies and R.J. Puddephatt, J. Chem. Soc. (A), 1968, 8, 1828.
128. F.P. Mullins, Can. J. Chem., 1970, 48, 1677.
129. K.M. Ali, D. Cunningham, M.J. Frazer, J.D. Donaldson and B.J. Senior, J. Chem. Soc. (A), 1969, 2836.
130. D.M. Barnhart, C.N. Caughlan and M. Ul.-Hague, Inorg. Chem., 1968, 7, 1135.
131. S.S. Sandu and S.S. Sandu, J. Inorg. Nucl. Chem., 1969, 31, 5, 1363.
132. E.V. Van Den Berghe and G.P. Van Der Kelen, J. Organometal. Chem., 1968, 11, 3, 479.
133. C.W. Hobbs and R.S. Tobias, Inorg. Chem., 1970, 2, 5, 1037.
134. C.A. Clausen and M.L. Good, Inorg. Chem., 1970, 2, 4, 817.
135. R.H. Herber and HWA Sheng Cheng, Inorg. Chem., 1969, 8, 10, 2145.
136. J.C. Hill, R.S. Drago and R.H. Herber, J. Amer. Chem. Soc., 1969, 91, 1644.
137. K. Nakamoto, "Infra-red Spectra of Inorganic and Co-ordination Compounds". Wiley, New York, 1963.
138. E.B. Wilson, J.C. Decius and P.C. Cross, "Molecular Vibrations". McGraw-Hill, New York, 1955.
139. R.E. Dodd, L.A. Woodward and H.L. Roberts, Trans. Faraday Soc., 1956, 52, 1052.
140. I.R. Beattie, M. Webster and G.W. Chantry, J. Chem. Soc. (Supp. 2), 1964, 6172.
141. G. ^{HERZBERG}~~Hertzberg~~, "Molecular Spectra and Molecular Structure". Van Nostrand, New York, 1945.
142. T.R. Gilson, Ph.D. Thesis, London, 1964.
143. R.G. Snyder and J.H. Schachtschneider, Spectrochim Acta, 1963, 19, 85.
144. I.R. Beattie and L. Rule, J. Chem. Soc., 1964, 3267.
145. R.F.M. White, "Nuclear Magnetic Resonance Spectroscopy and Inorganic Stereochemistry" in "Progress in Stereochemistry" 1968, 4, P 167. Eds. B.J. Aylett and M.M. Harris, Butterworths, London.

146. J.W. Emsley, J. Feeney and L.H. Sutcliffe, "High Resolution Nuclear Magnetic Resonance Spectroscopy", 1965, Oxford, Pergamon.
147. J. Chatt and R.G. Hayter, J. Chem. Soc., 1961, 2605.
148. M. Van Gorkam and G.E. Hall, Quart. Rev., 1968, 1, 22.
149. A. Abraham, "Principles of Nuclear Magnetism", Oxford, University Press, 1961, 480.
150. E.I. Snyder, J. Amer. Chem. Soc., 1963, 85, 2624.
151. E.L. Muetterties, J. Amer. Chem. Soc. 1960, 82, 1082.
152. I.P. Goldshtein, E.N. Gur'yanova and K.A. Kochesshkov, Proc. Akad. Sci. U.S.S.R., 1962, 144, 456.
153. I.R. Beattie, R. Hulme and L. Rule, J. Chem. Soc., 1965, 1581.
154. V. Doron and C. Fischer, Inorg. Chem., 1967, 6, 1917.
155. R.L. Mössbauer, Naturwiss, 1958, 45, 538 and Z.Physik, 1958, 151, 1 24.
156. R.H. Herber, J. Chem. Ed., 1965, 42, 180.
157. N.N. Greenwood and J.N.R. Ruddick, J. Chem. Soc. (A), 1967, 1679.
158. R.H. Herber and G.I. Parisi, Inorg. Chem. 1966, 5, 769.
159. M. von Laue, Sitzber, Math. Physik. K.I. Bayer, Akad. Wiss. Muenchen, 1912, 303.
160. W.L. Bragg, Proc. Cambridge Phil. Soc., 1913, 17, 43.
161. A.L. Patterson, Z. Krist., A90, (1935), 517.
162. M.J. ^{BUERGER}~~Bueger~~, "X-ray Crystallography", Wiley, New York, 1942.
163. M.J. ^{BUERGER}~~Bueger~~, "Crystal Structure Analysis", Wiley, New York, 1960.
164. E.W. Nuffield, "X-ray Diffraction Methods", Wiley, New York, 1966.
165. G.H. Stout and L.H. Jenson, "X-ray Structure Determination", (A Practical Guide), Macmillan, New York, 1968.
166. M.M. Woolfson, "An Introduction to X-ray Crystallography", Cambridge Univ. Press, 1970.
- 167a International Tables for X-ray Crystallography, I (Symmetry Groups), N.F.M. Henry and K. Lonsdale eds., Kynoch Press, Birmingham, 1952.
- 167b International Tables for X-ray Crystallography, III (Physical and Chemical Tables), C.H. MacGillavry and G.D. Rieck, eds., Kynoch Press, Birmingham, 1962.

168. L.H. Thomas and K. Umeda, J. Chem. Phys., 1957, 26, 293.
169. C.-I. Branden, Acta. Chem. Scand., 1963, 17, 759.
170. Y. Hermodsson, Acta. Cryst., 1960, 13, 656.
171. T.A. Dougherty, Diss. Abs., 1967, 28B, 83; T.A. Dougherty and R.E. McCarley, 152nd Abstracts Amer. Chem. Soc. Meeting, Sept. 1966, O, 121.
172. R.A. Walton, Quart. Rev., 1965, 19, 126.
173. H. Binas, Z. Anorg. Chem. 1967, 352, 271.
174. T.C. Furnas, "Single Crystal Orienter Instruction Manual", G.E.C. Milwaukee, 1957.
175. D.P. Shoemaker, Dept. Chem. Mit. Cambridge Mass., Unpublished Work.
176. G.G. Messmer, E.L. Amma and J.A. Ibers, Inorg. Chem., 1967, 6, 725.
177. L.E. Sutton et al "Interatomic Distances and Configuration in Molecules and Ions", Chem. Soc. London Special Publications, 11, 1958; 18, 1965.
178. M.F. Lappert, J. Chem. Soc., 1962, 542.
- 179a J.M. Miller and M. Onyszchuk, Can. J. Chem. 1964, 42, 1518.
- 179b J.M. Miller and M. Onyszchuk, Can. J. Chem. 1966, 44, 899.
180. M. Zackrisson and K.I. Alden, Acta. Chem. Scand., 1960, 14, 994.
181. J.E. Fergusson, D.K. Grant, R.H. Hickford and C.J. Wilkins, J. Chem. Soc., 1959, 99
182. R.C. Aggarwal, J.P. Guertin and M. Onyszchuk, in "Proceedings of the VIIIth International Conference on Coordination Chemistry", ed. V. Gutmann, Springer-Verlag, Vienna, 1964, p 198.
183. J.M. Miller and M. Onyszchuk, Proc. Chem. Soc. 1964, 290.
184. S.T. Zenchelsky and P.R. Segatto, J. Amer. Chem. Soc., 1958, 80, 4796.
185. D.P.N. Satchell and J.L. Wardell, J. Chem. Soc., 1964, 4134.
186. I. Lindquist and M. Zackrisson, Acta. Chem. Scand., 1960, 14, 453.
187. W. Heiber and E. Reindl, Z. Electrochem., 1940, 46, 549.
188. F.J. Cioff and S.T. Zenchelsky, J. Phys. Chem., 1963, 67, 357.

189. D.N. Miller and H.H. Sisler, J. Amer. Chem. Soc., 1955, 77, 4998 and 1956, 78, 6421.
190. R.C. Aggarwal and M. Onyszchuk, J. Inorg. Nuc. Chem. 1968, 30, 3351.
191. A. Marchand, J. Mendelsohn, M. Lebedeff and J. Valade, J. Organometal. Chem., 1969, 17, 379.
192. T.J. Lane, P.A. McCusker and B.C. Curran, J. Amer. Chem. Soc., 1942, 2076.
193. D. Cook, Canad. J. Chem., 1963, 41, 522.
194. K. Hensen and W. Sarholz, Theoret. Chim. Acta., 1968, 12, 206.
195. T. Danielsson, B. Nelander, S. Sunner and I. Wadso, Acta. Chem. Scand., 1964, 18, 995.
196. S. Sunner and I. Wadso, Acta. Chem. Scand., 1959, 13, 1, 97.
197. S. Sunner and I. Wadso, Science Tools, 1960, 13, 1.
198. I. Wadso, Acta. Chem. Scand., 1968, 22, 927.
199. P.R. Stroesser and S.J. Gill, Rev. Sci. Instr. 1967, 38, H.22.
200. N.N. Greenwood and P.G. Perkins, J. Inorg. Nuc. Chem. 1957, 4, 291.
201. E.M. Arnett, W.G. Bentrude, J.J. Burke and P. McDuggleby, J. Amer. Chem. Soc., 1965, 87, 7, 1541.
202. E. Calvet and H. Prat, "Recent Progress in MicroCalorimetry", Pergamon Press, 1963.
203. Handbook of Chemistry and Physics 17th Ed., The Chem. Rubber Co.,
204. G. Kegeles, J. Amer. Chem. Soc., 1940, 62, 3230.
205. U.N. Vasil/eva, M.A. Yutskovskaya and S.S. Medvedev, Dokl. Akad. Nauk, S.S.S.R., 1969, 188, 1, 351.

PLATE 1

CALORIMETER.

